



The impact of ocean acidification on microbial dynamics and activities - a mesocosm study in the Baltic Sea

Diplomarbeit

im Diplomstudiengang Marine Umweltwissenschaften
am Institut für Chemie und Biologie des Meeres
der Carl von Ossietzky Universität Oldenburg

vorgelegt von
Mascha Wurst

Erster und betreuender Gutachter:

Dr. Mirko Lunau

(AWI, Bremerhaven)

Zweiter Gutachter:

Prof. Dr. Wolfgang Ebenhöf

(ICBM, Oldenburg)

Oldenburg, 20. April 2008

Contents

LIST OF FIGURES IV

LIST OF TABLES IX

ABBREVIATIONS X

1 INTRODUCTION 1

 CARBONATE SYSTEM 3

 THE MARINE CARBON CYCLE 5

 MARINE PRIMARY PRODUCTION 7

 MICROBIAL LOOP 8

 HOW TO STUDY THE EFFECTS OF RISING CO₂ CONCENTRATION ON MARINE ENVIRONMENTS? 9

 THIS STUDY 10

2 MATERIALS AND METHODS - 13 -

SETUP AND SAMPLING - 13 -

MEASUREMENTS AND ANALYSES - 15 -

 PHYSICOCHEMICAL PARAMETERS - 15 -

 BIOGEOCHEMICAL PARAMETERS - 15 -

 AMINO ACIDS - 16 -

 TRANSPARENT EXOPOLYMER PARTICLES - 18 -

 PLANKTON ABUNDANCES - 19 -

 DIAZOTROPHIC CYANOBACTERIA DYNAMICS - 19 -

 PHYTOPLANKTON ACTIVITY - 19 -

 BACTERIAL DYNAMICS - 20 -

 HYDROLYTIC ENZYME ACTIVITIES - 21 -

 BACTERIAL ACTIVITIES - 23 -

 CALCULATION OF GROWTH RATES - 24 -

 STATISTICAL ANALYSES - 24 -

3 RESULTS - 25 -

EXPERIMENTAL BOUNDARY CONDITIONS	- 25 -
VERTICAL DISTRIBUTIONS (CTD MEASUREMENTS)	- 26 -
TEMPERATURE.....	- 26 -
SALINITY	- 28 -
PH AND PCO_2	- 29 -
THE PH AND PCO_2 HISTORY OF EVERY SINGLE MESOCOSM	- 32 -
BIOGEOCHEMICAL PROCESSES	- 35 -
PARTICULATE ORGANIC MATTER (POM).....	- 35 -
C:N:P RATIO	- 38 -
CHLOROPHYLL A AND NUTRIENTS	- 41 -
AMINO ACIDS	- 42 -
TRANSPARENT EXOPOLYMER PARTICLES	- 43 -
EUKARYOTIC PHYTOPLANKTON DYNAMICS	- 44 -
DIAZOTROPHIC CYANOBACTERIA DYNAMICS	- 45 -
PHYTOPLANKTON ACTIVITY	- 47 -
CO_2 UPTAKE.....	- 47 -
N_2 FIXATION.....	- 48 -
UNICELLULAR CYANOBACTERIA	- 50 -
BACTERIAL DYNAMICS	- 51 -
HYDROLYTIC ENZYME ACTIVITIES	- 53 -
A-GLUCOSIDASE.....	- 53 -
LEUCINE-AMINOPEPTIDASE	- 54 -
ALKALINE PHOSPHATASE	- 55 -
BACTERIAL ACTIVITIES	- 56 -
GROWTH RATES	- 57 -
4 DISCUSSION AND CONCLUSION	- 60 -
EXPERIMENTAL SETUP.....	- 60 -
EFFECTS OF INCREASING PCO_2 ON BIOGEOCHEMICAL PROCESSES	- 62 -
EFFECTS OF INCREASING PCO_2 ON MICROBIAL DYNAMICS AND ACTIVITIES	- 66 -
CONCLUSIONS.....	- 70 -
ACKNOWLEDGEMENTS	- 71 -

APPENDIX..... - 72 -
REFERENCES..... - 75 -

List of Figures

- FIGURE 1: SCHEMATIC VIEW OF THE COMPONENTS OF THE CLIMATE SYSTEM (BOLD), THEIR PROCESSES AND INTERACTIONS (THIN ARROWS) AND SOME ASPECTS THAT MAY CHANGE (BOLD ARROWS) (AFTER HOUGHTON ET AL. 2001). 1
- FIGURE 2: SCHEMATIC ILLUSTRATION OF THE CARBONATE SYSTEM IN THE OCEAN. CO_2 IS EXCHANGED BETWEEN ATMOSPHERE AND OCEAN VIA EQUILIBRATION OF CO_2 (G) AND DISSOLVED CO_2 . DISSOLVED CO_2 IS PART OF THE CARBONATE SYSTEM IN SEAWATER THAT INCLUDES BICARBONATE, HCO_3^- , AND CARBONATE ION, CO_3^{2-} (AFTER ZEEBE AND WOLF-GLADROW 2001). 4
- FIGURE 3: CYCLING OF ORGANIC MATTER AND MICROBIAL LOOP. INTERPLAY BETWEEN LIGHT, NUTRIENTS, TEMPERATURE, PRIMARY PRODUCTION OF PHYTOPLANKTON (CARBON DIOXIDE (CO_2) UPTAKE, NITROGEN (N_2) FIXATION), RESPIRATION OF OXYGEN (O_2), EXPORT OF PARTICULATE ORGANIC MATTER (POM), RELEASE OF DISSOLVED ORGANIC MATTER (DOM) AND BACTERIAL DEGRADATION PROCESSES OF DOM & POM (HYDROLYTIC ENZYME ACTIVITY (HEA), AND UPTAKE OF MONOMERIC DOM). THE DOM POOL CONSISTS OF DISSOLVED ORGANIC NITROGEN (DON, MAINLY AMINO ACIDS (AA)), DISSOLVED ORGANIC CARBON (DOC, MAINLY CARBOHYDRATES (CHO), AA, AND LIPIDS (L)) AND DISSOLVED ORGANIC PHOSPHOROUS (DOP). TRANSPARENT EXOPOLYMER PARTICLES (TEP) FORM FROM DOM PRECURSORS AND SUBSEQUENTLY PROMOTE SEDIMENTATION AND EXPORT OF POM. THE POM POOL CONSISTS OF PARTICULATE ORGANIC CARBON (POC), PARTICULATE ORGANIC NITROGEN (PON) AND PARTICULATE ORGANIC PHOSPHOROUS (POP) (M. LUNAU, AWI BREMERHAVEN). 12
- FIGURE 4: MAP OF NORTHERN EUROPE (INSET) AND OF THE BALTIC SEA INCLUDING THE SAMPLING AREA (MAP SOURCE: GOOGLE.MAPS); DRIFT OF THE MESOCOSMS DURING THE EXPERIMENT (11 DAYS, MODIFIED AFTER DR. K. VON BRÖCKEL, IFM-GEOMAR). - 13 -
- FIGURE 5: REACTION SCHEME OF THE ORTHO-PHTALDIALDEHYDE (OPA) DERIVATIZATION. - 17 -
- FIGURE 6: BOUNDARY CONDITIONS IN THE BALTIC SEA IN JULY 2007: WATER TEMPERATURE ($^{\circ}\text{C}$) (BLUE LINE) OF THE BALTIC AND WIND SPEED (M/S)(RED LINE).

LIST OF FIGURES

SAMPLING FREQUENCY OF MESOCOSMS IS MARKED WITH BLACK DOTS.	
ACIDIFICATION EVENTS ARE HIGHLIGHTED BY BOXES.....	- 25 -
FIGURE 7: COMPARISONS OF THE VERTICAL DISTRIBUTION OF WATER TEMPERATURES IN THE MESOCOSMS (MC) 1 - 6 AND IN THE BALTIC BEFORE (A) AND AFTER THE ACIDIFICATIONS (B, C, D) (SOLID LINES: 0 - 10 M, DOTTED LINES: 10 - 17.5 M) (DATA, K. SCHULZ).	- 26 -
FIGURE 8 : VERTICAL PROFILES OF WATER TEMPERATURE IN THE MESOCOSMS (MC) 1 - 6 AND IN THE BALTIC FOR 10 TH JULY (BLUE), 14 TH JULY (YELLOW), 16 TH JULY (RED) AND 20 TH JULY (GREEN). (SOLID LINES: 0 - 10 M, DOTTED LINES: 10 - 17.5 M) (DATA, K. SCHULZ)	- 27 -
FIGURE 9: VERTICAL PROFILES OF SALINITY IN THE MESOCOSMS (MC) 1 - 6 AND IN THE BALTIC FOR 10 TH JULY (BLUE), 14 TH JULY (YELLOW), 16 TH JULY (RED) AND 20 TH JULY (GREEN). (SOLID LINES: 0 - 10 M, DOTTED LINES: 10 - 17.5 M) (DATA, K. SCHULZ).....	- 29 -
FIGURE 10: VERTICAL PROFILES OF PCO ₂ (CALCULATED BY PH AND ALKALINITY)) IN THE MESOCOSMS (MC) 1 - 6 AND IN THE BALTIC FOR 10 TH JULY (BLUE), 14 TH JULY (YELLOW), 16 TH JULY (RED) AND 20 TH JULY (GREEN). (SOLID LINES: 0 - 10 M, DOTTED LINES: 10 - 17.5 M)	- 30 -
FIGURE 11: VERTICAL PROFILES OF PH IN THE MESOCOSMS (MC) 1 - 6 AND IN THE BALTIC FOR 10 TH JULY (BLUE), 14 TH JULY (YELLOW), 16 TH JULY (RED) AND 20 TH JULY (GREEN). (SOLID LINES: 0 - 10 M, DOTTED LINES: 10 - 17.5 M) (DATA, K. SCHULZ).....	- 31 -
FIGURE 12: RANGE OF PH (MEAN OF 0-10 M) IN THE MESOCOSMS (MC) 1-6 DURING THE ENTIRE EXPERIMENT (SOLID LINE: MEDIAN, DOTTED LINE: MEAN)	- 32 -
FIGURE 13: TEMPORAL DEVELOPMENT OF THE PCO ₂ CONCENTRATIONS IN THE MESOCOSMS (NOT, WEAKLY, MEDIUM AND STRONGLY ACIDIFIED) FOR THE 1 ST , 2 ND AND 3 RD ACIDIFICATION EXPERIMENTS.....	- 33 -
FIGURE 14: RANGE OF PCO ₂ CONCENTRATIONS IN THE MESOCOSMS (NOT, WEAKLY, MEDIUM AND STRONGLY ACIDIFIED) FOR THE 1 ST (A) AND 2 ND (B) ACIDIFICATION EXPERIMENT.	- 34 -

LIST OF FIGURES

FIGURE 15: MEANS OF PARTICULATE ORGANIC CARBON (POC) CONCENTRATIONS IN THE MESOCOSMS (NOT, WEAKLY, MEDIUM AND STRONGLY ACIDIFIED) FOR THE 1 ST (A) AND 2 ND (B) ACIDIFICATION EXPERIMENT (DATA, M. VOSS).	- 35 -
FIGURE 16: MEANS OF PARTICULATE ORGANIC NITROGEN (PON) CONCENTRATIONS IN THE MESOCOSMS (NOT, WEAKLY, MEDIUM AND STRONGLY ACIDIFIED) FOR THE 1 ST (A) AND 2 ND (B) ACIDIFICATION EXPERIMENT (DATA: M. VOSS).	- 36 -
FIGURE 17: MEANS OF PARTICULATE ORGANIC PHOSPHORUS (POP) CONCENTRATIONS IN THE MESOCOSMS (NOT, WEAKLY, MEDIUM AND STRONGLY ACIDIFIED) FOR THE 1 ST (A) AND 2 ND (B) ACIDIFICATION EXPERIMENT (DATA, K. ISENSEE).	- 37 -
FIGURE 18: MEANS OF THE CARBON/NITROGEN (C/N) RATIO (MOL/MOL) IN THE MESOCOSMS (NOT, WEAKLY, MEDIUM AND STRONGLY ACIDIFIED) FOR THE 1 ST (A) AND 2 ND (B) ACIDIFICATION EXPERIMENT (RED SOLID LINES: REDFIELD RATIO OF 6.6).	- 38 -
FIGURE 19: MEANS OF THE CARBON/PHOSPHORUS (C/P) RATIO IN THE MESOCOSMS (NOT, WEAKLY, MEDIUM AND STRONGLY ACIDIFIED) FOR THE 1 ST (A) AND 2 ND (B) ACIDIFICATION EXPERIMENT (RED SOLID LINES: REDFIELD RATIO OF 106).	- 39 -
FIGURE 20: MEANS OF THE NITROGEN/PHOSPHORUS (N/P) RATIO IN THE MESOCOSMS (NOT, WEAKLY, MEDIUM AND STRONGLY ACIDIFIED) FOR THE 1 ST (A) AND 2 ND (B) ACIDIFICATION EXPERIMENT (RED SOLID LINES: REDFIELD RATIO OF 16).	- 40 -
FIGURE 21: MEANS OF CHLOROPHYLL A (CHL A) CONCENTRATIONS IN THE MESOCOSMS (NOT, WEAKLY, MEDIUM AND STRONGLY ACIDIFIED) FOR THE 1 ST (A) AND 2 ND (B) ACIDIFICATION EXPERIMENT (DATA, P. FRITSCH).	- 41 -
FIGURE 22: MEANS OF DISSOLVED FREE AMINO ACID (DFAA) CONCENTRATIONS IN THE MESOCOSMS (NOT, WEAKLY, MEDIUM AND STRONGLY ACIDIFIED) FOR THE 1 ST (A) AND 2 ND (B) ACIDIFICATION EXPERIMENT.	- 42 -
FIGURE 23: MEANS OF TRANSPARENT EXOPOLYMER PARTICLES (TEP) IN THE MESOCOSMS (NOT, WEAKLY, MEDIUM AND STRONGLY ACIDIFIED) FOR THE 1 ST (A) AND 2 ND (B) ACIDIFICATION EXPERIMENT.	- 43 -
FIGURE 24: MEANS OF EUKARYOTIC PHYTOPLANKTON ABUNDANCES IN THE MESOCOSMS (NOT, WEAKLY, MEDIUM AND STRONGLY ACIDIFIED) FOR THE 1 ST (A)	

LIST OF FIGURES

AND 2 ND (B) ACIDIFICATION EXPERIMENT (DATA, H. JOHANSEN & A. GRÜTTMÜLLER).....	- 44 -
FIGURE 25: TEMPORAL DYNAMICS OF NODULARIA SPP. (A) AND APHANIZOMENON SPP. (B) IN THE MESOCOSMS (NOT, WEAKLY, MEDIUM AND STRONGLY ACIDIFIED) FOR THE 1 ST AND 2 ND ACIDIFICATION EXPERIMENT (1 UNIT = 100 µM) (DATA, K. HAYNERT).....	- 45 -
FIGURE 26: MEANS OF CO ₂ UPTAKE RATES OF ORGANISMS >10µM (BLACK) AND <10µM (GREY) IN THE MESOCOSMS (NOT, WEAKLY, MEDIUM AND STRONGLY ACIDIFIED) FOR THE 1 ST (A) AND 2 ND (B) ACIDIFICATION EXPERIMENT (DATA, M. VOSS)....	- 47 -
FIGURE 27: MEANS OF NITROGEN FIXATION (N ₂ FIX) RATES OF ORGANISMS >10µM (BLACK) AND <10µM (GREY) IN THE MESOCOSMS (NOT, WEAKLY, MEDIUM AND STRONGLY ACIDIFIED) FOR THE 1 ST (A) AND 2 ND (B) ACIDIFICATION EXPERIMENT (DATA, M. VOSS).	- 49 -
FIGURE 28: MEANS OF UNICELLULAR CYANOBACTERIA (DETERMINED BY FLOW CYTOMETRY) ABUNDANCES IN THE MESOCOSMS (NOT, WEAKLY, MEDIUM AND STRONGLY ACIDIFIED) FOR THE 1 ST (A) AND 2 ND (B) ACIDIFICATION EXPERIMENT (DATA, H. JOHANSEN & A. GRÜTTMÜLLER).	- 50 -
FIGURE 29: MEANS OF HETEROTROPHIC BACTERIA ABUNDANCES IN THE MESOCOSMS (NOT, WEAKLY, MEDIUM AND STRONGLY ACIDIFIED) FOR THE 1 ST (A) AND 2 ND (B) ACIDIFICATION EXPERIMENT (MEDIUM OF 2 ND ACIDIFICATION: N=1).....	- 51 -
FIGURE 30: LINEAR CORRELATIONS BETWEEN TRANSPARENT EXOPOLYMER PARTICLES (TEP) AND. CYANOBACTERIA (ORANGE) (A) AND TEP VS. HETEROTROPHIC BACTERIA (BLUE) (B). DATA OF THE NOT ACIDIFIED MESOCOSMS (1 ST ACIDIFICATION (RED) AND 2 ND ACIDIFICATION (BLACK)) WERE NEGLECTED. -	52
FIGURE 31: LINEAR MODEL FIT OF THE ENZYME EFFICIENCY (V _{MAX} /K _M) OF A-GLUCOSIDASE IN ALL MESOCOSMS AND DURING THE ENTIRE EXPERIMENT (MULTIPLE R(Z/XY) = 0.23, P = 0.2).	- 53 -
FIGURE 32: LINEAR MODEL FIT OF THE ENZYME EFFICIENCY (V _{MAX} /K _M) OF LEUCINE-AMINOPEPTIDASE IN ALL MESOCOSMS AND DURING THE ENTIRE EXPERIMENT (MULTIPLE R(Z/XY) = 0.68, P < 0.001).....	- 54 -

LIST OF FIGURES

FIGURE 33: LINEAR MODEL FIT OF THE ENZYME EFFICIENCY (V_{MAX}/K_M) OF ALKALINE PHOSPHATASE IN ALL MESOCOSMS AND DURING THE ENTIRE EXPERIMENT (MULTIPLE $R(Z/XY) = 0.68$, $P < 0.001$).....	- 55 -
FIGURE 34: MEANS OF L ^E UCINE (LEU) (A, B) AND THYMIDINE (THY) (C; D) UPTAKE RATES IN THE MESOCOSMS (NOT, WEAKLY, MEDIUM AND STRONGLY ACIDIFIED) FOR THE 1 ST AND 2 ND ACIDIFICATION EXPERIMENT.	- 56 -
FIGURE 35: TEMPORAL DYNAMICS OF HETEROTROPHIC BACTERIA ABUNDANCES IN THREE DIFFERENT (NOT (A), WEAKLY (B) AND STRONGLY (C) ACIDIFIED) MESOCOSMS FOR THE 2 ND ACIDIFICATION EXPERIMENT (ERROR BARS INDICATE ANALYTICAL ERRORS OF CYTOMETRICAL ANALYSES (4%)).....	- 57 -
FIGURE 36: TEMPORAL DYNAMICS OF UNICELLULAR CYANOBACTERIA ABUNDANCES IN THREE DIFFERENT (NOT (A), WEAKLY (B) AND STRONGLY (C) ACIDIFIED) MESOCOSMS FOR THE 2 ND ACIDIFICATION EXPERIMENT (ERROR BARS INDICATE ANALYTICAL ERRORS OF CYTOMETRICAL ANALYSES (8%)).....	- 58 -
FIGURE 37: GROWTH RATES OF UNICELLULAR CYANOBACTERIA (WHITE) AND HETEROTROPHIC BACTERIA (GREY) IN THREE DIFFERENT (NOT, WEAKLY AND STRONGLY ACIDIFIED) MESOCOSMS FOR THE 2 ND ACIDIFICATION EXPERIMENT.-	- 59 -
FIGURE 38: CHANGES IN NUTRIENT CHARACTERISTICS ACROSS A PRODUCTIVITY GRADIENT. (A-H COUPLING: AUTOTROPHIC-HETEROTROPHIC COUPLING) (FROM COTNER AND BIDDANDA 2002).....	- 69 -
FIGURE 39: DISSOLVED FREE AMINO ACID (DFAA) COMPOSITION IN THE MESOCOSMS (NOT, WEAKLY AND STRONGLY ACIDIFIED) OF THE 1 ST AND 2 ND ACIDIFICATION EXPERIMENT. TEMPORAL DEVELOPMENT WITHIN THE TREATMENTS AND ACIDIFICATION.	- 74 -

List of Tables

TABLE 1: SOLUBILITY OF 4-METHYLUMBELLIFERYL (MUF)- A-D-GLUCOSIDE, MUF-
PHOSPHATE AND L-LEUCINE 7-AMINO-4-METHYLCOUMARIN (AMC).- 21 -

TABLE 2: INITIAL VALUES OF MEASURED PARAMETERS BEFORE ACIDIFICATION AT ALL .. -
72 -

TABLE 3: SOLUBILITY OF MUF- AND AMC- LABELLED SUBSTRATE ANALOGUES- 73 -

Abbreviations

α -ABA	α -amino butyric acid
AMC	7-amino-4-methylcoumarin
approx.	approximately
AR4	4 th assessment report
ASN	asparagines
Bft	Beaufort
BPP	baterial protein production
Bq	Becquerel
C	carbon
C _A	carbonate alkalinity
CaCO ₃	calcium carbonate
CCM	CO ₂ concentrating system
CFCs	chlorofluorocarbons
CH ₄	methane
Chl a	chlorophyll a
CHO	carbohydrates
CO ₂	carbon dioxide
CO ₃ ²⁻	carbonate ion
CTD	conductivity, temperature, depth
DCAA	dissolved combined amino acids
DFAA	dissolved free amino acids
DIC	dissolved inorganic carbon
DMSO	dimethyl sulfoxide
DNA	desoxyribonucleic acid
DOC	dissolved organic carbon
DOM	dissolved organic matter
DON	dissolved organic nitrogen
DOP	dissolved organic phosphorous
e.g.	for example, <i>abbreviation of Latin 'exempli gratia'</i>
Em.	emission

ABBREVIATIONS

Ex.	Extinction
FL1	fluorescence 1
GCMs	global climate models
GDA	glutardialdehyde
GLN	glutamine
H ⁺	protons
HCl	hydrochloric acid
HCO ₃ ⁻	bicarbonate
HEA	hydrolytic enzyme activity
HMW	high-molecular-weight
HNA	high nucleic acid subgroup
H ₂ O	water vapour
H ₂ SO ₄	sulphuric acid
HPLC	high performance liquid chromatography
IPCC	Intergovernmental Panel on Climate Change
KOSMOS	Kiel Off-Shore Mesocosms for future Ocean Simulations
K _m	Michaelis constant (affinity for substrate)
LNA	low nucleic acid subgroup
MC	mesocosm
min ⁻¹	per minute
MUF	4-methylumbelliferyl
NaOH	sodium hydroxide
nm	nautical miles
N ₂	nitrogen
N ₂ O	nitrous oxide
NO ₃ ⁻	nitrate
O ₂	oxygen
O ₃	ozone
OPA	ortho-phtaldialdehyde
pCO ₂	carbon dioxide partial pressure
PE	polyethylene
PIC	particulate inorganic carbon

ABBREVIATIONS

POC	particulate organic carbon
POM	particulate organic matter
PON	particulate organic nitrogen
POP	particulate organic phosphorous
pH	pH is a measure of the acidity or alkalinity of a solution
PO ₄ ³⁻	phosphate
ppm	parts per million
RV	research vessel
RubisCO	Ribulose-1,5-bisphosphate carboxylase/oxygenase
sec ⁻¹	per second
SG1	SybrGreen I
SG2	SybrGreen II
Si	silicate
SOPRAN	Surface Ocean PRocesses in the Anthropocene
SSC	sidescatter
T _A	total alkalinity
TCA	trichloroacetic acid
TEP	transparent exopolymer particles
THDAA	total hydrolysable dissolved amino acids
TLZ	Technik- und Logistikzentrum
UV-vis.	ultraviolet-visible
V _{max}	maxiumin veloocity of enzyme
vs.	Versus
Xeq.	GumXanthan equivalents
°C	degree Celsius
³ H-Leu	³ [H]-leucine, tritiated leucine
³ H-TdR	³ [H]-thymidine, tritiated thymidine

1 Introduction

The earth's climate is a highly complex system usually separated in five major components: the atmosphere, the hydrosphere, the cryosphere, the land surface and the biosphere (Fig. 1). These components are influenced on the one hand by various external forcing mechanisms, such as solar irradiance and orbital patterns. But on the other hand, their chemical, physical and biological interactions and internal feedbacks play an important role. The components of the climate system are all linked by fluxes of mass, heat and momentum, although their composition, chemical and physical properties, structure and behaviour are very different (Houghton et al. 2001).

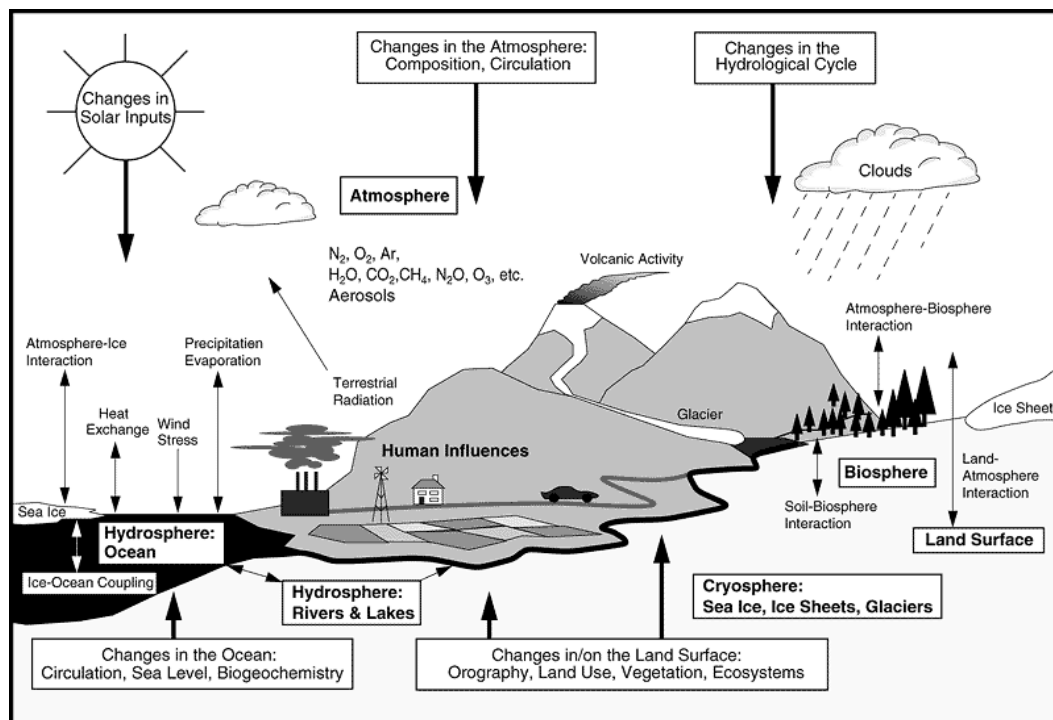


Figure 1: Schematic view of the components of the climate system (bold), their processes and interactions (thin arrows) and some aspects that may change (bold arrows) (after Houghton et al. 2001).

In recent years many attention was spent on investigating the changes of the atmospheric composition. The so called 'natural greenhouse effect' keeps the

earth's surface warm by trapping heat due to the greenhouse gases. The primary greenhouse gases are water vapour (H₂O), carbon dioxide (CO₂), methane (CH₄), nitrous oxide (N₂O) and ozone (O₃). Without these gases the earth's average surface temperature would be about -18°C, instead of 15°C (Houghton et al. 2001). The extent of change in climate, CO₂ and other climate-relevant gases is controlled by a variety of mechanisms. Among these mechanisms, biologically-driven reactions and feedbacks, involving both terrestrial and marine ecosystems, are tend to play a critical role (Riebesell 2004).

During the past 420,000 years before the industrial period the earth's climate system settled into a persistent pattern of glacial-interglacial cycles, with atmospheric CO₂ oscillating between 180 µatm in glacial and 280 µatm in interglacial times (Petit et al. 1999). Concentrations of atmospheric greenhouse gases and their radiative forcing have continued to increase as a result of human activities in the past 200 years. Since 1750 the increase of CO₂ emissions has been 31%, primarily due to fossil fuel use and changes in land use (Houghton et al. 2001). According to the 4th assessment report (AR4) of the Intergovernmental Panel on Climate Change (IPCC, 2007), the global atmospheric CO₂ concentration increased from a pre-industrial value of 280 µatm to 379 µatm in 2005. Current CO₂ concentration has not been exceeded during the past 650,000 years and likely not during the past 20 million years. The mean annual increase of CO₂ concentration was in average 1.9 µatm per year during the period from 1995 to 2005 (IPCC, 2007). Estimates of future atmospheric CO₂ concentrations, based on the IPCC 'business-as-usual' emission scenario (IS92a), predict that the CO₂ concentrations will rise by a factor of two relative to the present value (~380 µatm) in the year 2100, and could increase by a factor of three by the middle of the next century (Houghton et al. 2001).

About 98% of the CO₂ in the combined atmosphere-ocean system is dissolved in water. Atmospheric CO₂ reacts with water to bicarbonate and carbonate ions (see carbonate system) (Zeebe and Wolf-Gladrow 2001). If global emissions of

CO₂ from human activities continue to rise, the oceans will become more acidic by an average of 0.5 units (on the logarithmic scale of pH) (Caldeira and Wickett 2003; Raven 2005). Possible consequences of ocean acidification can range from physiological responses on organism level, changes in ecosystem structures, to shifts in biogeochemical cycling. Although the carbon cycle is most strongly affected by human activities, this anthropogenic influence has consequences for the earth system as a whole, since the carbon cycle is coupled with climate, water cycle, nutrient cycles and photosynthesis on land and in oceans (Falkowski et al. 2000; Riebesell 2004; Gruber and Galloway 2008).

Carbonate system

In order to understand the effect of rising atmospheric CO₂ concentrations on seawater chemistry, a fundamental knowledge of the carbonate system is needed.

Because of its solubility and chemical reactivity, CO₂ is taken up by the ocean much more effectively than other anthropogenic gases (e.g. chlorofluorocarbons (CFCs) and CH₄). Since pre-industrial times the world's oceans have absorbed nearly one third of the anthropogenic CO₂ emitted to the atmosphere (Sabine et al. 2004), making it the second largest sink for CO₂ after the atmosphere itself (Houghton et al. 2001).

At the surface ocean, where seawater is in contact with the atmosphere, gases (e.g. CO₂) can dissolve into the water and vice versa. In equilibrium the partial pressure of CO₂ (pCO₂) in the atmosphere equals the partial pressure of CO₂ in the surface ocean, which is related to the concentration of CO₂ by Henry's law:

$$CO_{2(aq)} = \alpha \cdot pCO_2 \quad (1)$$

where α is the solubility coefficient of CO₂ in seawater, which is temperature-, pressure- and salinity-dependent. When CO₂ reacts with seawater, it is hydrated to carbonic acid (H₂CO₃), which subsequently dissociated to

bicarbonate (HCO_3^-), carbonate ion (CO_3^{2-}) and protons (H^+) as shown in Figure 2 (Zeebe and Wolf-Gladrow 2001).

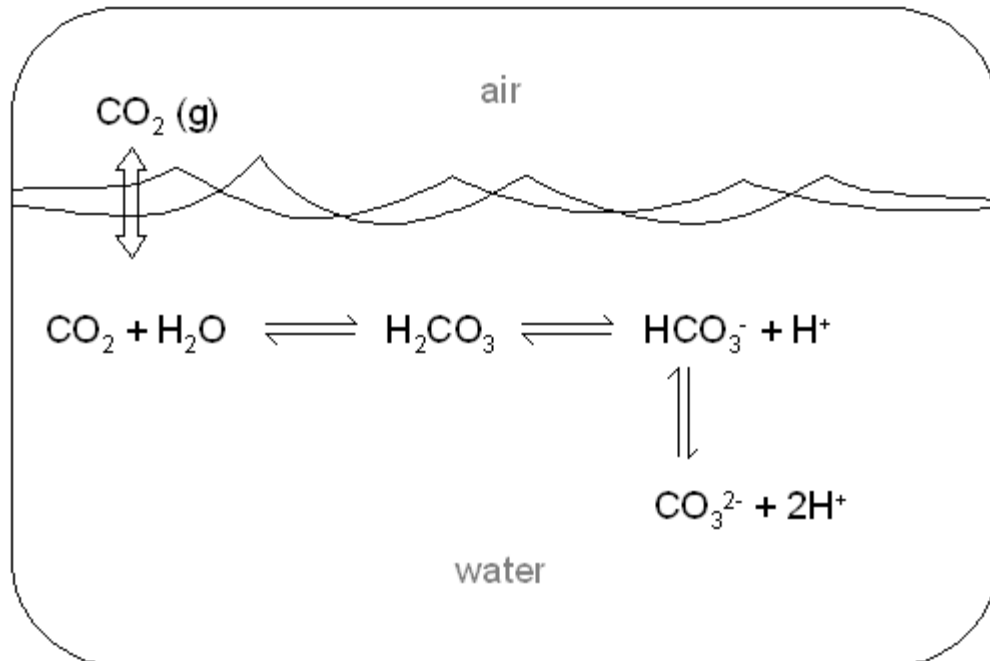


Figure 2: Schematic illustration of the carbonate system in the ocean. CO_2 is exchanged between atmosphere and ocean via equilibration of $\text{CO}_2(\text{g})$ and dissolved CO_2 . Dissolved CO_2 is part of the carbonate system in seawater that includes bicarbonate, HCO_3^- , and carbonate ion, CO_3^{2-} (after Zeebe and Wolf-Gladrow 2001).

The sum of all dissolved forms is called total dissolved inorganic carbon (DIC) and is given by:

$$\text{DIC} = \text{CO}_2 + \text{HCO}_3^- + \text{CO}_3^{2-} \quad (2)$$

A further quantitative parameter for the description of the carbonate system is the alkalinity, which is closely related to the charge balance in seawater. The total alkalinity (T_A) of seawater is a measure of the ability of a solution to neutralize acids to the equivalence point of HCO_3^- or CO_3^{2-} . The T_A consists of various components of seawater:

$$T_A = [HCO_3^-] + 2[CO_3^{2-}] + [B(OH)_4^-] + [OH^-] - [H^+] + \text{minor components} \quad (3)$$

where $[H^+]$ is the free concentration of hydrogen ion (Dickson, 1981).

At a typical surface ocean pH value of 8.2, less than 1% of dissolving CO_2 remains as dissolved CO_2 , while the rest is converted into HCO_3^- (~90%) and CO_3^{2-} (~9%) (Riebesell 2004). Because the pH is the negative decadic logarithm of the hydrogen-ion concentration, increasing atmospheric CO_2 concentrations lead to an increase of H^+ -ion concentration and a decrease of the pH. This acidification causes a shift of the pH-dependent equilibrium of the carbonate system towards higher proportions of CO_2 and lower proportions of CO_3^{2-} . This mechanism is called the buffer capacity of seawater as DIC forming anions react with H^+ -ions and thus buffer the system. Therefore, an invasion of anthropogenic CO_2 leads to an increase of DIC, but does not change T_A , because the charge balance is not affected. A more detailed description is given in Zeebe & Wolf-Gladrow (2001).

The marine carbon cycle

The global carbon cycle is a biogeochemical cycle by which carbon is exchanged between atmosphere, land and oceans of the Earth. The marine carbon cycle refers only to the fate of carbon in the oceans. The cycling of carbon in the marine environment involves both physical and biological processes and is a boundless system of inputs, fluxes, sinks and outputs. It includes the transfer of carbon from the atmosphere to the ocean, the fixation of carbon by phytoplankton, the flux of carbon through the marine food chain and the long-term fate of carbon in the marine environment.

Two of the most common processes involving carbon on land and in water, are utilization and release of CO_2 by photosynthesis and respiration, respectively. Marine biota contain comparatively low amounts of carbon (~3 Gt C) in contrast to terrestrial ecosystems (~500 Gt C plant biomass). However, the annual

amount of photosynthetically fixed carbon of marine primary producers (phytoplankton) is almost as high as of terrestrial biomass (103 Gt C a^{-1} and 120 Gt C a^{-1} , respectively) (Körtzinger 2006).

The marine biosphere operates like a biological pump. In the sunlit uppermost $\sim 100 \text{ m}$ of the ocean (euphotic zone), photosynthesis of phytoplankton serves as a source of oxygen and a sink for CO_2 and nutrients like nitrogen and phosphorous. Using the sunlight as their source of energy for growth, phytoplankton fix CO_2 into organic compounds like sugars. Whenever primary producers have enough DIC and light for photosynthesis the uptake of CO_2 continues, although nutrient concentrations are low. A consequence of this excess assimilation of carbon is extracellular release of organic matter. This release of organic matter is an important source for DOC in the upper ocean. A major fraction of DOC consists of polysaccharides, containing acidic sugars. This sticky organic matter coagulates into particles known as transparent exopolymer particles (TEP). TEP play an important role in aggregation, promoting the sedimentation of particles and thus export of organic and inorganic matter (Engel and Passow 2001; Passow 2002; Engel 2004b; Engel 2004a). The fixation of dissolved inorganic carbon (DIC) via photosynthesis and the vertical flux of particulate organic matter (POM), for example of TEP, dead organisms and/or fecal pellets, into deeper parts of the oceans cause a drawdown of CO_2 in the surface ocean and subsequently a supply of CO_2 from the atmosphere. On its way to the deeper ocean organic matter is either remineralized by bacteria (microbial loop) or it is deposited on and into the sediment. This is called the organic carbon or soft-tissue pump. Hence, the ocean is commonly regarded as a carbon sink.

Contrariwise, a second biological carbon pump, the carbonate carbon pump or hard-tissue pump can be a source of CO_2 for the atmosphere. The formation of particulate inorganic carbon (PIC) involves a net release of CO_2 , which can be used for photosynthesis or is released into the atmosphere. A major source of PIC is calcium carbonate (CaCO_3), which is produced by calcification of for example calcifying algae species. Thus, the carbonate pump refers to the sinking of particulate inorganic carbon (PIC) to the deep ocean. The rain-ratio represents the relative ratio of the two biological carbon pumps (PIC/POC ratio),

thus, the relative importance of inorganic to organic carbon in exported biogenic matter.

An acidification of ocean waters will potentially change the productivity of autotrophic phytoplankton and subsequently affect the efficiency of the biological carbon pump in the future, as recently hypothesized by Riebesell et al. (2007). From this hypothesis follows that the stoichiometric composition of C:N:P may alter in the future. This would subsequently change microbial processes and biogeochemical cycling.

Marine primary production

Several studies have shown that some macroalgae (Gao et al. 1993), diatoms (Riebesell et al. 1993) and cyanobacteria (Qiu and Gao 2002; Barcelos E Ramos et al. 2007) exhibit higher photosynthesis rates under CO₂ enrichment. The overall oceanic primary production was shown to be higher under increased CO₂ concentrations (Hein and Sand-Jensen 1997), influenced by the species composition of phytoplankton assemblages.

Photosynthetic carbon fixation of marine phytoplankton has been reported to be affected by elevated pCO₂ concentrations (Riebesell et al. 1993; Rothschild 1994; Hein and Sand-Jensen 1997; Raven 2003; Leonardos and Geider 2005). The processes of photosynthetic carbon fixation and diazotrophic N₂ fixation are both energy demanding processes. Cyanobacteria have to invest significant amounts of energy to concentrate CO₂ at the site of carboxylation, due to the relatively low affinity of their main carboxylating enzyme RubisCO (Ribulose-1,5-bisphosphate carboxylase/oxygenase) (Tortell 2000). This causes a competition and reduction of energy for other cellular processes, such as protein synthesis and carbon acquisition (Kaplan and Reinhold 1999). In response to increasing CO₂ availability cyanobacteria are known to down-regulate their CO₂ concentrating mechanism (CCM) and allocate energy to other cellular processes (Giordano et al. 2005). Thus, the energetic benefit at

elevated CO_2 may be higher in cyanobacteria compared to other phytoplanktonic groups with RubisCOs characterized by higher CO_2 affinities.

Microbial loop

Within the marine carbon cycle, the microbial loop describe a trophic pathway, where DOM is reintroduced to the food web through the incorporation into bacteria (Azam et al. 1983) (Fig. 3). Bacteria are consumed mostly by protists such as flagellates and ciliates. These protists, in turn, are consumed by larger aquatic organisms (for example small crustaceans like copepods). Thus, the recycling of this organic matter into the food web results in additional energy available to higher trophic levels (e.g. fish). The DOM is introduced into aquatic environments from several sources, such as the leakage of fixed carbon from algal cells or the exudation by microbes. DOM is also produced by the breakdown and dissolution of organic particles. In turn, ~30% of the DOC incorporated into bacteria is respired and released as CO_2 (Stoderegger and Herndl 1998).

Heterotrophic bacteria play a major role in organic matter cycling (e.g. Cole et al. 1988; Azam 1998; Azam and Malfatti 2007). Their dynamics and activities depend on the availability of DOM either in form of monomeric substances or dissolved free amino acids, which can directly transferred into the cell (Chrost 1991). This directly utilizable DOM limits the growth rate and metabolism of heterotrophic bacteria. However, the majority (>95%) of organic matter in aquatic ecosystems is composed of polymeric, high molecular weight (HMW) compounds, like polysaccharides, proteins, lipids etc., which means that only a small portion of total DOM is readily utilizable in natural waters (Muenster 1985; Jorgensen 1987). Various aquatic microorganisms are able to efficiently utilize polymeric DOM by enzymatic hydrolysis (Hoppe 1983; Chrost et al. 1989).

The efficiency of the microbial loop can be determined by bacterial incorporation of radiolabeled substrates like ^3H -thymidine (Fuhrman and Azam 1982; Kirchman et al. 1982), and ^3H -leucine (Simon and Azam 1989).

How to study the effects of rising CO₂ concentration on marine environments?

There are several possibilities to study the effects of rising CO₂ concentration on marine environments.

Perturbation studies can be conducted on a laboratory scale for example in batch cultures or in chemostat systems. Batch cultures are determined by the starting conditions and follow their own dynamic thereafter (e.g. Barcelos E Ramos et al. 2007). The chemostat is an open system, in which organisms can be grown continuously in a well defined physiological state (e.g. Sciandra et al. 2003; e.g. Koch 2007). While laboratory investigations and bottle incubation experiments on small scales have the advantage of being easier to handle, the dynamics of a natural environment with interactions e.g. on trophic levels are not well simulated. Field studies with respect to rising CO₂ concentrations were conducted in mesocosm experiments (Engel et al. 2005; Grossart et al. 2006; Riebesell et al. 2007). The use of mesocosms allows to study ecosystems under semi-natural conditions in large bodies of sea-water from a few hundred litres to dozens of cubic meters including all its organisms. Until recently, mesocosms were only deployed close to the coast within protected areas. Newly developed free-floating offshore mesocosms can be used in open waters with the advantage of e.g. covering natural light and temperature variability and different kinds of environments.

Ecosystem models are a useful and important tool to predict the patterns of carbon flux, primarily regarding to potential consequences of climate change (Falkowski et al. 2000; Gruber and Galloway 2008). Numerous simulations of coupled atmosphere-ocean global climate models (GCMs) or biogeochemical models has been carried out, including projections into the 21st century. But most models do not include microbial processes on organism level, mainly, due to our limited knowledge of the factors and processes that determine the abundance, distribution and activities of key groups of marine organisms. These

uncertainties affect our ability to predict specific responses (Falkowski et al. 2000), for example, to ocean acidification. The impact of microorganisms on biogeochemical cycles must be addressed on nanometre (molecular) to millimetre scale to make useful predictions of how marine ecosystems in the ocean may respond to global change (Azam and Malfatti 2007).

This study

In the Baltic Sea, N₂ fixation by diazotrophic cyanobacteria is an important factor that determines overall growth and biomass of autotrophic plankton and, thereby, primary production. As in most other marine environments, phytoplankton blooms in the Baltic Sea are controlled by nitrogen (N₂) (Graneli et al. 1990; Tamminen 1995). The advantage of diazotrophic cyanobacteria is the capability of using atmospheric N₂ as their sole source of nitrogen (Niemi 1979). Blooms of diazotrophic cyanobacteria mainly consist of small-sized picocyanobacteria (*Synechococcus spp.*) and larger, colony-forming, filamentous, heterocystous, N₂ fixing cyanobacteria (*Nodularia spumigena*, *Aphanizomenon flos-aquae* and *Anabaena spp.*) (Stal et al. 2003). During summer in the Baltic Sea, in areas where the N:P ratio is below the Redfield ratio of 16, blooms of diazotrophic cyanobacteria develop. But not only the N:P ratio is an important factor, an adequate concentration of both elements is essential for bloom formation (De Nobel 1997).

In this study offshore mesocosms were used to investigate the impact of rising pCO₂ concentration on a natural plankton community in the Baltic Sea.

Recent studies revealed that oceanic primary production increases with rising CO₂ (Fig. 3) (Hein and Sand-Jensen 1997). An acidification of ocean waters will potentially change the productivity of autotrophic phytoplankton and subsequently the efficiency of the biological carbon pump in the future. From a biogeochemical point of view the elemental composition of C:N:P will change, and subsequently alter biogeochemical cycling and vertical export of organic and inorganic matter (Riebesell et al. 2007). This will affect the recycling of

organic matter within the microbial loop. Linked to phytoplankton, an increase of the availability of DOM will increase heterotrophic bacterial activity and productivity, and therefore growth and/or abundance (Grossart et al. 2006). Preliminary studies indicate that enzyme efficiencies decrease with decreasing pH (Piontek et al. 2007a; Piontek et al. 2007b; Lunau et al. 2008).

In order to reliably predict consequences of ocean acidification on microbial dynamics and activities, there is a great necessity for repeated studies under controlled environmental conditions.

In this study rising pCO₂ concentrations were simulated in offshore mesocosms by the addition of hydrochloric acid. Low concentrations of Chlorophyll *a* and low primary production revealed a non-bloom situation. Our study shows that acidification of Baltic Sea water led to a loss of POC over time. The perturbation by hydrochloric acid induced a community shift from eukaryotes to prokaryotes. However, in contrast to hydrolytic enzyme efficiencies, microbial uptake rates of DOM were not influenced by the acid treatment. Autotrophic unicellular cyanobacteria outcompeted heterotrophic bacteria under strong acidic conditions.

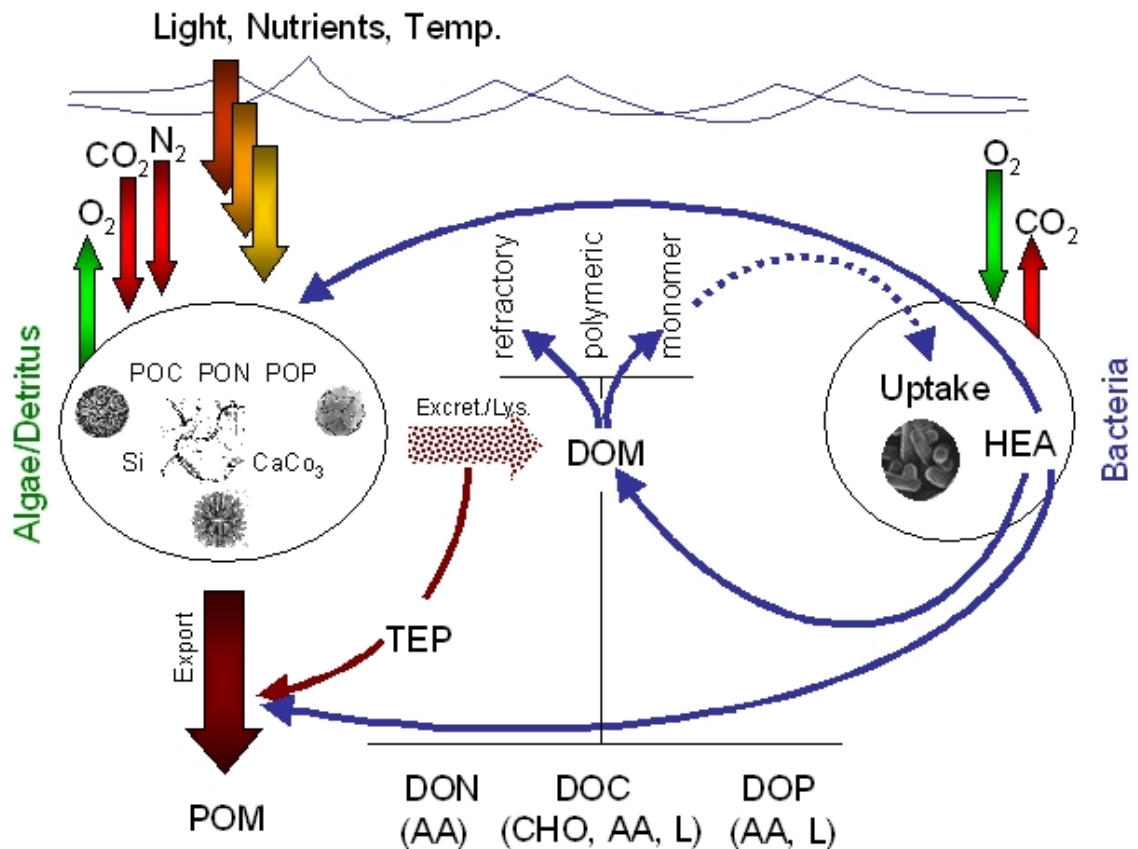


Figure 3: Cycling of organic matter and microbial loop. Interplay between light, nutrients, temperature, primary production of phytoplankton (carbon dioxide (CO_2) uptake, nitrogen (N_2) fixation), respiration of oxygen (O_2), export of particulate organic matter (POM), release of dissolved organic matter (DOM) and bacterial degradation processes of DOM & POM (hydrolytic enzyme activity (HEA), and uptake of monomeric DOM). The DOM pool consists of dissolved organic nitrogen (DON, mainly amino acids (AA)), dissolved organic carbon (DOC, mainly carbohydrates (CHO), AA, and lipids (L)) and dissolved organic phosphorous (DOP). Transparent Exopolymer Particles (TEP) form from DOM precursors and subsequently promote sedimentation and export of POM. The POM pool consists of particulate organic carbon (POC), particulate organic nitrogen (PON) and particulate organic phosphorous (POP) (M. Lunau, AWI Bremerhaven).

2 Materials and methods

In this study we measured the effect of Baltic Sea acidification on microbial dynamics and activities. Offshore mesocosms were used to simulate different levels of carbon dioxide partial pressure ($p\text{CO}_2$). This work was done in the frame of the project SOPRAN (Surface Ocean PRocesses in the ANthropocene).

Setup and sampling

The offshore mesocosm experiment was carried out during a research cruise with the RV Alkor (AL-302) and the RV Heincke (HE-273) in the Baltic Sea in July 2007. The experimental system was designed by the IFM-GEOMAR. Briefly, the KOSMOS (Kiel Off-Shore Mesocosms for future Ocean Simulations), constructed by the TLZ (Technik- und Logistikzentrum) of the IFM-GEOMAR, facilitate the use of free-drifting mesocosms offshore.

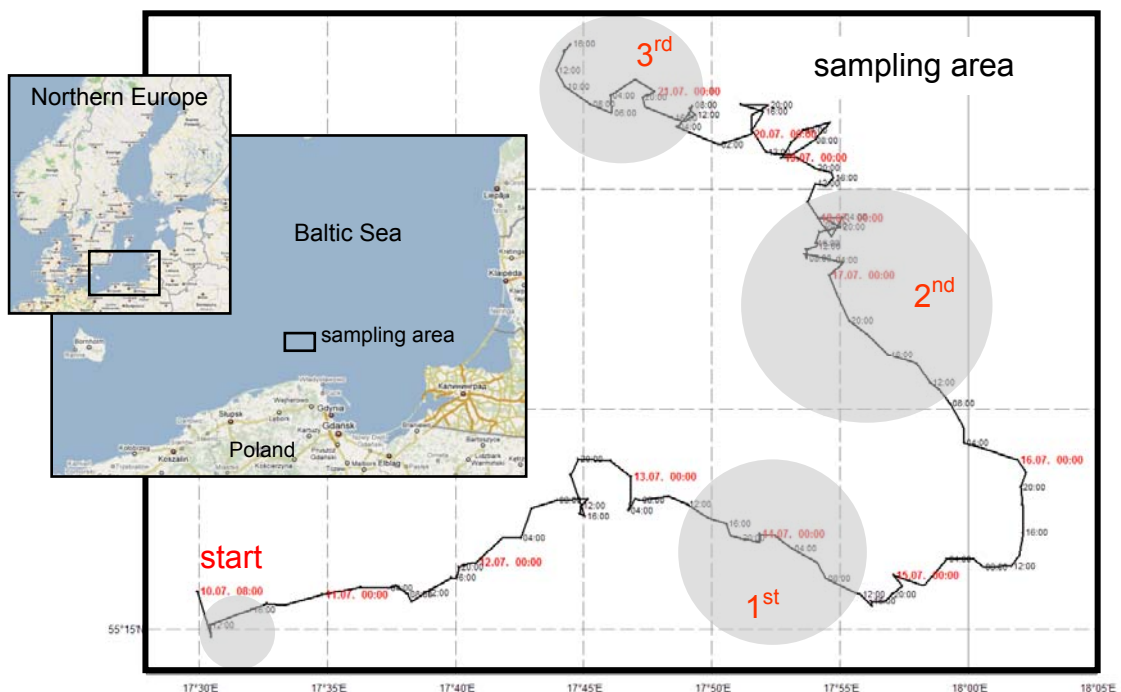


Figure 4: Map of northern Europe (inset) and of the Baltic Sea including the sampling area (map source: google.maps); Drift of the mesocosms during the experiment (11 days, modified after Dr. K. von Bröckel, IFM-GEOMAR)

Section 2: Material and methods

The sampling area is shown in Figure 4. The six mesocosms were launched at the 10th of July and then connected to each other by tampen. They were taken back on board RV Alkor at the 21st of July just before a storm came up. Throughout the 11 days of the experiment, the mesocosms drifted approx. 55 nautical miles (nm) along a transect between 55°15'N, 17°30'E and 55°17'N, 18°02'E and 55°29'N, 17°45'E as shown in Figure 4.

Six mesocosms (ca. 60 m³, diameter of 2 m, 20 m water depth) were used with six different pCO₂ levels to simulate a large CO₂ gradient. Different amounts of HCl (3.75 M) in a range of 0 – 110 µmol were added to acidify the water masses in the mesocosms by using a mixing spindle.

Due to the weather conditions five mesocosms were acidified three times. At the 10th of July reference measurements of all mesocosms were performed before the first HCl-treatment of the mesocosms to determine how equal the enclosed water masses were. Initial values of all parameter can be found in Table 2 in the appendix. Mesocosm 4 was used as a reference during the experiment, since it was not treated.

The first acidification was performed at the 13th of July at 12 am. The six mesocosms were sampled at two times: 6 hours and 24 hours after the acidification. The second acidification was performed at the 16th of July at 11 am. Three days after the first acidification the five mesocosms were already conditioned with HCl. The mesocosms were sampled at two times, 6 h and 25 h after acidification. The sampling frequency for three mesocosms was increased as a result of the fast changes observed after the first acidification. Thus, mesocosm 2, 4 and 5 were additionally sampled at 18.5 h, 21.5 h, 29.5 h, 33 h and 42.5 h after acidification. The third acidification was performed at the 20th of July at 10 am. Due to the breakage of three mesocosms (1, 3 and 4) during a storm beforehand just three mesocosms (2, 5 and 6) were acidified. The Baltic was used as an alternate reference, as the untreated control mesocosm 4 was out of order. Sampling was performed at 2.5 h, 4.75 h, 6.5 h, 10 h, 18 h, 22 h and 25.5 h after the third acidification.

Integrated water samples of the upper 10 m of the water column were taken out of each mesocosm during calm weather from a zodiac by using a pressure controlled sampling device (Hydrobios, Kiel). The samples were directly transferred into 250 ml Polyethylene (PE)- bottles and brought on board ship for further treatment as soon as possible.

Measurements and analyses

Physicochemical parameters

Nautical, meteorological and ship-specific data were monitored by the ship's data distribution system 'DATADIS' (Böning Automationstechnologie GmbH & Co. KG, Ganderkesee, Germany). Conductivity, temperature and depth (CTD) as well as salinity and pH measurements were conducted daily (unless the weather conditions did not allow measurements for safety reasons) by K. Schulz (IFM-GEOMAR, Kiel, unpublished data). Furthermore, pCO₂ values were calculated from pH and alkalinity. On the basis of no more than one pH measurement per day, pH values for sampling times were calculated. A linear development between two or three measured pH values were presumed and the slope of the linear regression was used for calculation. In addition pCO₂ concentrations were calculated using the function of pH (CTD) and calculated pCO₂ for all sampling times.

Distinct pCO₂ measurements were maintained less frequently using a CO₂/H₂O analyzer LI-6262 (LI-COR Biosciences) by R. Schmidt (Baltic Sea Research Institute, Warnemünde, unpublished data).

Biogeochemical parameters

POC and PON were analyzed with a C/N analyzer (CHN-O-rapid) by M.Voss (Baltic Sea Research Institute, Warnemünde). Concentrations of particulate

organic phosphorous (POP) were analyzed by K. Isensee (Baltic Sea Research Institute, Warnemünde). POP concentrations were determined by alkaline sulphate oxidation according to Koroleff & Grasshoff (1983). Concentrations of Chlorophyll *a* (Chl *a*) and nutrients were analyzed by P. Fritsche (IFM-Geomar, Kiel) following standard procedures.

Amino acids

Subsamples for dissolved free amino acids (DFAA) and total hydrolysable dissolved amino acids (THDAA) were filtered on board through 0.45 µm TUFFRYN® membrane filters (Acrodisc, Whatman) und kept frozen for three weeks at -20°C until analysis in the lab. Concentrations of DFAA and THDAA were analysed by high performance liquid chromatography (HPLC) after pre-column derivatization with ortho-phthaldialdehyde (OPA) (Lindroth and Mopper 1979). Chromatographic separation method was carried out with an Agilent HPLC-device (1100 Series) using an Alltima reverse-phase column (C-18, 5 µm, 250 mm, Alltech) in combination with an Analytical Guard (Agilent) precolumn. The detection of dye-labelled amino acids (OPA derivatization) was performed by a fluorescence detector (extinction: 342 nm, emission: 440 nm).

Section 2: Material and methods

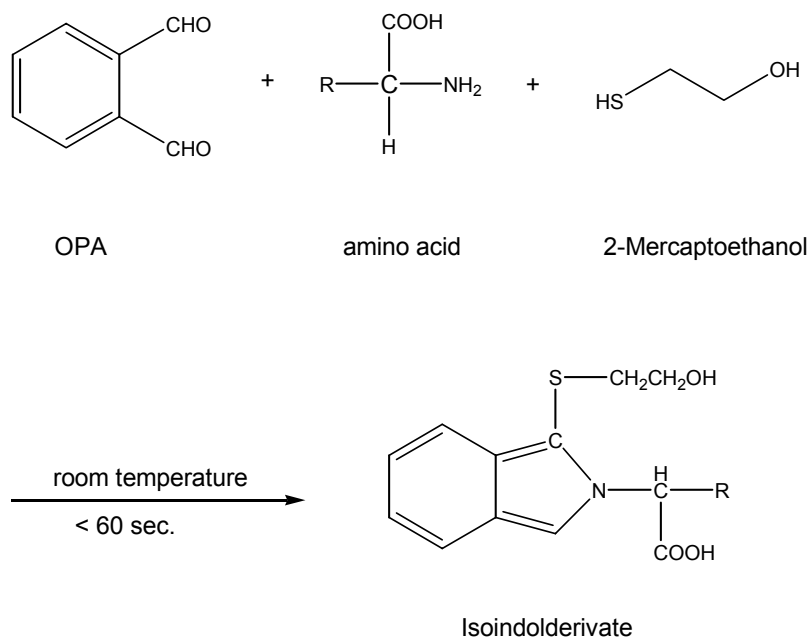


Figure 5: Reaction scheme of the ortho-phthalaldehyde (OPA) derivatization.

The DFAA were measured directly after addition of the internal standard α -amino butyric acid (α -ABA, final concentration of 30 nM). Prior to injection, the sample was derivatized with OPA (Fig. 5) and the reaction was stopped by adding glacial acetic acid (pH <5 after addition).

The THDAA were analysed as DFAA after hydrolysis with 6N HCl at 155°C for one hour in glass ampoules, sealed under nitrogen. Before hydrolysis 500 μ l of unfiltered subsamples were spiked with the internal standard (α -ABA, final concentration of 100 nM) and ascorbic acid (10 μ g ml⁻¹ final concentration) was added to prevent oxidation of amino acids by nitrate. Prior to analysis 500 μ l of the hydrolysed samples were neutralised with 6N NaOH and diluted by double-distilled water to a final dilution of 1:4.

An external standard (Agilent amino acid standard spiked with α -ABA, glutamine (GLN) and asparagine (ASN)) was used to identify and quantify the amino acids. Response factors of the amino acids related to α -ABA were calculated.

The concentration of dissolved combined amino acids (DCAA) was calculated by subtracting the DFAA from the THDAA.

Transparent Exopolymer Particles

Transparent Exopolymer Particles (TEP) were determined colorimetrically according to the method described by Passow & Alldredge (1995). Briefly, subsamples of 30 ml were filtered gently at low, constant vacuum (<200 Hg) onto polycarbonate filters (0.45 µm Nuclepore, Whatman). TEP were stained for three seconds with 1 ml of a 0.02% aqueous solution of the polysaccharide-specific dye alcian blue in 0.06% acetic acid (pH 2.5). Before use, the staining solution was filtered (0.2 µm) to avoid particles in the dye solution. After staining, the filters were rinsed with deionised water to remove excess dye. All filters were prepared in triplicates and stored at -20°C until analysis within 2 months.

Due to reaggregation processes and prefiltration, the dye content of staining solutions decreases with age. Therefore, a calibration of the staining solution was necessary to compare samples measured with different batches of staining solution. The calibration factor was determined by relating dry weight measurements of Gum Xanthan particles retained on filters to their staining capacity as described by Passow and Alldredge (1995) according to equation 4.

$$calibration\ factor = \frac{dry\ weight_{standard} [\mu g\ l^{-1}]}{\left((absorption_{average} - absorption_{blank}) * filtered\ volume [l]^{-1} \right)} \quad (4)$$

Dry weights of a calibration standard solution, prepared by mixing ~ 15 mg of Gum Xanthan with 200 ml deionised water and grinding step by step into TEP-sized particles, were examined by filtering 0.5 – 2 ml aliquots onto preweighed filters. The filters were dried at 60°C overnight and stored in a desiccator. Alcian blue stainable particles were measured by filtering 0.5 – 2 ml of the calibration standard and staining as described above. The calculated calibration factor for this study was 33.33.

The stain bonded to particles present in the samples was extracted by soaking the filters in 6 ml of 80% sulphuric acid (H₂SO₄) for 2 h. The absorption of dye-

labelled TEP was measured at 787 nm against deionised water with an UV-vis. spectrophotometer (Shimadzu UV-1700 PharmaSpec).

Concentration of TEP was expressed in Gum Xanthan equivalents [$\mu\text{g l}^{-1}$] and was determined from equation 5.

$$TEP_{conc.} = (absorption_{sample} - absorption_{blank}) * filtered\ volume\ [l] * calibration\ factor\ [\mu\text{g}] \quad (5)$$

Plankton abundances

Abundances of unicellular cyanobacteria, nano- and picoplankton (diatoms and green algae) were analyzed by H. Johansen and A. Grützmüller (Baltic Sea Research Institute, Warnemünde) using Flow Cytometry following standard procedures. Eukaryotic phytoplankton abundances were calculated by the sum of nano- and picoplankton.

Diazotrophic cyanobacteria dynamics

Abundances of diazotrophic bacteria were analyzed by K. Haynert (Baltic Sea Research Institute, Warnemünde) using fluorescence microscopy. Abundances of *Nodularia* spp. and *Aphanizomenon* spp. are given in units l^{-1} , whereas one unit is equivalent to 100 μm .

Phytoplankton activity

Autotrophic production rates of organisms larger and smaller than 10 μm were analyzed by M. Voss (Baltic Sea Research Institute, Warnemünde). Nitrogen (N_2) fixation and CO_2 uptake were measured using ^{13}C labelled bicarbonate solution and $^{15}\text{N}_2$ enriched gas according to the method described by Montoya et al. (1996). A more detailed description is given in Voss et al. (2006). The

incubations of the samples were conducted with about 75% light intensity and incubations times ranged from 3.5 to 8 h depending on the time of the day (light).

Bacterial dynamics

Subsamples for bacterial cell counts were preserved with two different fixations: glutardialdehyde (GDA, AppliChem; final concentration of 1.1%) and Dekafald (contained DMDM Hydantonin and less than 1% formaldehyde, Jan Dekker Nederland B.V., Netherlands; final concentration of 4.4%). For each preservative, duplicates were prepared and stored at -20°C until further analysis. Samples were analyzed by flow cytometry (FACSCalibur, Beckton Dickinson, USA) within 2 months. All the cytometrical analyses were done following exactly the same protocol, keeping all settings constant.

Prior to analyses nucleic acid was stained by SybrGreen I (SG1) and SybrGreen II (SG2) (Invitrogen, Karlsruhe, Germany). Each dye working solution was prepared freshly every day by diluting the stock solution (10000x) 1:40 with dimethyl sulfoxide (DMSO, Sigma), followed by a 1:40 dilution with the sample (final dilution 10^{-3} , final concentration 6.25x). As an internal standard yellow-green fluorescent latex beads (0.94 μm diameter, Polyscience, USA) were used for the volume normalization of counted events. TruCount beads (Beckton Dickinson) were used for daily intercalibration according to del Giorgio et al. (1996) and Gasol & del Giorgio (2000).

The instrument was equipped with an air cooled argon laser (15 mW, Ex. 488 nm). Green fluorescence intensity (GFL) was detected with the standard filter setup (Em. 530 +/- 15 nm) as fluorescence 1 (FL1). Photomultiplier voltages were adjusted so that the bacterial populations were centered in the channels corresponding to the second and third logarithmic decade for fluorescence and the second decade for sidescatter (SSC). Analyses were performed at the lowest flow rate (approx. 14 $\mu\text{l min}^{-1}$). Event range was between 300 and 900 sec^{-1} . A threshold for FL1 was set in order to remove

background noise and to enhance processing speed. Manual gating was used after visual inspection of the dot plot of SSC vs. FL1 to define a region of interest.

Data were stored as list-mode files and subsequently displayed and calculated either with CellQuest software version 3.3 or WinMDI (version 2.8; J. Trotter, The Scripps Institute, Flow Cytometry Core Facility, La Jolla, USA).

Hydrolytic enzyme activities

Rates of hydrolytic enzyme activities were determined by kinetic measurements using 4-methylumbelliferyl (MUF) and 7-amino-4-methylcoumarin (AMC) labelled substrate analogues. Model substrate initial stock solutions (5 mM) of MUF- α -D-glucoside, MUF-phosphate and L-Leucine-AMC were prepared according to Table 1. Please note, that all solutions have always to be kept in the dark (Hoppe, 1983).

Table 1: Solubility of 4-methylumbelliferyl (MUF)- α -D-glucoside, MUF- phosphate and L-Leucine 7-amino-4-methylcoumarin (AMC).

substrate analogue	solubility			
	Hoppe et al. (1983)	Chrost et al. (1989)	Chrost et al. (2006)	this study
MUF α -D-glucoside	Methylcellosolve			Methylcellosolve
MUF phosphate	Methylcellosolve	H ₂ O	H ₂ O	H ₂ O (deionised)
L-Leucine AMC	Methylcellosolve	H ₂ O	Ethanol 96%	Ethanol 96%

For this study kinetics of α -glucosidase, phosphatase and leucine-aminopeptidase were analyzed. A complete list of substrate analogues tested in this experiment can be found in the appendix.

A set of five different concentrations for each substrate analogue (156.25, 312.50, 625, 1250, 2500 μ M) were prepared by dilution of the initial stock solutions with sterile deionised H₂O. These stock solutions were kept at -30°C less than two weeks. Prior to our experiment 96-well plates were prepared, allowing numerous replicates and high sample throughput. Aliquots of each

Section 2: Material and methods

substrate analogue (20 μ l) and of each concentration in triplicates were pipetted into 96-well plates. These prepared 96-well plates were kept frozen, until kinetic measurements were conducted.

Subsamples of 230 μ l of the six mesocosms were transferred into the prepared wells of the plate immediately after sampling. A multichannel pipette was used to fasten this procedure. Thus, final concentrations of substrate solutions were 12.5, 25, 50, 100 and 200 μ M. Initial fluorescence (t_0) was measured shortly after the addition of samples to the substrate analogue aliquots by using a microplate reader (BMG Labtech FLUOstar OPTIMA, Germany), which is equipped with a xenon flash lamp. Excitation and emission filters were adjusted to the fluorochrome characteristics (355 and 460 nm, respectively). Incubations were performed for 1h at *in situ* temperature in the dark. The amount of measured fluorescence intensity is proportional to the amount of hydrolyzed substrate analogue. The difference between the start-stop measurement is needed to calculate the maximal velocity (V_{max}) and the half saturation constant (K_m).

Because the intensity of fluorescence is influenced by pH, calibration curves of MUF and AMC solutions with different pH were determined. In order to correct the fluorescence intensity change due to different pH levels in the samples, a calibration factor is necessary. MUF- and AMC- solutions (solved in sterile, deionised H₂O) were prepared in four different concentrations (final 0.156, 0.325, 1.25 and 2.5 μ M). The initial stock solutions of MUF and AMC were diluted in 50mM MOPS buffer solutions with six different pH values (6.5, 7, 7.5, 8, 8.5 and 9). The fluorescence intensities were measured in 96-well plates as described above. The calibration factor was determined by relating the different MUF respectively AMC concentrations to the obtained fluorescence intensities. In respect to different pH, this relationship was characterized by different slopes. For calculation of the pH-corrected fluorescence intensities a polynomial fit was used to relate the slopes to pH. The equations of the polynomial fit were used for correction.

Enzyme efficiency (V_{max}/K_m) was calculated from hyperbolic fitting of kinetic measurements using the corrected fluorescence intensities. Kinetics of the five different concentrations were calculated (simple ligand binding, one site saturation) for the three replicates and for t_0 and t_1 separately, using the software SigmaPlot (Version 10.0, Systat Software, Inc., Germany). The mean of the fits of the three replicates were calculated for t_0 and t_1 . V_{max} and K_m of the averaged difference of t_1 and t_0 was calculated again as described above.

Turnover rates of the substrate analogues at non saturating concentrations (1.56 μM) were taken from this fit.

Bacterial activities

Rates of leucine uptake were determined by incorporation of $^3\text{[H]}$ -leucine (^3H -Leu) and thymidine uptake by incorporation of $^3\text{[H]}$ -thymidine (^3H -TdR), roughly followed the protocols described by Simon & Azam (1989) and Fuhrman & Azam (1982), respectively. Triplicate 1.5 ml samples and a pre-fixed blank were incubated at *in situ* temperature in the dark for 1 h: one set was amended with ^3H -Leu (5.29×10^{12} Bq mmol^{-1} ; (Moravek Biochemicals, Inc., California, USA)) at a final concentration of 80 nM and a second set received ^3H -TdR (2.52×10^{12} Bq mmol^{-1} ; (Moravek Biochemicals, Inc., California, USA)) at a final concentration of 80 nM. Incubations were stopped by adding formaldehyde buffered with 4% (v/v) boric acid. After 15 min of fixation, samples were centrifuged with $\text{RCF} = 6240 \times g$ at 4°C for 10 min and the supernatants were gently removed by suction. Pellets were resuspended in ice-cold 5% trichloroacetic acid (TCA). Thereafter, samples were centrifuged at 4°C for 10 min and aspirated again. Only the samples of the first set (^3H -Leu incorporation) were additionally washed with 1.5 ml of 80% ethanol, centrifuged at 4°C for 10 min and aspirated again. Finally samples were dissolved in 1.5 ml scintillation cocktail (Ultima Gold, PerkinElmer) and kept refrigerated until radio-assay analysis using a TriCarb (1600 TR) liquid scintillation counter within four weeks.

Calculation of growth rates

Growth rates of unicellular cyanobacteria and heterotrophic bacteria were calculated by using the following equation:

$$\text{growth rate } (t_0, t) = \left(\frac{A(t)}{A(t_0)} \right)^{\frac{1}{N}} - 1 \quad (6)$$

where $N = t - t_0$ is the number of time units between t_0 and t , and A is the parameter at the certain time t .

Statistical Analyses

Statistical analyses were performed with the software SigmaStat version 3.5 (Systat Software, Inc., Germany).

3 Results

Experimental boundary conditions

The experiment was conducted from 10th until 21st of July 2007. The discontinuance of sampling as shown in Figure 6 was due to the weather conditions. Sampling of the mesocosms was impossible as result of mean wind speed of 7.7 m/s (4 Bft), with maximums up to 12-15 m/s, and wave heights up to 2.5-3 m. Above wave heights of 1.5 m (at 4 Bft, wind speed 5-8 m/s) the water of the mesocosms exchanged occasionally with surrounding Baltic Sea water. At wave heights above 2.5 m the mesocosms became instable and bounced for- and backwards, thus water exchanged frequently. In this work equal water exchanged is assumed for all mesocosms. Throughout the entire experiment the water temperature of the Baltic increased from ~12°C to ~17°C. The mesocosms were acidified three times due to the boundary conditions.

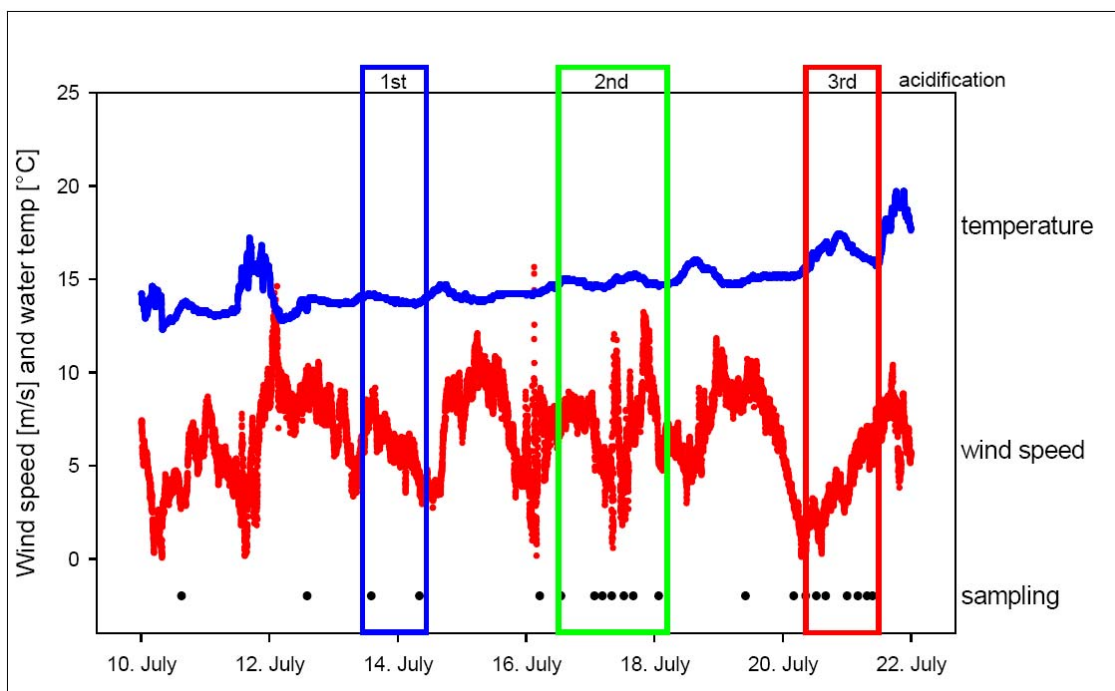


Figure 6: Boundary conditions in the Baltic Sea in July 2007: Water temperature (°C) (blue line) of the Baltic and wind speed (m/s)(red line). Sampling frequency of mesocosms is marked with black dots. Acidification events are highlighted by boxes.

Vertical distributions (CTD measurements)

We focused on the upper 10 m of the mesocosms, which were sampled by an integrating sampler. The vertical distributions of water temperature, salinity, pCO₂ and pH are given in the following.

Temperature

At the start of the experiments at the 10th of July, before acidification at all, the water temperatures in the mesocosms differed in the upper 4 m considerably (Fig. 7, A). Compared to the Baltic, in the mesocosms the water temperatures of the surface layer (~1 m) were about 1 to 1.5°C warmer, whereas from 4 m down to 17.5 m only slight differences were observed. After the 1st acidification mean water temperatures down to 10 m were approx. 1°C warmer than mean temperatures at the 10th of July (Fig. 7, B). In the upper 3 m water temperatures were about 1°C warmer. The Baltic differed from the mesocosms in the surface layer (~1 m) by 0.5°C. A thermocline established at about 10 m depth in the Baltic, whereas water temperatures in the mesocosms decreased slowly from 13.5 to 12.5°C from 10 to 17.5 m. After the 2nd acidification the decrease of the water temperatures with depth was almost linear from 15°C in the surface layer to 14°C at 10 m depth in the mesocosms (Fig. 7, C). The Baltic water was about 0.2°C warmer and followed the same trend down to 10 m. A thermocline was observed in the Baltic but not in the mesocosms. However, mean water temperatures were slightly higher after the 2nd acidification.

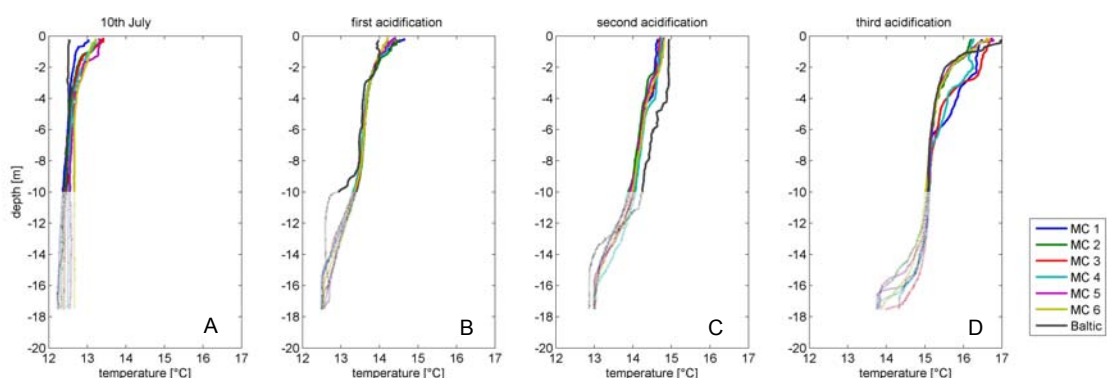


Figure 7: Comparisons of the vertical distribution of water temperatures in the mesocosms (MC) 1 - 6 and in the Baltic before (A) and after the acidifications (B, C, D) (solid lines: 0 - 10 m, dotted lines: 10 - 17.5 m) (data, K. Schulz).

During the experiment a maximum water temperature of more than 17°C was observed in the surface layer of the Baltic after the third acidification (Fig. 7, D). The changes of water temperatures with depth were more variable for mesocosms (MCs) 1, 3 and 4, especially in the upper 6 m, since these mesocosms were broken prior to the 3rd acidification and were not acidified again. Water temperatures of the Baltic and of the remaining MCs 2, 5 and 6 were almost 2°C warmer in the upper 2 m than water temperatures from 2 to 10 m and did not differ from each other.

The increase of water temperatures in the upper 10 m during the experiment was observed in all mesocosms as well as in the Baltic (Fig. 8). The differences in the mesocosms between the 10th of July and the 1st acidification were almost equal. After the 2nd acidification water temperatures in the surface layer did not increase as much as before, whereas after the 3rd acidification the water temperatures in the upper 2 m showed huge variability.

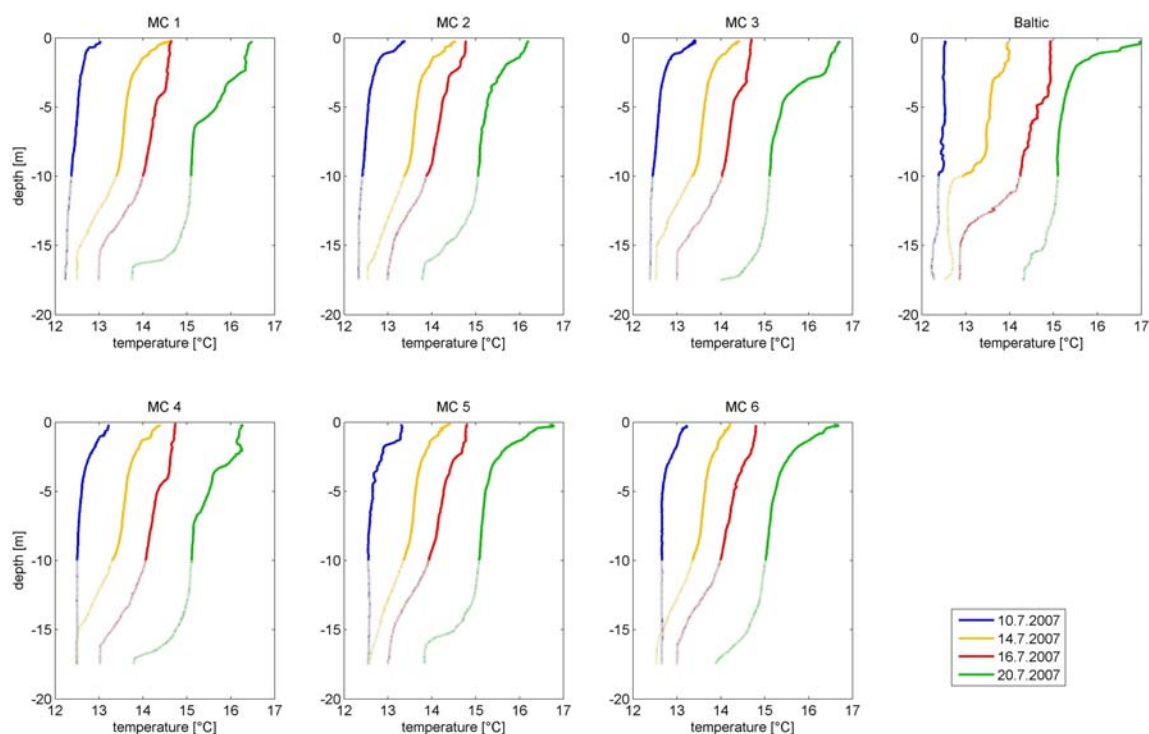


Figure 8 : Vertical profiles of water temperature in the mesocosms (MC) 1 - 6 and in the Baltic for 10th July (blue), 14th July (yellow), 16th July (red) and 20th July (green). (solid lines: 0 - 10 m, dotted lines: 10 - 17.5 m) (data, K. Schulz)

Salinity

Salinity showed mean values of ~7.5 psu in the upper 10 m in all mesocosms and in the Baltic at the 10th of July (blue lines, Fig. 9). The salinity varied about 0.1 psu at the surface layers. A decrease of salinity was observed after 4 - 6 days, during the 1st and 2nd acidification (yellow and red lines). In the Baltic the decrease was about 0.1 psu, while it varied between the mesocosms. However, it was not more than +/- 0.05 psu. After the 3rd acidification (green lines) the vertical distribution of the salinity differed immensely. Compared to the Baltic (~7.4 psu, surface layer varied), the salinity of the remaining three mesocosms (MC 2, 5 and 6) decreased with depth and varied from each other. In mesocosms 2 and 6 the salinity was higher after the 3rd acidification compared to the 1st and 2nd acidification and followed an increasing trend from surface to 10 m. The salinity in MC 5 further decreased to surface value of ~7.4 psu and followed an increasing trend down to 10 m depth. Since Mcs 1, 3, and 4 were broken prior to the 3rd acidification and not acidified a third time, the mean salinity equalled Baltic Sea values.

Salinity measurements reveal that below 10 m an inflow of surrounding seawater occurred in almost all mesocosms due to broken bottoms.

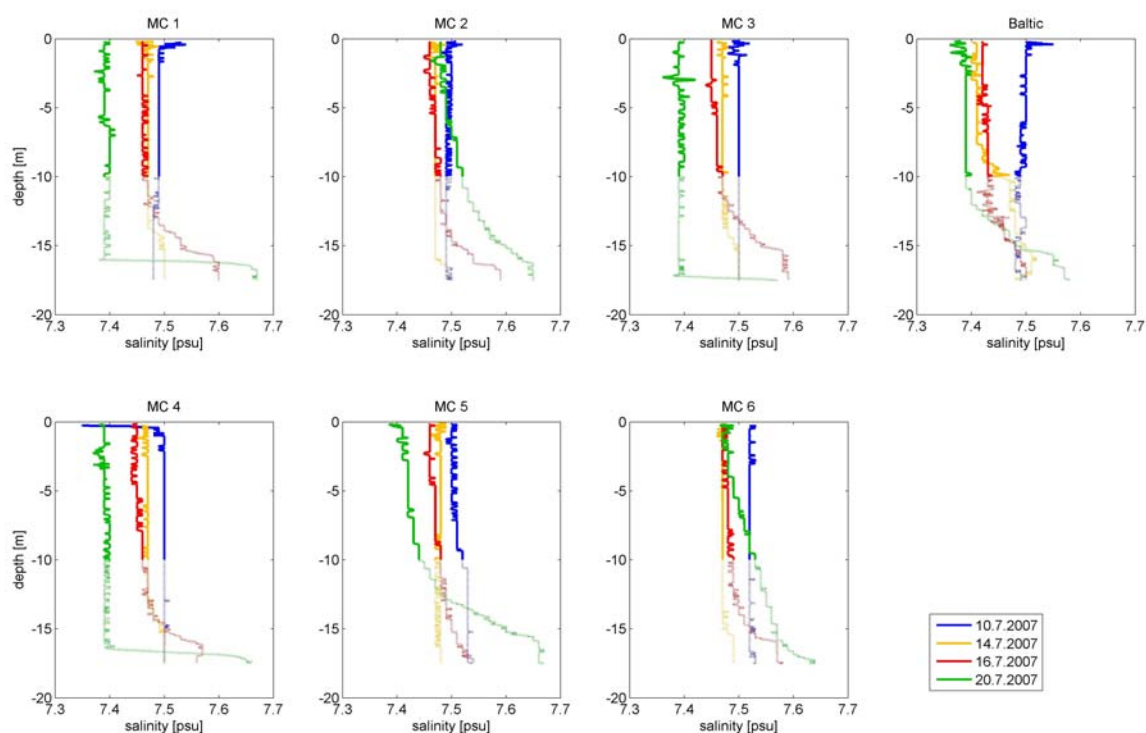


Figure 9: Vertical profiles of salinity in the mesocosms (MC) 1 - 6 and in the Baltic for 10th July (blue), 14th July (yellow), 16th July (red) and 20th July (green). (solid lines: 0 - 10 m, dotted lines: 10 - 17.5 m) (data, K. Schulz)

pH and pCO₂

The variability of the vertical distribution of the experimental elevated pCO₂ concentrations in the mesocosms was related with the overall amount of added HCl (Fig. 10). The higher the amount of HCl (respectively the concentration of pCO₂), the higher were vertical heterogeneities. After the 1st acidification (yellow line) the vertical distribution of the pCO₂ in the upper 10 m did not vary much in MCs 2 and 6, but were differently enhanced compared to the reference measurements at the 10th of July. The higher the pCO₂ concentration the higher was the vertical variability in MCs 1, 3, and 5 after the 1st acidification. After the 2nd acidification (red line, Fig. 10) the vertical variability was even stronger in

MC 1, 3, and 5 than after the 1st acidification. The importance of the vertical variability was underlined in MC 1 in the upper 10 m of the 2nd acidification, where pCO₂ values range from 1100 µatm up to a maximum of more than 3000 µatm.

After the 3rd acidification (green line, Fig. 10) the vertical distribution of pCO₂ in the remaining MCs 2, 5 and 6 was consistent. The pCO₂ concentrations were differently enhanced compared to the reference measurements at the 10th of July.

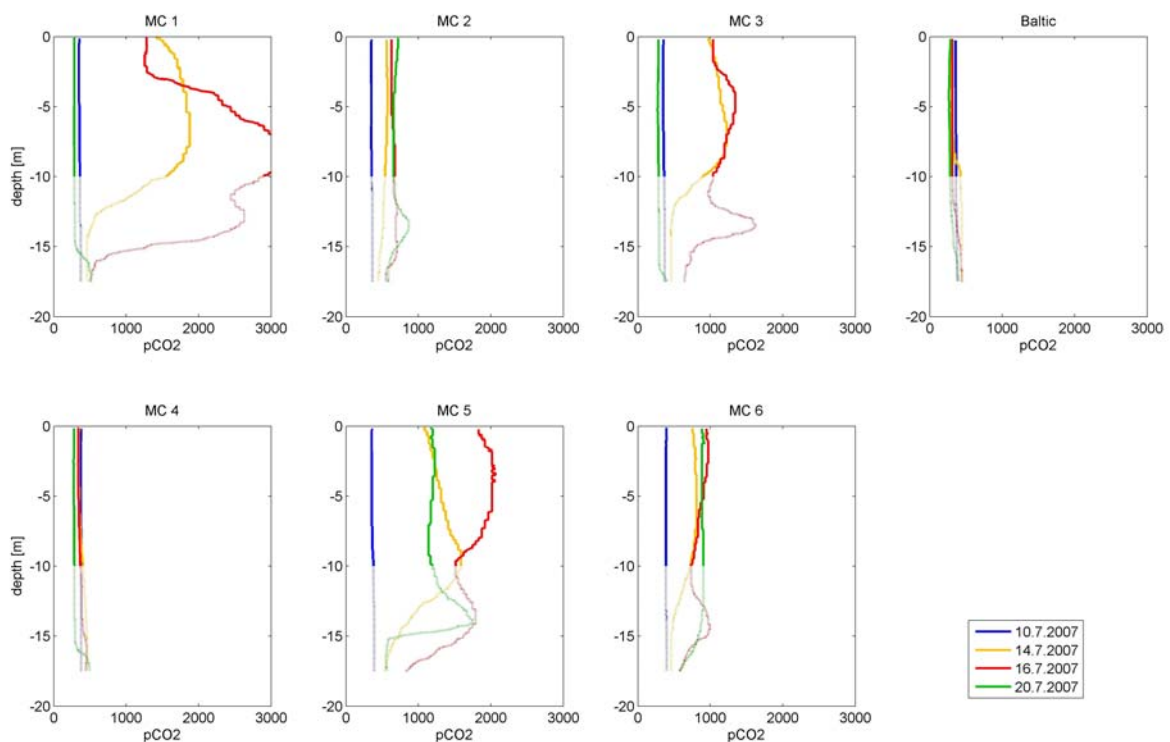


Figure 10: Vertical profiles of pCO₂ (calculated by pH and alkalinity) in the mesocosms (MC) 1 - 6 and in the Baltic for 10th July (blue), 14th July (yellow), 16th July (red) and 20th July (green). (solid lines: 0 - 10 m, dotted lines: 10 - 17.5 m)

Similar patterns were found for the vertical distribution of pH (Fig. 11). Slight differences in pH were observed in the Baltic and in the reference mesocosm 4 during the experiment, where the pH increased from 8 to 8.2 over time. Initial pH values of 8.1 (blue lines) were equal in all mesocosms. After the 1st

acidification (yellow lines) the pH artificially decreased in MC 2 to 7.9 and in MC 6 to 7.8 compared to the reference measurement. In MC 3, 5 and 1 the pH varied vertically, but mean values were about 7.6, 7.5 and 7.4, respectively. After the 2nd acidification (red lines) in MC 2 and MC 6 the pH was 7.8 and 7.7, respectively. In MC 3 and 5 the pH varied vertically again, but mean values were about 7.6 and 7.4, respectively. The vertical variability of MC 1 ranged from 7.6 to 7.2, with the mean value of 7.4.

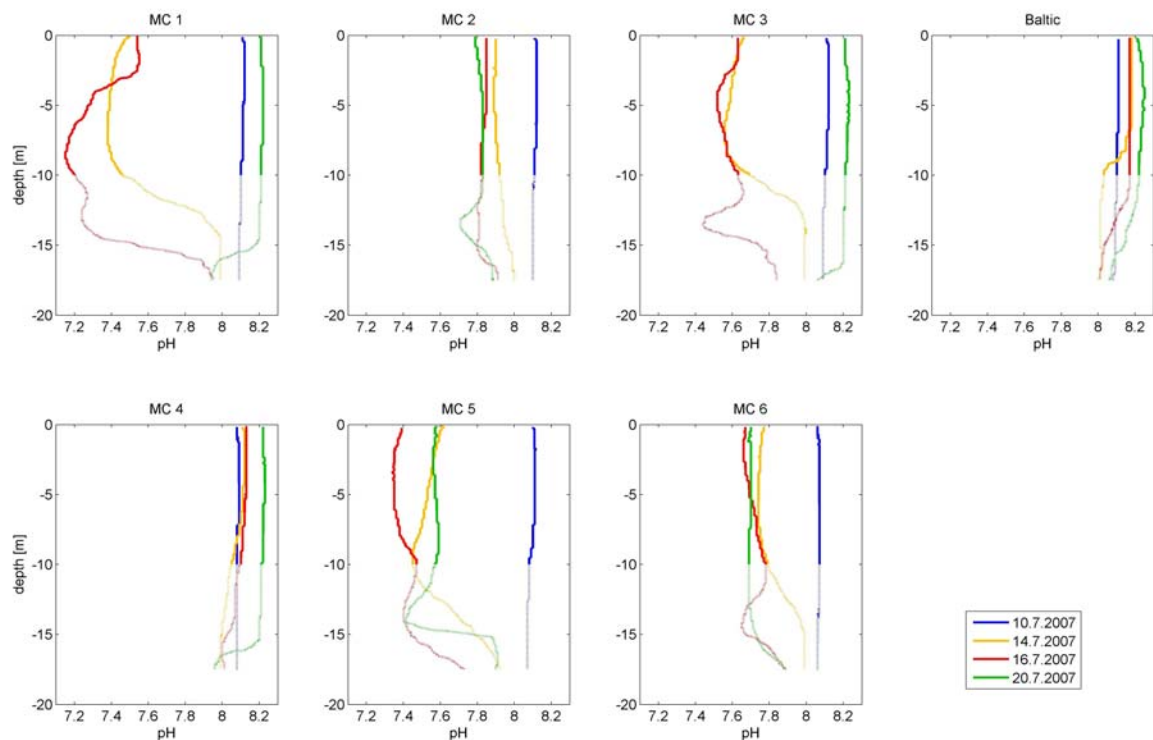


Figure 11: Vertical profiles of pH in the mesocosms (MC) 1 - 6 and in the Baltic for 10th July (blue), 14th July (yellow), 16th July (red) and 20th July (green). (solid lines: 0 - 10 m, dotted lines: 10 - 17.5 m) (data, K. Schulz)

Despite the fact that there was an exchange of water due to the boundary conditions and therefore mesocosm damages, the CTD values indicate that the upper 10 m of the water column (of the mesocosms whose data were used for this thesis) were only slightly affected.

The pH and pCO₂ history of every single mesocosm

The addition of HCl to five of six mesocosms led to different levels of acidification (respectively pCO₂). During the whole experiment each mesocosm was treated differently and the range of pH varied considerably. While the pH (mean of 0-10 m) of the untreated mesocosm MC 4 varied between 8.1 and 8.2, the range in MC 5 for example differed between 7.4 and 8.1 (Fig. 12). The scope of the acidifications was to establish a gradient of diverse steady pH, but the pH and pCO₂ concentrations were not constant over time and changed more or less fast back to values near present day.

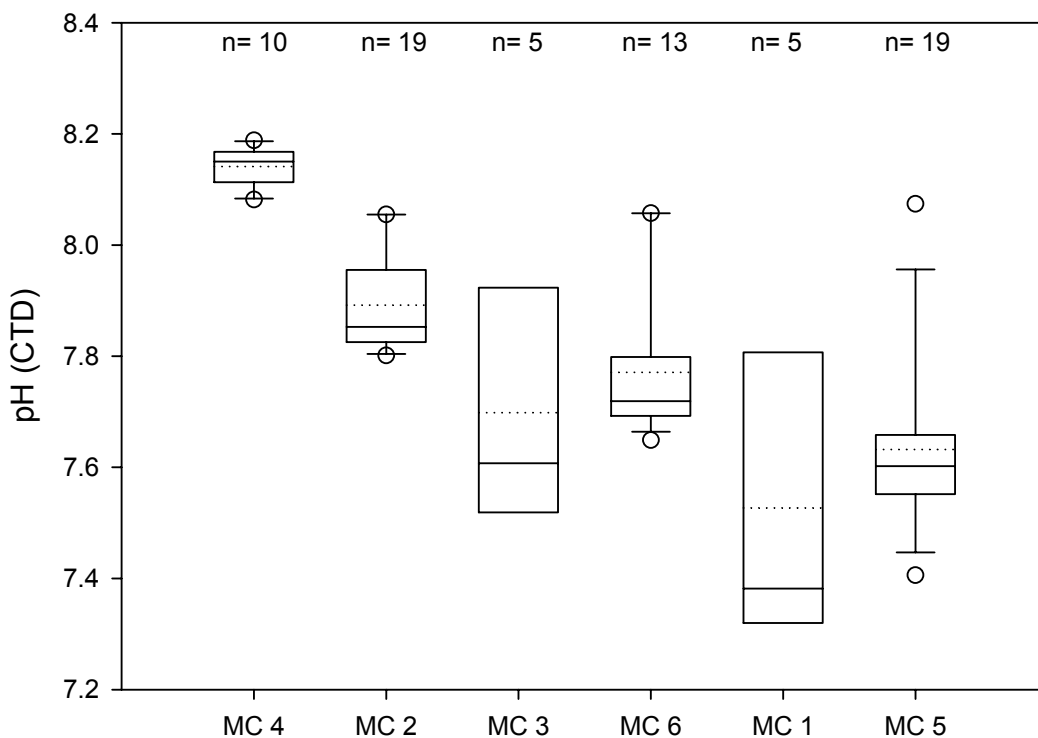


Figure 12: Range of pH (mean of 0-10 m) in the mesocosms (MC) 1-6 during the entire experiment (solid line: median, dotted line: mean)

The more acidic mesocosms changed faster with time than the less acidified mesocosms due to the more pronounced gradient between sea surface/air. Thus, the rebalance to present day values was not linear. Based on the fact that

the pH range of the untreated mesocosm 4 was stable over time, it was used as a reference in this study.

Since mesocosms 1 and 3 were sampled less frequently ($n=5$) compared to the other mesocosms and their pH values varied over a large range, data of mesocosms 1 and 3 are not included in the analyses.

The temporal development of the $p\text{CO}_2$ concentrations in the differently HCl-treated mesocosms (MC 4 \triangleq not, MC 2 \triangleq weak, MC 6 \triangleq medium and MC 5 \triangleq strong) showed this decreasing trend within each acidification experiment (Fig. 13). Data of the 3rd acidification experiment are not included in this diploma thesis, because the not acidified reference mesocosm was not available anymore. Additionally, it can not be ensured that the first 10 m of the three remaining mesocosms were not affected by mesocosm damages and water exchange with surrounding Baltic Sea water during this last acidification experiment.

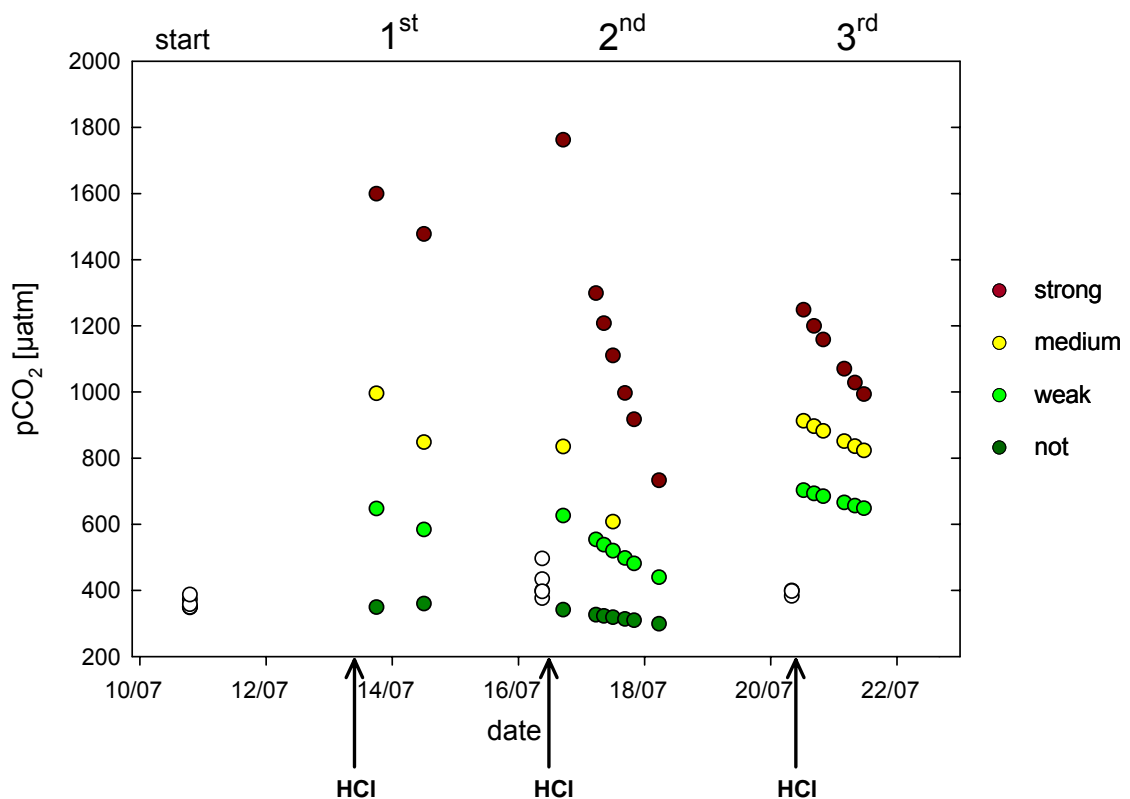


Figure 13: Temporal development of the $p\text{CO}_2$ concentrations in the mesocosms (not, weakly, medium and strongly acidified) for the 1st, 2nd and 3rd acidification experiments.

For further data analyses, means were calculated for the different mesocosms representing different ranges of $p\text{CO}_2$ concentrations for the 1st and 2nd acidification experiment. Please note, that the categorized range of $p\text{CO}_2$ concentrations in the mesocosms differed between the 1st to the 2nd acidification experiment (Fig. 14).

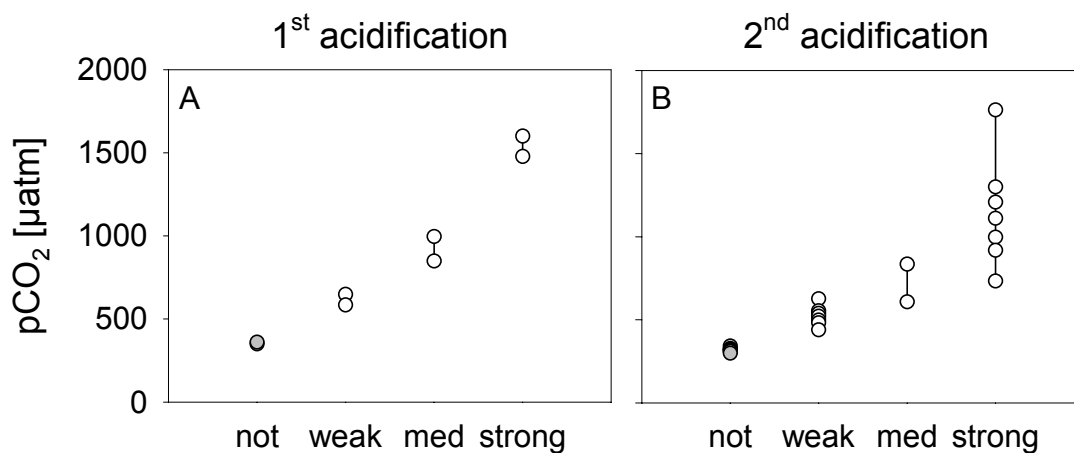


Figure 14: Range of $p\text{CO}_2$ concentrations in the mesocosms (not, weakly, medium and strongly acidified) for the 1st (A) and 2nd (B) acidification experiment.

This two acidifications were analysed as two different acidification experiments, which certainly had a temporal relation to each other, but also differences in their abiotic environments and $p\text{CO}_2$ ranges from one to the other acidification experiment.

Biogeochemical processes

Particulate Organic Matter (POM)

To address possible consequences of ocean acidification, the effects of elevated pCO₂ concentrations on biogeochemical level were studied in this field experiment.

Mean concentrations of particulate organic carbon (POC) did not show any significant response to the HCl treatment during the 1st acidification experiment (Fig. 15, A). However, after the 2nd acidification POC concentrations were significantly enhanced in the not acidified mesocosm compared to the mesocosms that experienced acid treatment (ANOVA, Holm-Sidak, $p = 0.01$; Fig. 15, B). Mean POC concentrations of the acidified mesocosms were significantly reduced after the 2nd acidification when compared to the 1st (ANOVA on ranks, Dunn's, $p = 0.005$).

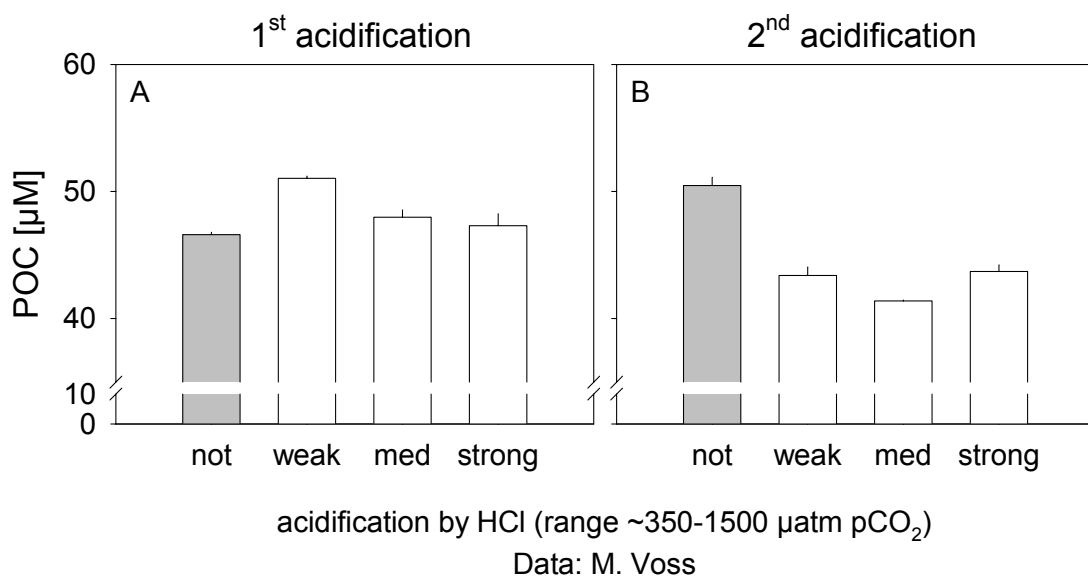


Figure 15: Means of Particulate Organic Carbon (POC) concentrations in the mesocosms (not, weakly, medium and strongly acidified) for the 1st (A) and 2nd (B) acidification experiment (data, M. Voss).

Mean concentrations of particulate organic nitrogen (PON) did not vary significantly with increasing pCO₂ concentrations between the 1st and 2nd acidification experiment (Fig. 16).

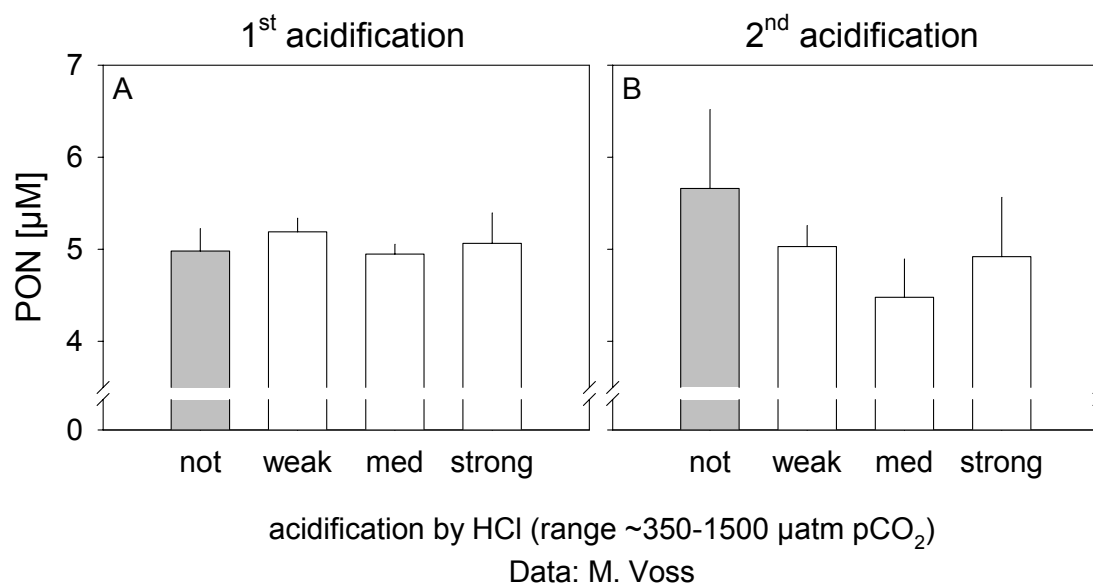


Figure 16: Means of Particulate Organic Nitrogen (PON) concentrations in the mesocosms (not, weakly, medium and strongly acidified) for the 1st (A) and 2nd (B) acidification experiment (data: M. Voss).

Particulate organic phosphorus (POP) concentrations (means) did not change significantly under elevated $p\text{CO}_2$ concentrations during the 1st and 2nd acidification experiment (Fig. 17). However, in contrast to the 1st acidification experiment mean POP concentrations were significantly reduced in the mesocosms that experienced acid treatment after the 2nd acidification (ANOVA, Holm-Sidak, $p = 0.01$).

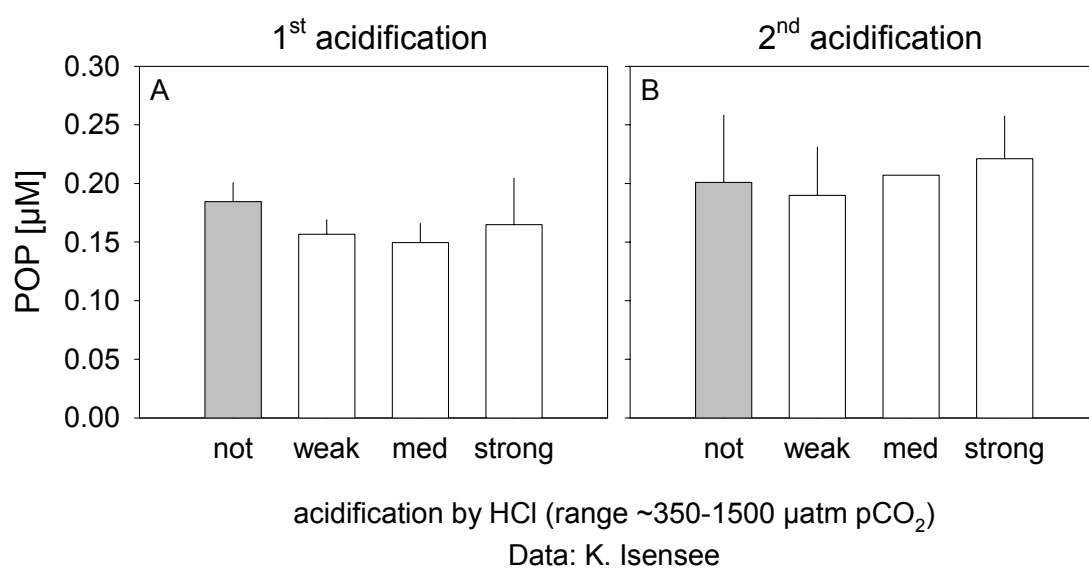


Figure 17: Means of Particulate Organic Phosphorus (POP) concentrations in the mesocosms (not, weakly, medium and strongly acidified) for the 1st (A) and 2nd (B) acidification experiment (data, K. Isensee).

C:N:P ratio

During the 1st and 2nd acidification experiment means of the particulate carbon/nitrogen (C/N) ratio (mol/mol) did not change significantly neither under elevated pCO₂ concentrations nor over time (Fig. 18). Mean C/N ratios were higher in all mesocosms during both experiments. as expected by the canonical Redfield ratio of 6.6 .

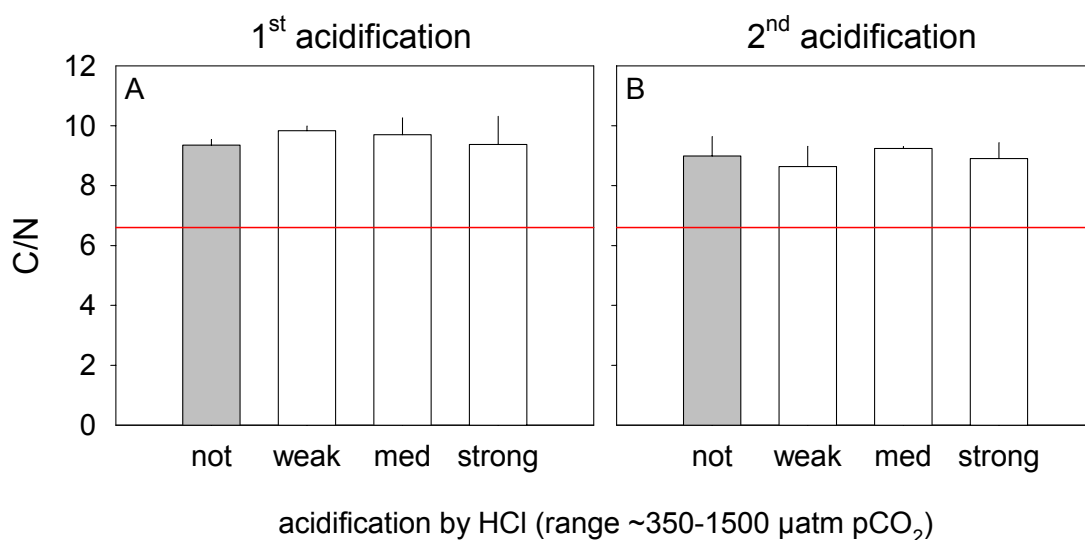


Figure 18: Means of the carbon/nitrogen (C/N) ratio (mol/mol) in the mesocosms (not, weakly, medium and strongly acidified) for the 1st (A) and 2nd (B) acidification experiment (red solid lines: Redfield ratio of 6.6).

For both experiments no significant difference between the different HCl treatments were observed for means of the particulate carbon/phosphorus (C/P) ratios (Fig. 19). However, mean C/P ratios of the HCl treated mesocosms were significantly higher during the 1st compared to the 2nd acidification experiment (ANOVA on ranks, Dunn's, $p = 0.001$).

Mean C/P ratios were three to two times higher during the 1st respectively 2nd experiment compared to the Redfield ratio of 106.

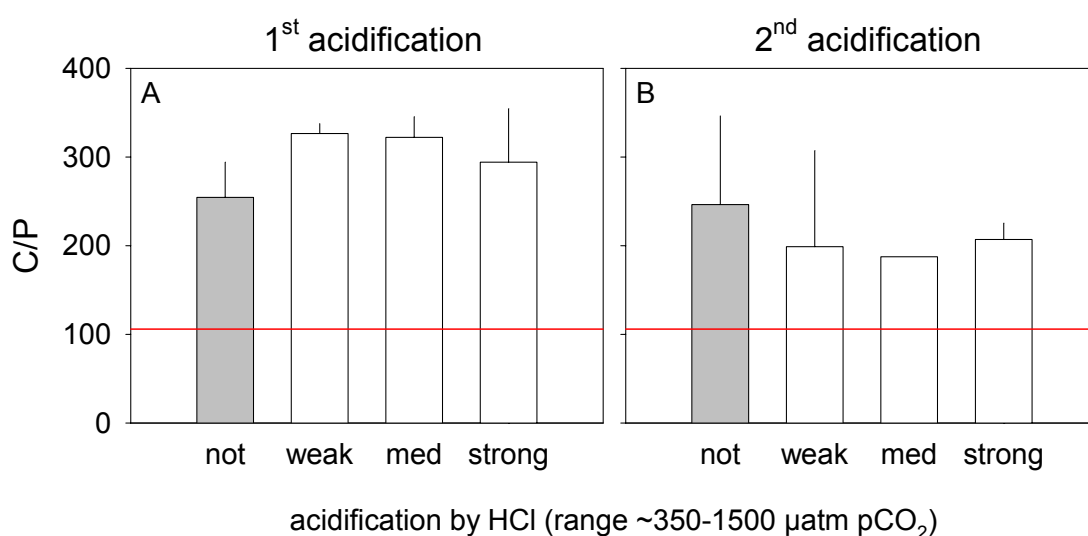


Figure 19: Means of the carbon/phosphorus (C/P) ratio in the mesocosms (not, weakly, medium and strongly acidified) for the 1st (A) and 2nd (B) acidification experiment (red solid lines: Redfield ratio of 106).

Means of the particulate nitrogen/phosphorus (N/P) ratio did not change significantly with increasing $p\text{CO}_2$ concentrations during the 1st and 2nd acidification experiment and varied between ~25 and ~30 (Fig. 20). However, in contrast to the 1st acidification experiment mean N/P ratios were significantly reduced in the mesocosms that experienced acid treatment after the 2nd acidification (ANOVA, Holm-Sidak, $p = 0.009$).

Moreover, means of the N/P ratio were enhanced twofold compared to the Redfield ratio of 16.

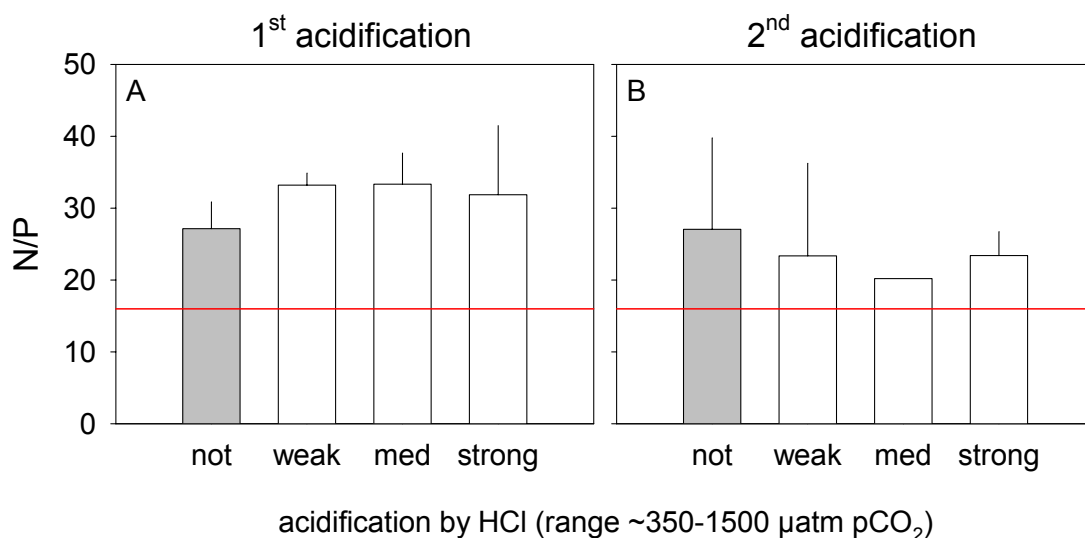


Figure 20: Means of the nitrogen/phosphorus (N/P) ratio in the mesocosms (not, weakly, medium and strongly acidified) for the 1st (A) and 2nd (B) acidification experiment (red solid lines: Redfield ratio of 16).

Chlorophyll a and nutrients

Chlorophyll *a* (Chl *a*) and nutrient concentrations were low in the Baltic, when this campaign took place. Concentrations of nitrate (NO_3^-) were at the detection limit. Phosphate (PO_4^{3-}) concentrations were $0.22 (\pm 0.04) \mu\text{mol l}^{-1}$ and decreased by $0.1 \mu\text{mol l}^{-1}$ in all mesocosms over time (date not shown). Chl *a* concentration was $2.13 (\pm 0.26) \mu\text{g l}^{-1}$ and did not change significantly. Overall the experiment was conducted in a non-bloom situation (Fig. 21).

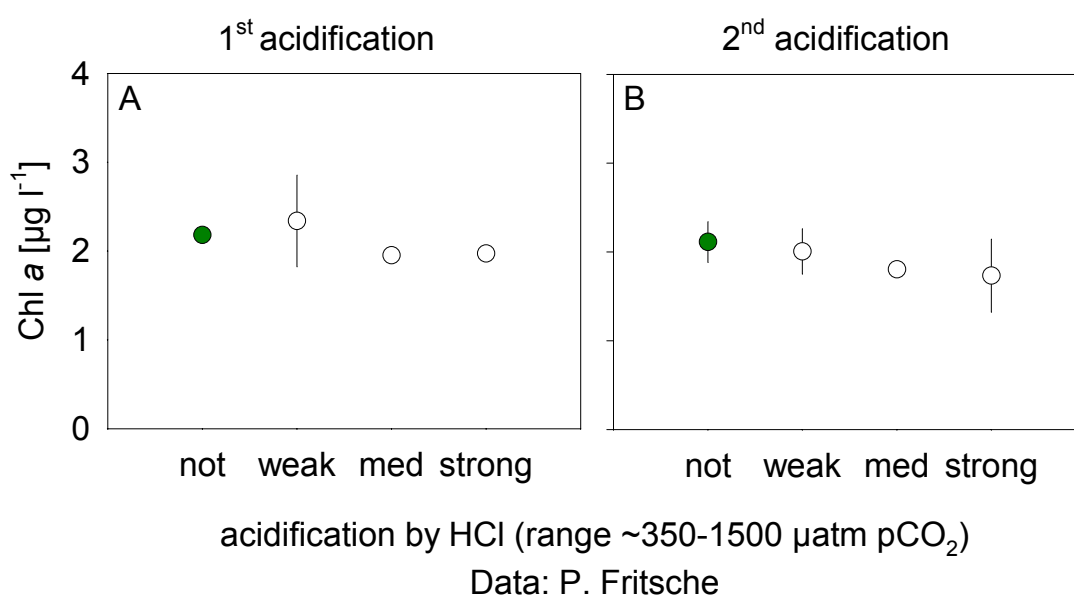


Figure 21: Means of Chlorophyll *a* (Chl *a*) concentrations in the mesocosms (not, weakly, medium and strongly acidified) for the 1st (A) and 2nd (B) acidification experiment (data, P. Fritsche).

Amino acids

Mean concentrations of dissolved free amino acids (DFAA) did not change significantly with increasing $p\text{CO}_2$ concentrations during the 1st and 2nd acidification experiment (Fig. 22), although diurnal variabilities were observed (data not shown). During the 1st acidification experiment DFAA concentrations were significantly higher compared to the 2nd experiment (ANOVA on ranks, Dunn's, $p = 0.032$).

In general concentrations of DFAA were ~50% lower during both experiments in all mesocosms compared to the mean start concentration of 131.6 nM .

The composition of the DFAA showed differences by comparing the three acidification experiments (data not shown, appendix (Fig. 39)). However, the DFAA composition did not show a direct response to the strength of acid treatment.

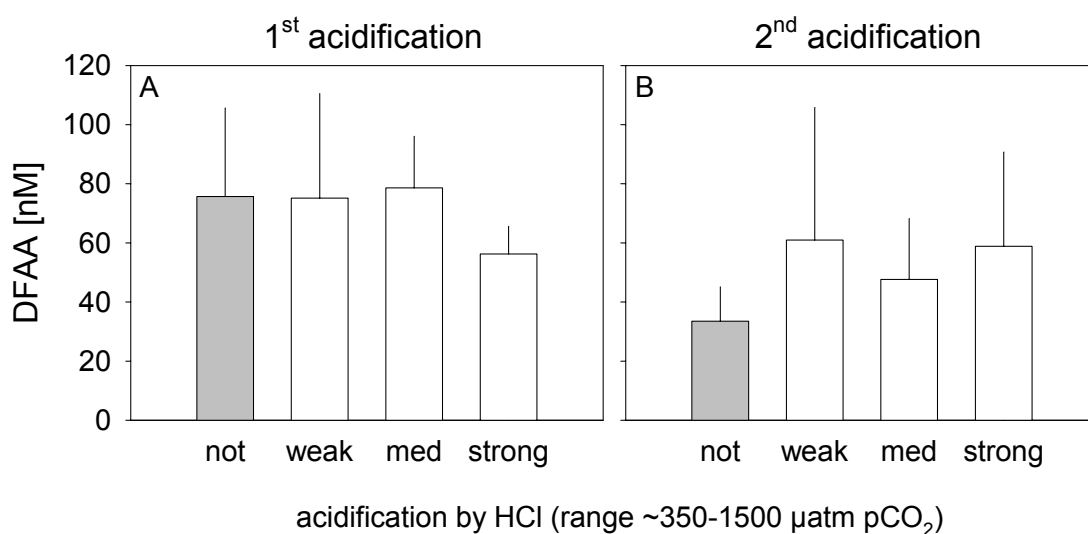


Figure 22: Means of dissolved free amino acid (DFAA) concentrations in the mesocosms (not, weakly, medium and strongly acidified) for the 1st (A) and 2nd (B) acidification experiment.

Transparent Exopolymer Particles

Dynamics of Transparent Exopolymer Particles (TEP) are a good indication for biologically-driven changes of the carbon-pool. In this study mean concentrations of TEP were considerable low between ~60 and ~100 μg GumXanthan equivalents (Xeq.) l^{-1} (Fig. 23). After the 1st acidification TEP concentrations of the not acidified mesocosm did not change compared to the weakly acidified mesocosm (Fig. 23, A). However mean concentrations of TEP significantly decreased with increasing pCO_2 concentrations from the weakly to the strongly acidified mesocosm (ANOVA on ranks, Turkey, $p = 0.013$). During the 2nd acidification experiment a significant difference was observed between the not acidified and the mesocosms that experienced acid treatment (Fig. 23, B, (ANOVA, Holm-Sidak, $p = 0.001$)). TEP concentrations increased over time in the not acidified mesocosm (t-test, $p < 0.001$).

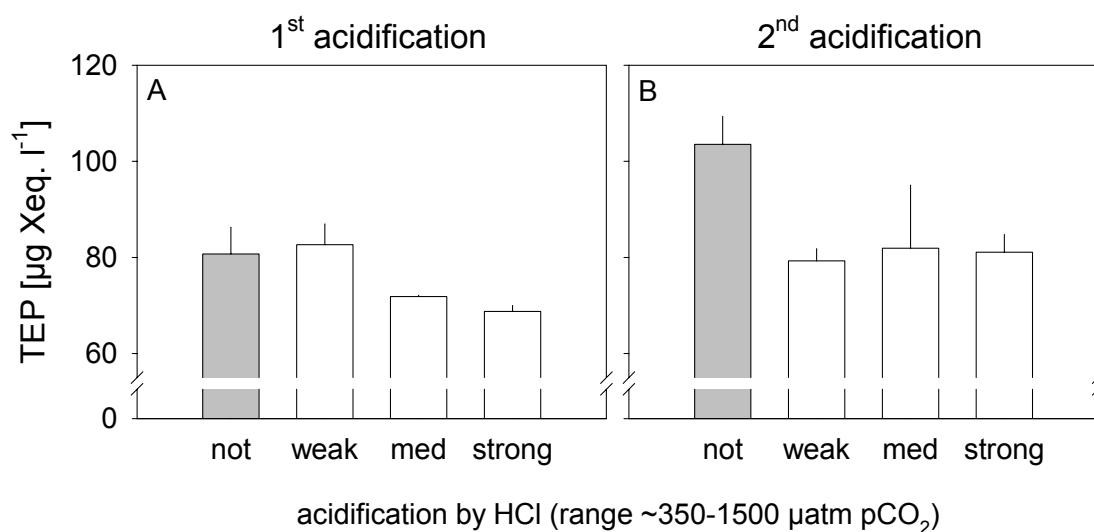


Figure 23: Means of Transparent Exopolymer Particles (TEP) in the mesocosms (not, weakly, medium and strongly acidified) for the 1st (A) and 2nd (B) acidification experiment.

Eukaryotic phytoplankton dynamics

Phytoplankton plays a major role in biogeochemical cycling of inorganic and organic matter, and is known as main TEP producer. Mean abundance of eukaryotic phytoplankton, determined by flow-cytometry, decreased significantly (linear regression analysis, $r^2 = 0.97$; $p = 0.016$) from $4.28 (\pm 0.01) \times 10^4$ cells ml^{-1} to $2.33 (\pm 0.86) \times 10^4$ cells ml^{-1} with increasing pCO_2 concentrations after the 1st acidification (Fig. 24, A). During the 2nd acidification experiment the highest mean abundance was observed in the not acidified mesocosm, which was significantly higher compared to the abundance in the acidified mesocosms (Fig. 24, B, (ANOVA, Holm-Sidak, $p < 0.001$)). The lowest abundance of eukaryotic phytoplankton after the 2nd acidification was found in the medium acidified mesocosm (ANOVA, Holm-Sidak, $p < 0.001$).

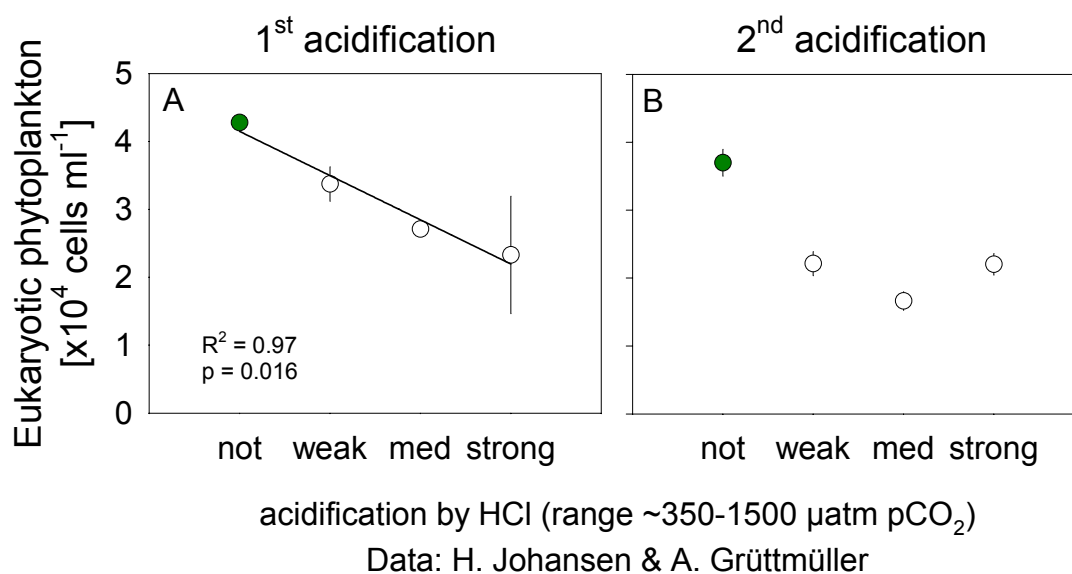


Figure 24: Means of eukaryotic phytoplankton abundances in the mesocosms (not, weakly, medium and strongly acidified) for the 1st (A) and 2nd (B) acidification experiment (data, H. Johansen & A. Grützmüller).

Diazotrophic cyanobacteria dynamics

Abundances of diazotrophic cyanobacteria *Nodularia spp.* and *Aphanizomenon spp.* were determined by fluorescence microscopy.

Abundances of *Nodularia spp.* did not change significantly between the different treatments during the 1st and 2nd acidification experiment (Fig. 25. A). But abundances decreased from ~3000 to ~900 units l⁻¹ (one unit = 100 μ m) over time from the 1st to the 2nd acidification experiment.

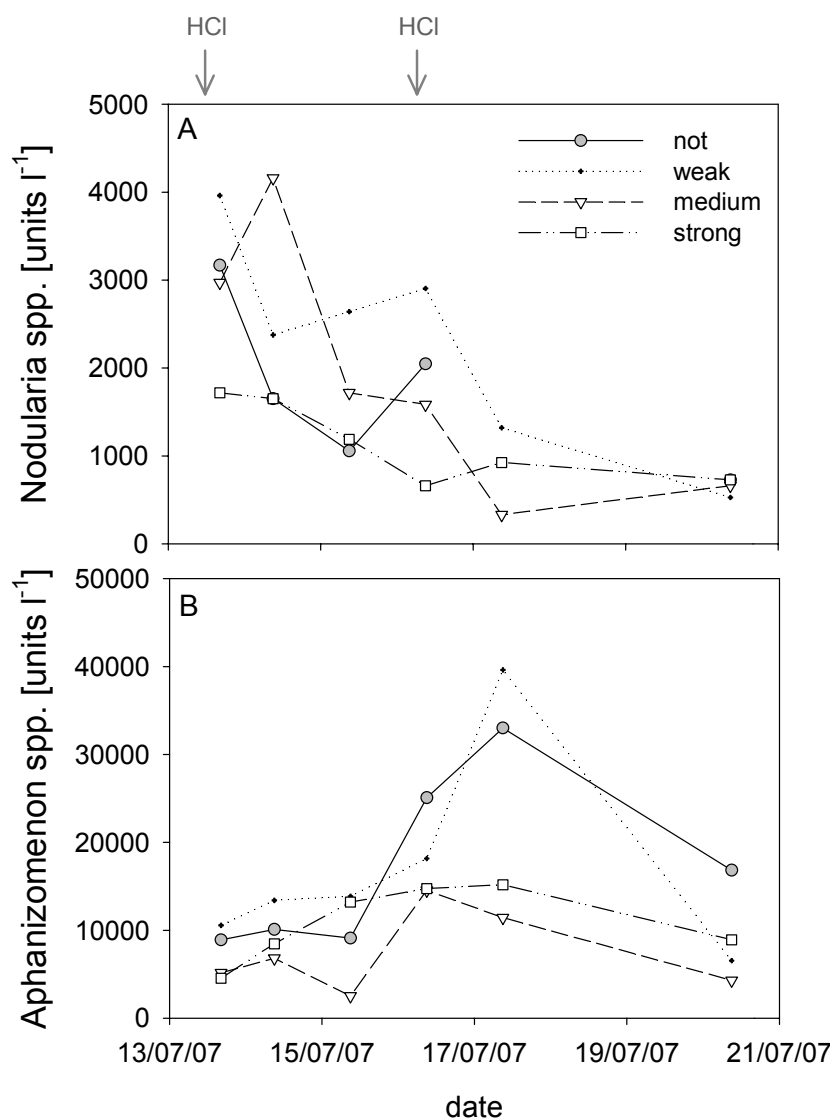


Figure 25: Temporal dynamics of *Nodularia spp.* (A) and *Aphanizomenon spp.* (B) in the mesocosms (not, weakly, medium and strongly acidified) for the 1st and 2nd acidification experiment (1 unit = 100 μ m) (data, K. Haynert).

Abundances of *Aphanizomenon spp.* were not significantly different during the 1st experiment, whereas during the 2nd acidification experiment abundances of the not and weakly acidified mesocosms increased compared to the medium and strongly acidified mesocosm (Fig. 25, B). In contrast to *Nodularia spp.*, abundances of *Aphanizomenon spp.* increased in the not and weakly acidified mesocosms over time.

Phytoplankton activity

Autotrophic rates, CO₂ uptake and nitrogen (N₂) fixation, were measured in order to follow the impact of increasing CO₂ concentrations on the physiology of the autotrophs.

CO₂ uptake

In general CO₂ uptake rates were low, ranging from 0.02 to 0.25 μmol l⁻¹ h⁻¹ (Fig. 26). The CO₂ uptake was dominated by organisms smaller than 10 μm (grey bars) during the entire experiment. Mean CO₂ uptake rates of organisms larger than 10 μm (black bars) were not significantly affected by the HCl treatment during the 1st and the 2nd acidification experiment. Furthermore only CO₂ uptake rates of organisms larger than 10 μm decreased significantly from the 1st to the 2nd acidification experiment (ANOVA on ranks, Dunn's, p<0.001).

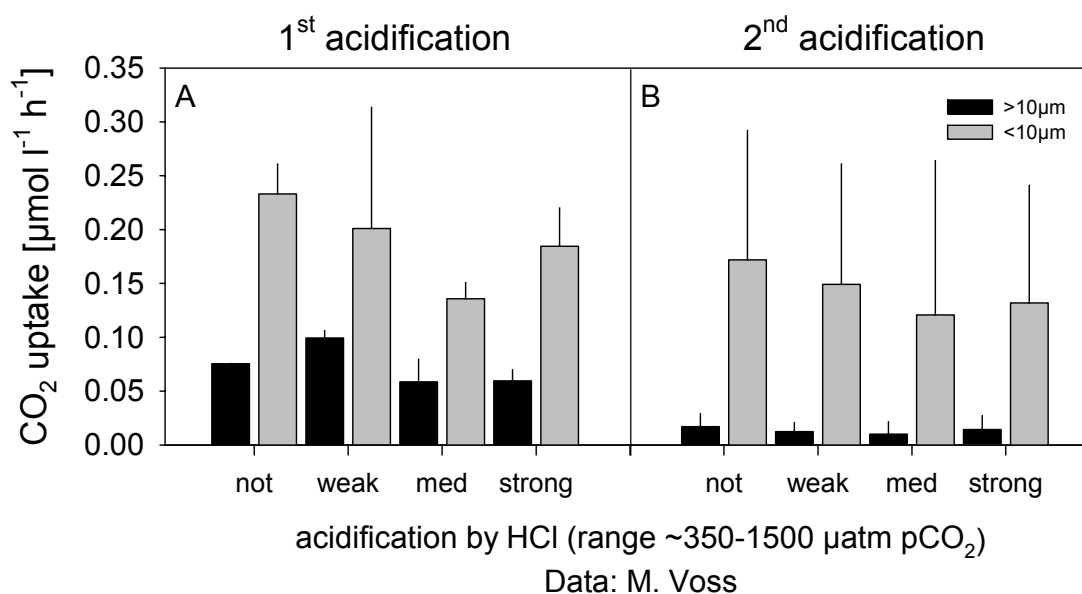


Figure 26: Means of CO₂ uptake rates of organisms >10 μm (black) and <10 μm (grey) in the mesocosms (not, weakly, medium and strongly acidified) for the 1st (A) and 2nd (B) acidification experiment (data, M. Voss).

Thus, the proportion of the CO₂ uptake of organisms smaller to larger than 10 µm increased significantly from the 1st to the 2nd acidification experiment (ANOVA on ranks, Dunn's, $p < 0.001$). The large error bars are due to the diurnal variability (data not shown).

N₂ fixation

Overall N₂ fixation rates were low between 0.25 and 3 nmol l⁻¹ h⁻¹ (Fig. 27).

Mean N₂ fixation rates of organisms larger 10 µm (black bars) did not change with increasing pCO₂ concentrations during the 1st acidification experiment (Fig. 27, A). After the 2nd acidification mean N₂ fixation rates in the larger than 10 µm size class were significantly higher in the not acidified mesocosm than in the HCl-treated mesocosms (Fig. 27, B, (ANOVA, Holm-Sidak, $p = 0.004$)).

Mean N₂ fixation rates of organisms smaller than 10 µm (grey bars) did not change significantly neither with increasing pCO₂ concentrations during the 1st and the 2nd acidification experiment nor over time from the 1st to the 2nd acidification experiment (Fig. 27).

Finally N₂ fixation was dominated by organisms smaller than 10 µm, due to the decrease of mean N₂ fixation rates of organisms larger than 10 µm over time. Thus the proportion of N₂ fixation rates of organisms smaller to larger than 10 µm increased significantly from the 1st to the 2nd acidification experiment (ANOVA on ranks, Dunn's, $p < 0.001$).

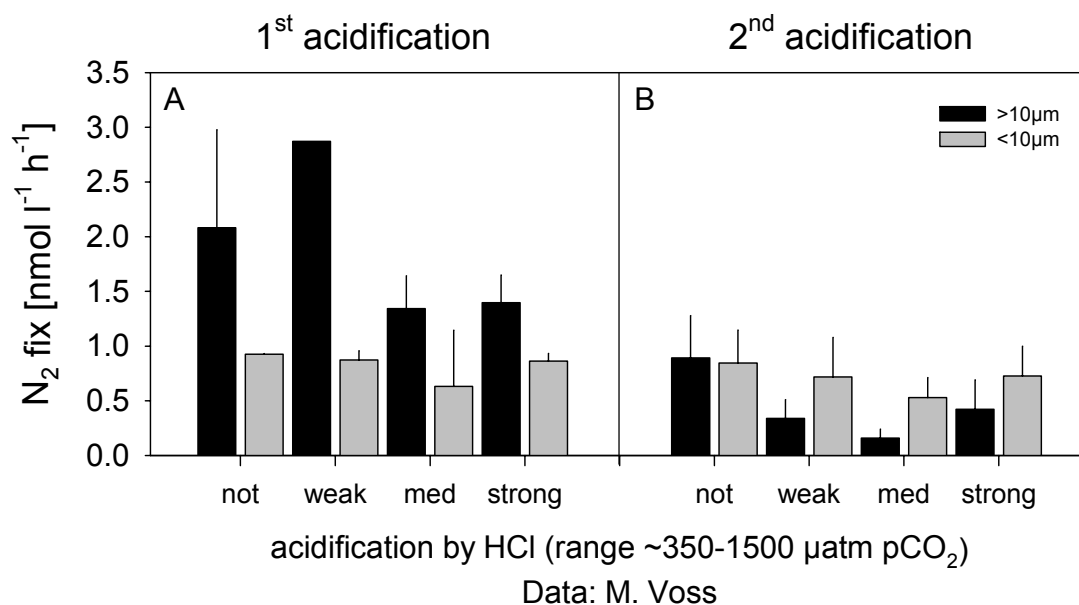


Figure 27: Means of nitrogen fixation (N_2 fix) rates of organisms $>10\mu\text{m}$ (black) and $<10\mu\text{m}$ (grey) in the mesocosms (not, weakly, medium and strongly acidified) for the 1st (A) and 2nd (B) acidification experiment (data, M. Voss).

Unicellular cyanobacteria

Mean numbers of unicellular cyanobacteria, determined by Flow Cytometry, did not respond significantly to increasing pCO₂ concentrations after the 1st and 2nd acidification (Fig. 28). No significant differences were observed from the 1st to the 2nd acidification experiment, although mean numbers of small cyanobacteria increased slightly in the not acidified mesocosms.

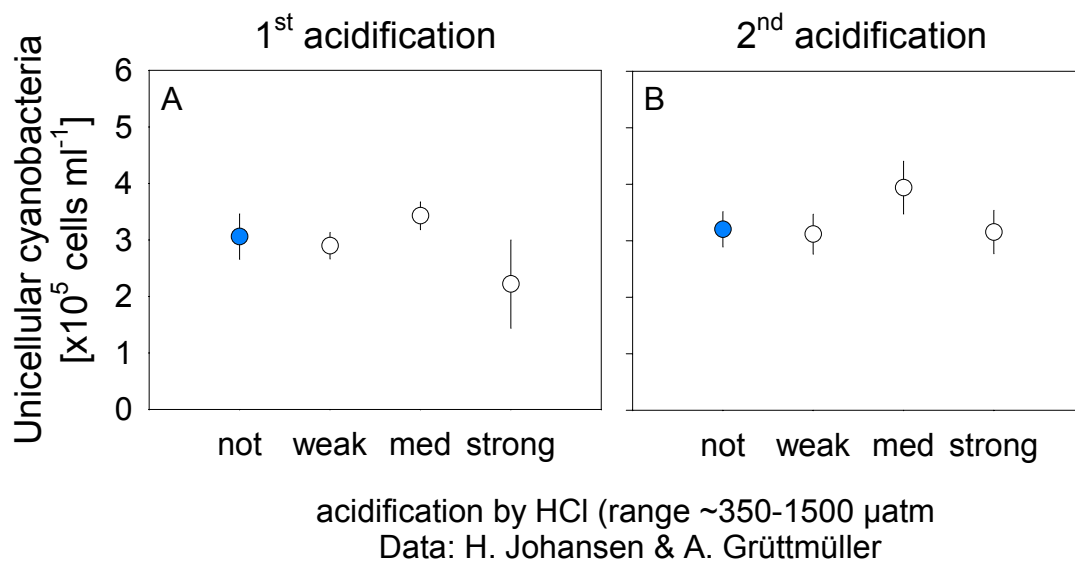


Figure 28: Means of unicellular cyanobacteria (determined by Flow Cytometry) abundances in the mesocosms (not, weakly, medium and strongly acidified) for the 1st (A) and 2nd (B) acidification experiment (data, H. Johansen & A. Grützmüller).

Bacterial dynamics

Mean abundances of heterotrophic bacteria (determined by Flow Cytometry) did not show any significant response to the HCl treatment after the 1st acidification (Fig. 29, A). During the 2nd acidification experiment significantly increased numbers of heterotrophic bacteria were observed in the not acidified mesocosm compared to the mesocosms that experienced acid treatment (Fig. 29, B, (ANOVA, Holm-Sidak, $p < 0.001$)). By comparing the abundance in the different mesocosms between the 1st and 2nd acidification experiment separately, statistically significant enhanced numbers of heterotrophic bacteria were observed in the not, weakly and strongly acidified mesocosms after the 2nd acidification (t-test, $p_{\text{not}} = 0.008$, $p_{\text{weak}} = 0.013$, $p_{\text{strong}} = 0.032$).

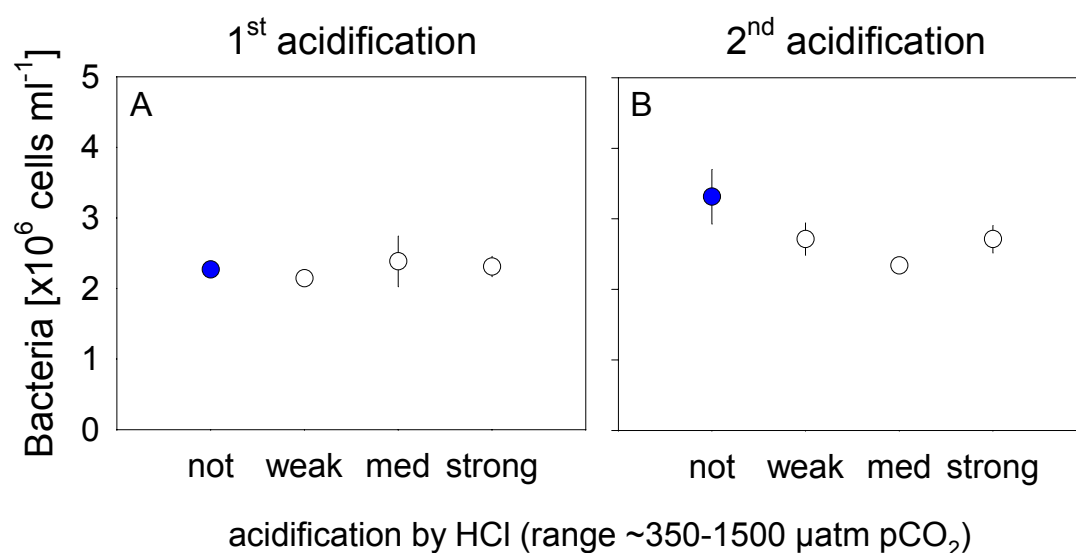


Figure 29: Means of heterotrophic bacteria abundances in the mesocosms (not, weakly, medium and strongly acidified) for the 1st (A) and 2nd (B) acidification experiment (medium of 2nd acidification: $n=1$).

Since TEP abiotically form from dissolved organic precursors, mainly released by marine organisms, it is likely, that changes in TEP dynamics were correlated with the dynamics of eukaryotic phytoplankton, cyanobacteria and heterotrophic bacteria.

Indeed, TEP dynamics were significantly correlated with the dynamics of cyanobacteria in all HCl-treated mesocosms during both experiments (Fig. 30, A, (linear regression analysis, $r^2 = 0.95$, $p = 0.003$)). A strong correlation was also found between the dynamics of heterotrophic bacteria and TEP (Fig. 30, B, (linear regression analysis, $r^2 = 0.98$, $p = 0.005$)). Please note, that TEP vs. $p\text{CO}_2$ and TEP vs. eukaryotic phytoplankton did not show any correlation at all.

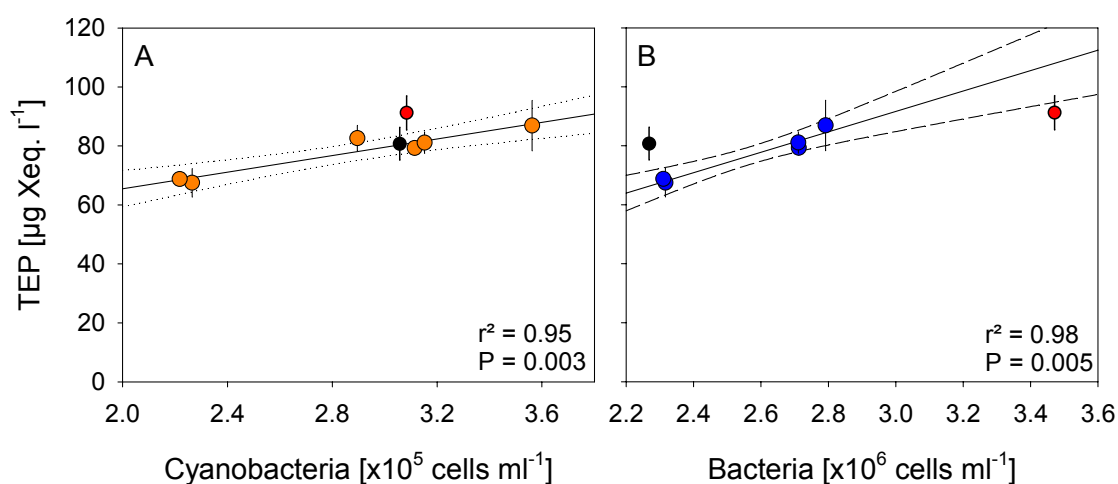


Figure 30: Linear Correlations between Transparent Exopolymer Particles (TEP) and cyanobacteria (orange) (A) and TEP vs. heterotrophic bacteria (blue) (B). Data of the not acidified mesocosms (1st acidification (red) and 2nd acidification (black)) were neglected.

Hydrolytic enzyme activities

In order to follow the impact of decreasing pH on the microbial degradation of organic matter enzyme efficiency (V_{\max}/K_m) of α -glucosidase, leucine-aminopeptidase and alkaline phosphatase were measured by substrate kinetics using MUF- and AMC-labelled substrate analogues.

α -glucosidase

In general turnover rates of α -glucosidase were low ($0.021 \pm 0.007 \mu\text{mol l}^{-1} \text{h}^{-1}$). The enzyme efficiency (V_{\max}/K_m) of α -glucosidase was only little affected by pH during the entire experiment and varied only slightly over time (Fig. 31).

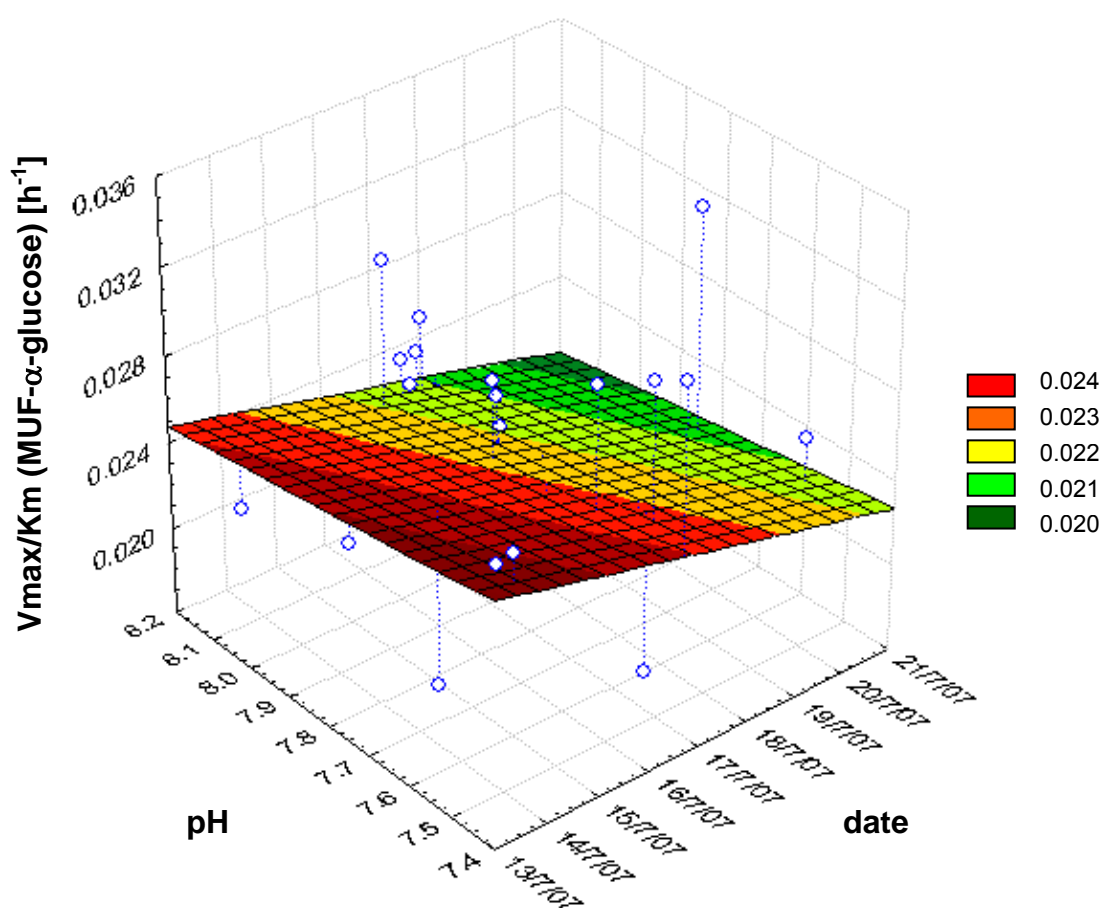


Figure 31: Linear model fit of the enzyme efficiency (V_{\max}/K_m) of α -glucosidase in all mesocosms and during the entire experiment (multiple $R(z/xy) = 0.23$, $p = 0.2$).

Leucine-aminopeptidase

In contrast to α -glucosidase the enzyme efficiency of leucine-aminopeptidase was more sensitive to changes in pH and dropped almost by 60 to 70% under strong acidification (Fig. 32). The high ratio of V_{max} vs. K_m indicate a high efficiency in substrate turnover (mean leucine turnover was $1.2 \pm 0.4 \mu\text{mol l}^{-1} \text{h}^{-1}$). Over time a slight increase of the ratio of V_{max} vs. K_m was observed. Enzyme efficiency of leucine-aminopeptidase decreased in average by $\sim 40\%$ with decreasing pH from 8.1 to 7.6.

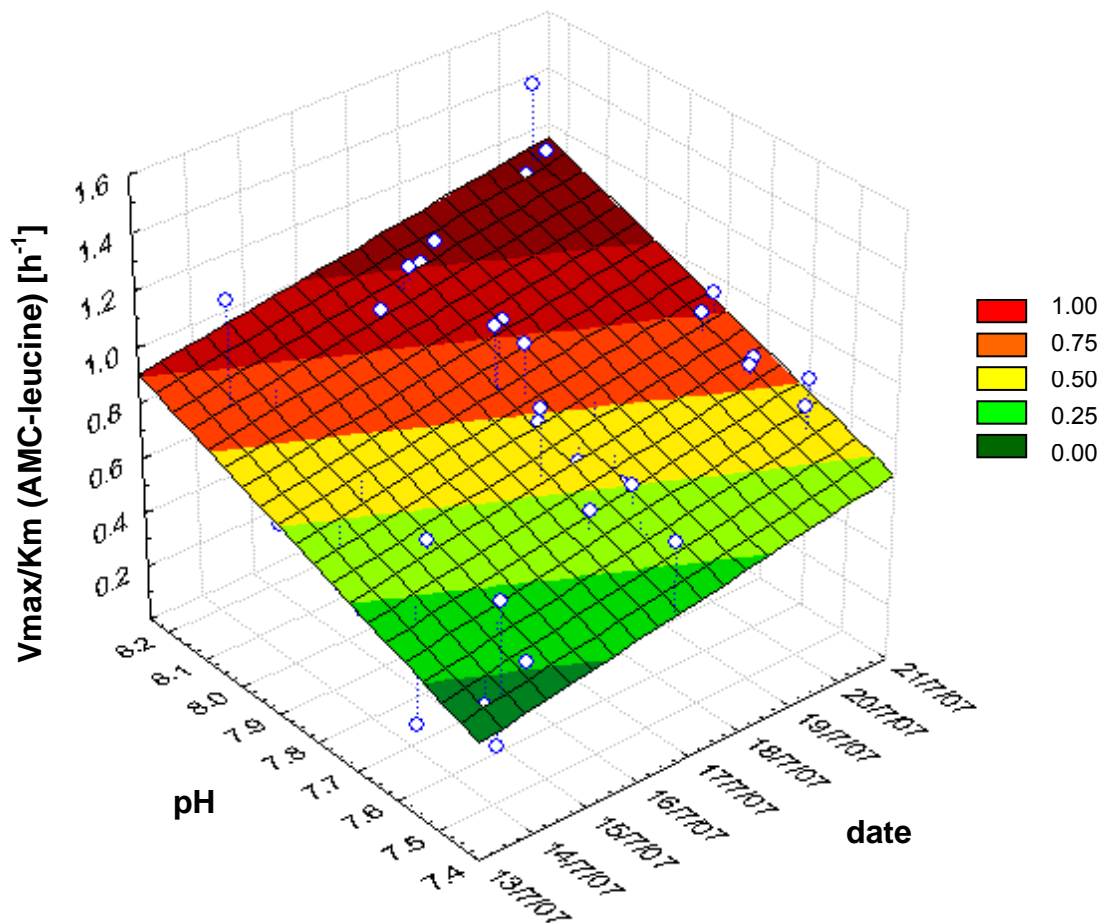


Figure 32: Linear model fit of the enzyme efficiency (V_{max}/K_m) of leucine-aminopeptidase in all mesocosms and during the entire experiment (multiple $R(z/xy) = 0.68$, $p < 0.001$).

Alkaline phosphatase

Activity of alkaline phosphatase did not change over time during the entire experiment, but responded noticeably to the HCl treatments (Fig. 33). The calculated linear model shows a pronounced decrease in the V_{\max}/K_m ratio of ~20% with decreasing pH. Mean phosphate turnover was $0.85 \pm 0.1 \mu\text{mol l}^{-1} \text{h}^{-1}$.

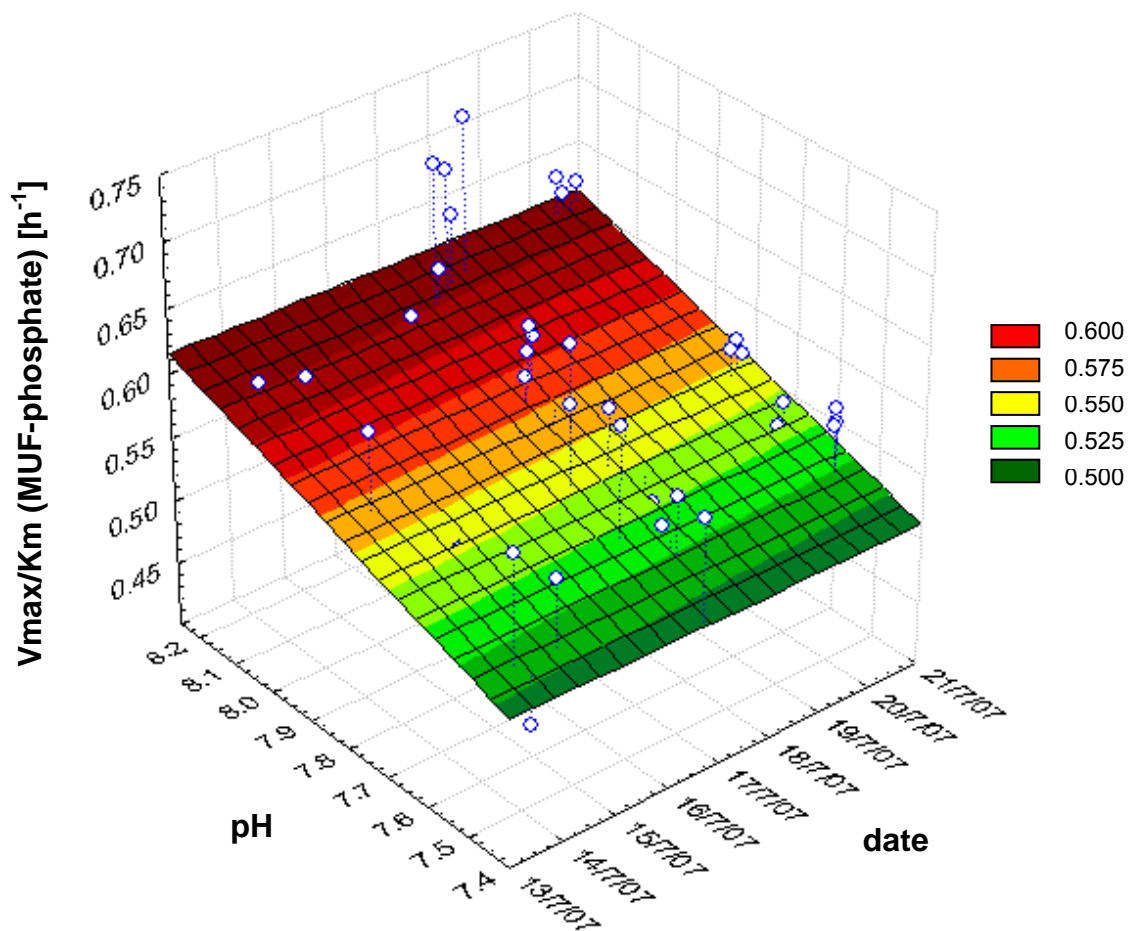


Figure 33: Linear model fit of the enzyme efficiency (V_{\max}/K_m) of alkaline phosphatase in all mesocosms and during the entire experiment (multiple $R(z/xy) = 0.68$, $p < 0.001$).

Bacterial activities

Microbial activity was measured by uptake of radiolabeled ^3H -Leucine (Leu) and ^3H -Thymidine (Thy). Uptake rates were high and ranged from 3.2 and 17.2 $\text{nmol l}^{-1} \text{h}^{-1}$, and 2.4 and 8.9 $\text{nmol l}^{-1} \text{h}^{-1}$, respectively.

However, mean leucine uptake rates (proxy for biomass production) did not change significantly under elevated pCO_2 concentrations neither during the 1st nor during the 2nd acidification experiment (Fig. 34, A, B). By comparing the 1st and 2nd acidification experiment, statistically significant differences were observed, since leucine uptake rates were on average four times higher after the 1st than after the 2nd acidification (ANOVA on ranks, Dunn's, $p < 0.001$). The large error bars are due to the diurnal variability.

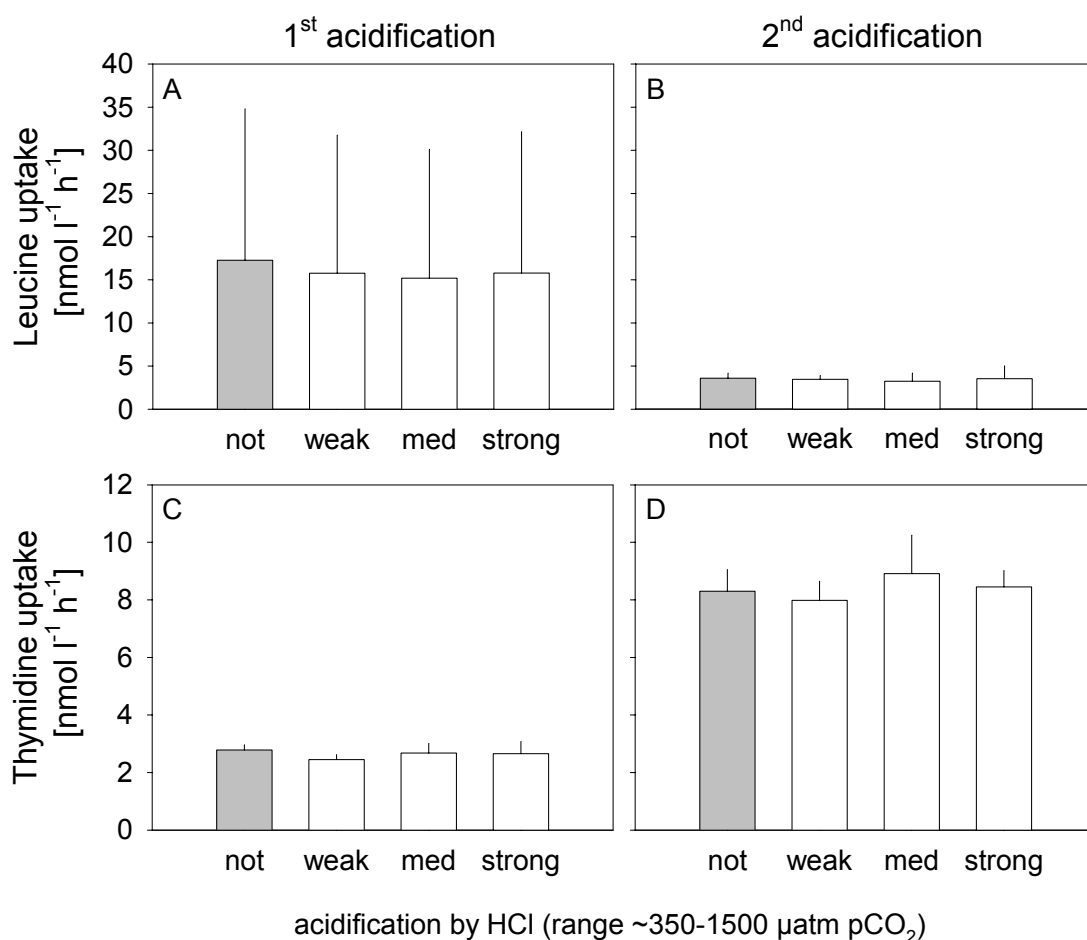


Figure 34: Means of leucine (Leu) (A, B) and thymidine (Thy) (C; D) uptake rates in the mesocosms (not, weakly, medium and strongly acidified) for the 1st and 2nd acidification experiment.

A complementary pattern was found for thymidine uptake rates (proxy for cell deviation). No significant response to the acid treatment was observed during the 1st and the 2nd acidification experiment (Fig. 34, C, D). Means of thymidine uptake rates significantly increased from ~2 to ~8 nmol l⁻¹ h⁻¹ from the 1st to the 2nd acidification experiment (ANOVA on ranks, Dunn's, $p < 0.001$).

However, the proportion of leucine vs. thymidine uptake decreased significantly from the 1st to the 2nd acidification experiment indicating a shift to smaller bacteria (ANOVA on ranks, Dunn's, $p < 0.001$).

Growth rates

Unfortunately we have only a small data set (2nd acidification) which allows to calculate growth rates. From this data it is obvious, that a significant increase of heterotrophic bacteria abundances over time was observed in the not and weakly acidified, but not in the strongly acidified mesocosm (Fig. 35). Furthermore, the slope of the not acidified mesocosm was ~60% higher than of the weakly acidified mesocosm.

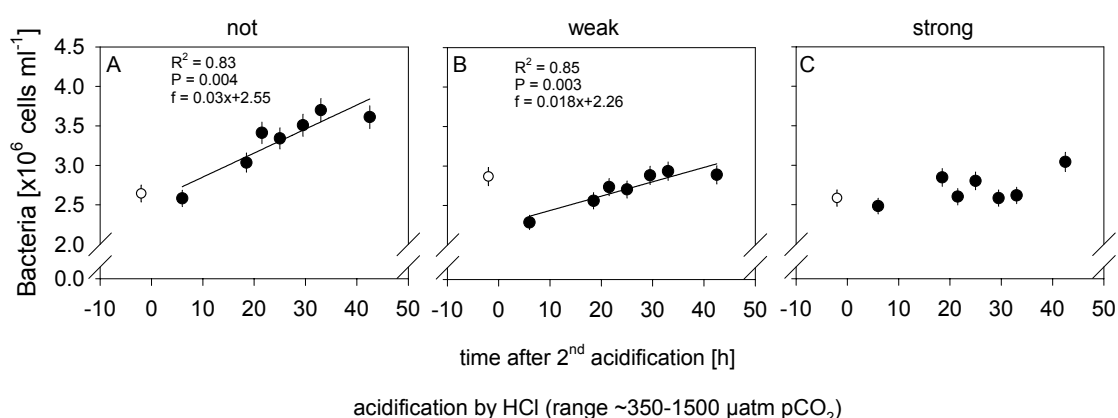


Figure 35: Temporal dynamics of heterotrophic bacteria abundances in three different (not (A), weakly (B) and strongly (C) acidified) mesocosms for the 2nd acidification experiment (error bars indicate analytical errors of cytometrical analyses (4%)).

The complementary pattern was seen for the unicellular cyanobacteria. Abundance of these prokaryotes did not significantly increase over time in the not and weakly acidified mesocosms (Fig. 36). In fact a significant temporal increase of cyanobacteria abundance was observed only with strong acidification.

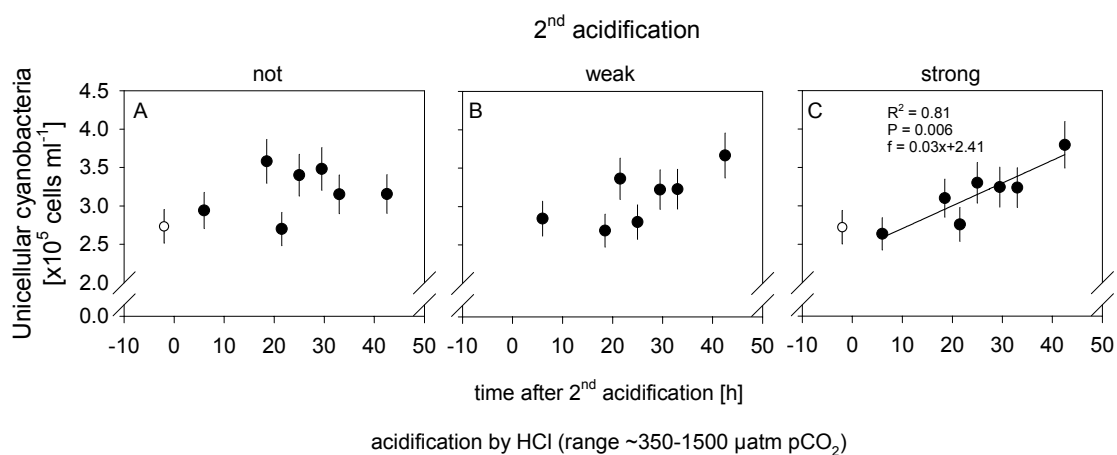


Figure 36: Temporal dynamics of unicellular cyanobacteria abundances in three different (not (A), weakly (B) and strongly (C) acidified) mesocosms for the 2nd acidification experiment (error bars indicate analytical errors of cytometrical analyses (8%)).

Calculated growth rates of unicellular cyanobacteria and heterotrophic bacteria changed with increasing pCO_2 concentrations (Fig. 37). Compared to the unicellular cyanobacteria the growth rate of heterotrophic bacteria was ~80 % higher in the not acidified mesocosm, whereas in the weakly acidified mesocosm growth rates equalled. In the strong acidified mesocosm the growth rate of the unicellular cyanobacteria was ~40% higher than the growth rate of the heterotrophic bacteria.

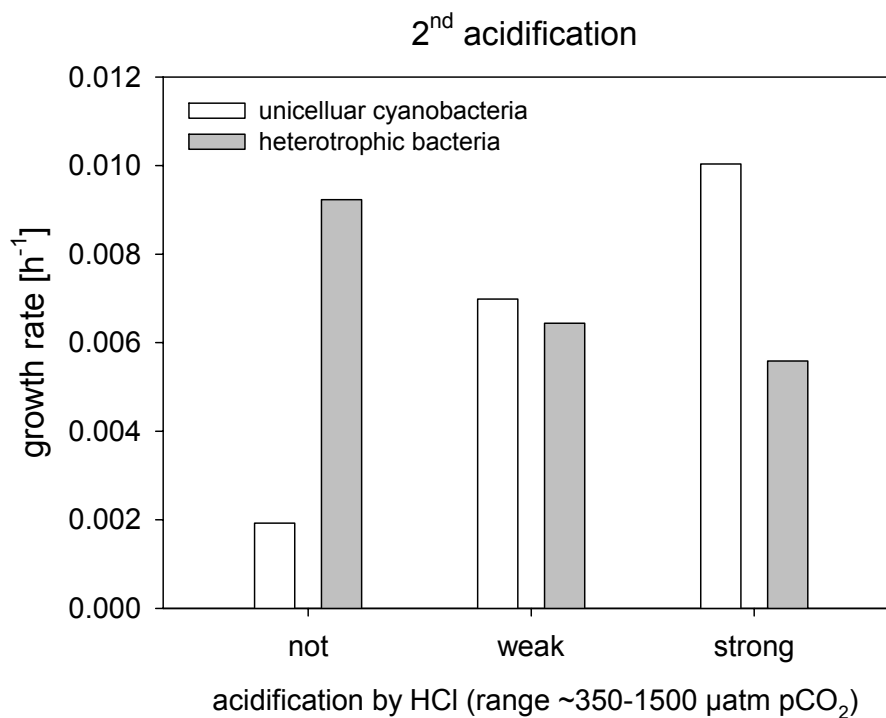


Figure 37: Growth rates of unicellular cyanobacteria (white) and heterotrophic bacteria (grey) in three different (not, weakly and strongly acidified) mesocosms for the 2^{nd} acidification experiment.

These findings may indicate a competition between heterotrophic bacteria and unicellular cyanobacteria during the 2^{nd} acidification experiment.

4 Discussion and conclusion

Our knowledge of factors and processes that determine the abundance, distribution and activities of marine microorganisms regarding to global change is limited. These uncertainties affect our ability to predict specific responses to the acidification of marine environments (Falkowski et al. 2000; Gruber and Galloway 2008). The mechanisms that underlie the contribution of microorganisms in marine food webs and biogeochemical cycles need to be assessed on nanometer to micrometer scale in order to make reliable predictions with respect to the response of the ocean to global change.

Experimental setup

In general, testing the impact of enhanced pCO₂ concentrations on natural aquatic ecosystems is a difficult task. While laboratory studies and bottle incubation experiments have the advantage of being highly reproducible when CO₂ concentrations were adjusted by aeration or addition of either acidic or alkaline solutions, the dynamics of a natural environment are not well simulated. Free-floating offshore mesocosms provide a reasonable alternative to *in-situ* perturbation experiments by allowing the study of whole ecosystems under semi-natural conditions in open waters. The mesocosms, which were used for the very first time in this study, are still in the beginning of their technical development and have to be further improved to sustain naturally occurring boundary conditions (e.g. high wind speeds, waves, up- and down-movements etc.). Due to unusual weather conditions for summer times (strong wind events and therefore wave heights between 1.5 and 2.5 m), some mesocosms had been damaged (mainly, broken bottom plates) over the time of the entire experiment. Even though the mesocosms would have resisted the extreme boundary conditions during the entire experiment, sampling of the mesocosms

is and will remain a problem during strong wind events, when waves are too high to allow the use of zodiacs for sampling.

However, usually in summer times the Baltic Sea provides calm open waters, which was certainly not the case in July 2007, when this mesocosm manipulation experiment took place. The upper 10 m of the water column inside the mesocosms was only slightly affected by exchange during the duration of the single experiments (1st and 2nd acidification), even if it was observed regularly in between. Please note, that in this work only data from those mesocosms and depth are discussed, which were not affected by mixing and water exchange as inferred from vertical CTD measurements from inside the mesocosms.

In contrast to a land-based mesocosm study at the European Union Large Scale Facility (LSF) in the Raunefjorden (in Bergen, Norway) in 2001 (Engel et al. 2005), the offshore mesocosms used here were not air-tight covered by domes. Hence, the pCO₂ concentrations in the weakly buffered Baltic Sea water rapidly equilibrated with the atmosphere. Since phytoplankton activity was very low in this study, the huge variability in pCO₂ and thus in pH cannot be explained by photosynthetic activity, which can account for up to 30% of diurnal variability of CO₂ in the upper water column during summer time (Yamashita et al. 1993). In order to study long-term CO₂ effects on natural aquatic ecosystems, an experimental setup is required, which provides low variability in seawater chemistry within different treatments. An alternative experimental setup was used in the study of Engel and colleagues (2005), where the enclosed water masses in the land-based mesocosms were acidified by aeration and a fumigation of the tents was maintained to keep the CO₂ partial pressure of the overlying air at a constant level. Furthermore, they reported low variability in seawater chemistry (pCO₂, pH, alkalinity and inorganic nutrients) within their treatments. Unfortunately, this experimental setup can not be used for offshore mesocosms due to logistical reasons. Therefore, more developmental work on acidification techniques and monitoring of seawater chemistry offshore have to be done.

Moreover, the huge $p\text{CO}_2$ gradient applied in this study (mean $p\text{CO}_2$ of 1600 μatm in the strongest acidified mesocosm) reflects a future CO_2 scenario, which exceeds model predictions of 540 - 970 μatm for the year 2100 (IPCC emission scenario, IS92 (Houghton et al. 2001)). For environmental, public and political concerns a gradient of $p\text{CO}_2$ concentrations up to ~ 1000 μatm might be more relevant. Furthermore, an experimental setup of three different $p\text{CO}_2$ concentrations up to ~ 1000 μatm and replicates may help to facilitate data interpretation.

Since the acidification of the mesocosms was repeated three times and due to the narrow intervals of continuous observations, our conclusions can only account for short term effects of CO_2 enrichment by HCl addition in a weakly buffered aquatic environment.

Effects of increasing $p\text{CO}_2$ on biogeochemical processes

In this field study, the effects of different $p\text{CO}_2$ concentrations on a natural phytoplankton community were investigated to address possible consequences of future ocean acidification. An acidification of ocean waters will potentially change the productivity of autotrophic phytoplankton and subsequently the efficiency of the biological carbon pump in the future, as recently hypothesized by Riebesell et al. (2007). This hypothesis implies potential changes in stoichiometry of organic matter in the future. This would subsequently alter microbial processes and biogeochemical cycling.

In contrast to what we expected, the situation in the Baltic in 2007 was characterized by low concentrations of Chl *a*, low primary production, low autotrophic activity and low concentrations of nutrients. Limitation in nitrate (below the detection limit, low DFAA) but not in phosphorus (conc) indicated a non-bloom situation. The elemental composition of organic matter in this mesocosm study was much higher than the canonical Redfield ratio of 106:16:1 (Redfield et al. 1963). Although several studies showed a high species-specific

variability in the elemental stoichiometry (Sterner and Elser 2002), our results support the assumption of a low productive system with low amounts of freshly produced POM.

The increase of POC concentration (~8%) in the control mesocosm was mainly due to the increased TEP concentration and increased biomass of heterotrophic bacteria. For calculation of the carbon content of TEP, a conversion factor of 0.75 was applied (Engel and Passow 2001). The carbon content of heterotrophic bacteria of 20 fg C cell⁻¹ was assumed according to Lee & Fuhrman (1987). TEP is known to have a high carbon content, because it mainly consists of polysaccharides. Therefore, the increased TEP concentration and higher cell abundance of heterotrophic bacteria can explain the increased POC concentration in the control mesocosm.

The substantial loss of POC concentrations (~10%) after 5 days due to perturbation by HCl-treatment can either be explained by enhanced vertical export of particulate material to deeper layers or by a degradation of biomass. Although the main POC proportion (80%) was owing to the smaller than 10 µm fraction, this loss of POC can only partly be accounted to the smaller than 10 µm size fraction (50%) (data not shown). Decreasing abundances of eukaryotic phytoplankton may indicate also a loss of POC (<10 µm), but did not explain this loss alone. Since abundances of heterotrophic bacteria, unicellular bacteria and concentrations of TEP did not decrease after the 2nd acidification, it is assumed that the unidentified part of the POC loss in the fraction smaller than 10 µm was exported into deeper layer of the mesocosm (below 10 m). Reduced TEP concentrations related to high CO₂ may be due to increased sedimentation rates. Eukaryotic phytoplankton and diazotrophic cyanobacteria decayed after acidification and over time, respectively. On the way down into deeper layer of the mesocosms, cell lysis and degradation processes will change the POM pool, recycle some of the organic matter back into the food web. During this process, refractory particulate and dissolved matter may be produced, and sedimentation processes of POM may increase due to the existence of TEP.

Our data showed that POC loss in the fraction larger than 10 μm was mainly due to the decay of the abundances of *Nodularia spp.* before the 2nd acidification. Although abundances of *Aphanizomenon spp.* increased after the 2nd acidification, a proliferation of *Aphanizomenon spp.* over *Nodularia spp.* (Stal et al. 2003) only occurred in the control and weakly acidified mesocosm. Therefore, strong HCl-treatment inhibited the growth of *Aphanizomenon spp.*, and influenced their dynamic compared to the control mesocosm. In accordance with results of this study, Caraco and Miller (1998) also suggested that the abundance of *Aphanizomenon flos aquae* is negatively affected by the impact of decreasing pH.

Temporally increasing POP concentrations in the HCl-treated mesocosms indicate an indirect response of the community change to phosphorous acquisition. Due to the higher availability of DOM (loss of filamentous cyanobacteria), heterotrophic bacteria and primarily unicellular cyanobacteria were favored. Since phosphate was not limited, it is likely that a P accumulation in the form of polyphosphate (poly-P) occurred.

While the C:N ratios remained nearly constant during the whole experiment, C:P ratios decreased significantly after the 2nd HCl-treatment due to the observed loss in POC and increase of POP concentrations. Recent studies indicate that phytoplankton species differ in their CO₂ requirement, suggesting large differences in CO₂-sensitivity between major phytoplankton taxonomic groups (Riebesell 2004). The effects of elevated inorganic carbon and CO₂ availability revealed considerable changes in phytoplankton elemental composition of C:N:P even though these differences were highly species-specific (Burkhardt and Riebesell 1997; Burkhardt et al. 1999; Gervais and Riebesell 2001; Riebesell et al. 2007). Barcelos e Ramos et al. (2007) investigated the effects of CO₂-induced changes in seawater chemistry on *Trichodesmium*, a colony-forming cyanobacterium. Carbon, nitrogen and phosphorus cellular contents, and cell dimensions decreased with rising CO₂ as a result of doubled cell division rate during their study. While C:P and N:P ratios more than doubled, C:N ratios remained without change. Their findings would imply a higher productivity of N-limited oligotrophic oceans, P limitation and

increase biological carbon sequestration in the ocean. In contrast to our study, the effects of rising CO₂ were investigated during exponential growth of *Trichodesmium*. Prevailing environmental conditions play an important role when investigating (1) changes in the ecosystem community structure and (2) changes due to HCl treatment. The response to rising CO₂ of a low primary productive system may therefore differ from a nutrient-repleted high primary productive system. In our case the C:N:P ratio was much higher than the Redfield ratio and primary production was very low. A lowering of C:P may therefore be the consequence of POC loss 5 days after acidification.

Effects of increasing pCO₂ on microbial dynamics and activities

Dynamics of eukaryotic phytoplankton, diatoms and green algae, were sensitive to the acidification. Abundances of *Nodularia* spp. decreased over time regardless to the acid treatment, whereas abundances of *Aphanizomenon* spp. increased in the control and weakly acidified mesocosms. The composition of diazotrophic cyanobacteria shifted between the two species in the control mesocosm, as it was also observed by Stal et al. (2003). But in contrast to our findings, their results showed a proliferation of *Nodularia spumigena* over *A. flos aquae* during a plankton bloom, mainly due to different photosynthetic and N₂ fixation potentials. As it was also suggested by Stal et al. (2003), dynamical developments of species composition depend on the prevailing environmental conditions. Our study took place during a non-bloom situation, where phosphate was not limited. Kononen et al. (1996) suggested that *Nodularia* spp. is favoured in situations when nutrients are limited, due to their ability to grow on intracellular P-storage for several days (more than one cell division) (Huber and Hamel 1985). Furthermore, their study revealed, that *Nodularia* spp. and *Aphanizomenon* spp. have different nutrient uptake kinetics. A higher affinity of *Nodularia* spp. than *Aphanizomenon* spp. for phosphate has been observed by Kononen et al. (1996). Thus, the observed temporal decrease of *Nodularia* spp. and the increase of *Aphanizomenon* spp. were due to sufficient nutrient supply. Moreover, the perturbation by the acid treatment caused an inhibition of the growth of *Aphanizomenon* spp. under low pH, as it was also suggested by Caraco and Miller (1998). Hence, among these interactions of natural succession and direct or indirect effect of HCl treatment, it is assumed that nutrient uptake kinetics may change in the future, possibly due to disadvantageous pH optima for nutrient uptake enzymes in cyanobacteria. Additionally the decrease of N₂ fixation rates of organisms larger than 10 µm as well as CO₂ uptake (over time as well as HCl-induced) was due to the shift of the two species. *Nodularia* spp. has 80% more heterocysts than *Aphanizomenon* spp. (Stal et al. 2003). This physiological difference explains

the significant decrease N₂ fixation from the 1st to the 2nd acidification, and the HCl-induced differences during the 2nd acidification experiment.

These findings are in accordance with growth of unicellular cyanobacteria, which can be mixotroph. Obviously, after the storm between the 1st and 2nd acidification the water masses were mixed and the prokaryotes had enough DOM for growth. This assumption is supported by autotrophic and heterotrophic activities. CO₂ uptake and N₂ fixation rates of unicellular cyanobacteria remained unchanged, but became a significant dominance in overall N₂ fixation. Our data suggest, therefore, that a perturbation by hydrochloric acid induced a community shift from eukaryotes to prokaryotes.

While CO₂ uptake and N₂ fixation of unicellular cyanobacteria were not influenced by the acid treatment, the decline of diazotrophic cyanobacteria caused lower autotrophic rates. Since unicellular cyanobacteria abundances were also not negatively affected by HCl treatment, their CO₂ uptake and N₂ fixation remained stable. This obvious advantage of being not directly affected by HCl treatment, was also observed for heterotrophic bacteria.

Heterotrophic activities of bacteria shifted relatively from biomass production to cell deviation, but were not directly influenced by the acid treatment. Leucine (proxy for biomass production) was considered to be taken up exclusively by heterotrophic bacteria (Kirchman et al. 1985; Riemann and Azam 1992), until Kamjunke & Jähnichen (2000) reported significant leucine incorporation of unicellular cyanobacteria. Recently, Hietanen et al. (2002) showed, that even filamentous cyanobacteria (like *Nodularia spp.*) are capable to incorporate leucine depending on the trophic state of the system. We can not be sure, that diazotrophic cyanobacteria incorporate radiolabelled leucine in the beginning of our study and therefore may falsify our results. But after the 2nd acidification, when abundances of diazotrophic cyanobacteria decreased, and the activity shifted relatively to cell deviation, these uptake rates of leucine and thymidine can only account for heterotrophic bacteria and unicellular cyanobacteria. In

contrast to leucine, based on present knowledge, thymidine is taken up exclusively by heterotrophic bacteria (Fuhrman and Azam 1982).

Although heterotrophic bacteria play a major role in organic matter cycling (e.g. Cole et al. 1988; Azam 1998; Azam and Malfatti 2007), observed effects of increased pCO₂ on their dynamics and activities are rare. In this study bacterial activity (thymidine incorporation) increased temporally, and was not directly affected by the acid treatment. Recent studies (Coffin et al. 2004; Grossart et al. 2006) showed pCO₂ related effects on bacterial production. While the results of the study by Coffin et al. (2004) suggest that the bacterial production in the deep ocean is moderately sensitive to seawater acidification (mild acidification did not inhibit production, may even enhance it), Grossart et al. (2006) pointed out, that the effects of changes in pCO₂ on bacterial activities are mainly indirectly linked to phytoplankton and presumably to particle dynamics.

Our results suggest that the high bacterial biomass production rates (leucine incorporation) could be interfered by cyanobacteria and that the temporal increasing cell deviation rates (thymidine incorporation) were mainly linked to the high organic matter availability and utilization. Hence, it is suggested that microbial uptake rates were not directly influenced by an increase in pCO₂.

Unicellular cyanobacteria and heterotrophic bacteria profited of the organic matter, which resulted e.g. from cell lysis and exudation. I assume, that these osmotrophic prokaryotes competed for utilization of organic matter. Low nanomolar concentrations of DFAA and very high leucine-aminopeptidase efficiency refer to rapid turnover of leucine. Cottner and Biddanda (2002) suggest a tight coupling of heterotrophs and autotrophs in low productivity systems, when nutrients are primarily organic and dissolved, prokaryotic heterotrophic respiration is equal or greater than primary production (Fig. 38).

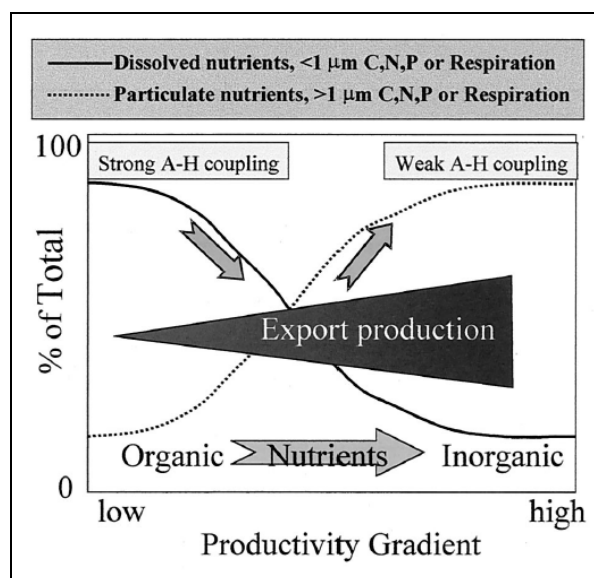


Figure 38: Changes in nutrient characteristics across a productivity gradient. (A-H coupling: autotrophic-heterotrophic coupling) (from Cotner and Biddanda 2002).

The effect of the HCl treatment on autotrophic-heterotrophic competition for nutrient utilization was partly conditioned by the fact, that some very few known unicellular cyanobacteria species are capable of fixing N_2 , when it is clearly ecologically advantageous (Zehr et al. 2001). In cases of N limitation and low amounts of utilizable DOM, these unicellular cyanobacteria acquire their nutrients for growth and metabolism more easily. In addition to this privilege of some unicellular cyanobacteria, our results indicate that the heterotrophic bacteria seem to be inhibited in acquiring nutrients with increasing pCO_2 regarding to their growth dynamics after the 2nd acidification. Enzyme efficiencies of alkaline phosphatase and leucine-aminopeptidase decreased (<60-70% and 20%, respectively) in response to the acid treatment. Furthermore, the slight increase of the enzyme efficiency of leucine-aminopeptidase over time under low pH conditions lead to possible changes in the substrate affinity. Overall, dynamics and calculated growth rates of unicellular cyanobacteria and heterotrophic bacteria, as well as lower enzyme efficiencies of heterotrophic bacteria lead to the assumption that unicellular cyanobacteria outcompeted heterotrophic bacteria under strong acidified

conditions. Our results suggest that CO₂-induced decrease of hydrolytical enzyme efficiencies lead to a competition between heterotrophs and autotrophs.

Conclusions

In order to investigate the impact of ocean acidification on microbial dynamics and activities, community structure and prevailing environmental conditions have to be considered. In the present study, the situation was characterized as a low productive system. Efficiencies of microbial exoenzymes decreased with decreasing pH, while microbial uptake rates were not affected by acidification. Autotrophic unicellular cyanobacteria outcompeted heterotrophic bacteria in strongly acidified mesocosms (pH 7.5). This shift in the community structure may have the potential to affect degradation and stoichiometry of organic matter in the Baltic Sea. Observed short-term effects suggest ocean acidification to potentially change trophic structures and interactions on the ecosystem level. The mechanisms that underlie the contribution of microorganisms in marine food webs and biogeochemical cycles need to be assessed on nanometer to micrometer scale in order to make reliable predictions with respect to the response of the ocean to global change. However, these complex, cascading trophic interactions need further investigations to serve as a reliable basis for accurate ecosystem models.

Acknowledgements

My special thanks go to my supervisor Dr. Mirko Lunau! Thank you for giving me the opportunity to broaden my mind and my knowledge. I really appreciated to work and discuss with you. Thanks for your support, for new perspectives, for good advice and fruitful comments!

Thanks to Prof. Dr. Wolfgang Ebenhöf for the good modelling seminars during my studies and for kindly being the secondary referee of this diploma thesis!

I would also like to thank Dr. Anja Engel for scientific discussions and helpful comments. I greatly appreciate the scientific discussions and the practical help of all participants of the SOPRAN 2007 cruise in the Baltic Sea. Thanks to Maren Voss, Kai Schulz, Robert Schmidt, Kirsten Isensee, Henning Johansen, Annett Grützmüller, Peter Fritsche and Kristin Haynert for kindly providing their data! I also thank the crew of RV Heincke and RV Alkor for their professional support. I am grateful to Dr. Hans-Peter Grossart for all the conversations and good advice. Thank you for analytical and technical support in your lab. Many thanks to Nicole Händel, Judith Piontek and Corinna Borchard for practical support, proofreading, helpful comments and the nice atmosphere in our working group!

I would also like to thank the institutions, that funded this work: the BMBF (SOPRAN, Theme 2), the Leibniz- and the Helmholtz Association (HZ-NG 102) and the Leibniz-Institute of Freshwater Ecology and Inland-Fisheries (IGB).

Dir, Helge, danke ich für die Kraft, die Motivation, das Verständnis und die Unterstützung während der letzten Jahre. Du hast mich stets ermutigt, meine Interessen zu verfolgen und hast immer ein offenes Ohr für mich gehabt. Danke!

Meiner Familie danke ich aus tiefstem Herzen für die Unterstützung, das Vertrauen und die Liebe!

Appendix

Table 2: Initial values of measured parameters before acidification at all

parameter	MC 1	MC 2	MC 3	MC 4	MC 5	MC 6
calculated pH (0-10m)	8.113	8.118	8.116	8.086	8.105	8.069
calculated pCO ₂ (0-10m) [µatm]	351.444	348.010	349.568	372.981	357.677	387.113
POC [µM]	45.765	53.074	49.986	55.989	60.945	61.717
PON [µM]	4.073	3.908	3.864	4.342	4.401	7.438
POP [µM]	nn	0.088	nn	nn	0.053	nn
C/N [mol/mol]	11.237	13.582	12.936	12.895	13.847	8.298
C/P [mol/mol]	nn	604.411	nn	nn	1139.448	nn
N/P [mol/mol]	nn	44.501	nn	nn	82.287	nn
CHI a [µg l ⁻¹]	2.092	2.094	2.194	1.890	2.043	1.956
DFAA [nM]	145.879	198.908	131.678	106.726	106.629	99.572
TEP [µg Xeq. l ⁻¹]	72.742	70.929	68.672	71.558	71.743	71.928
eukaryotic phytoplankton [x10 ⁴ cells ml ⁻¹]	2.232	nn	nn	nn	nn	nn
Nodularia spp [units l ⁻¹]	nn	nn	nn	nn	4158	2970
Aphanizomenon spp [units l ⁻¹]	nn	nn	nn	nn	6798	5148
CO ₂ UT total [µmol l ⁻¹ h ⁻¹]	nn	nn	0.066	0.151	nn	0.191
CO ₂ UT >10 [µmol l ⁻¹ h ⁻¹]	nn	0.011	0.006	0.007	nn	0.006
CO ₂ UT <10 [µmol l ⁻¹ h ⁻¹]	0.069	nn	0.060	0.144	0.197	0.185
N ₂ fix total [nmol l ⁻¹ h ⁻¹]	0.265	0.044	0.162	0.381	0.608	0.764
N ₂ fix >10 [nmol l ⁻¹ h ⁻¹]	0.196	0.043	0.142	0.190	0.112	0.138
N ₂ fix <10 [nmol l ⁻¹ h ⁻¹]	0.069	0.001	0.020	0.192	0.496	0.625
unicellular cyanobacteria [x10 ⁵ cells ml ⁻¹]	3.699	nn	nn	nn	nn	nn
bacteria [x10 ⁶ cells ml ⁻¹]	2.288	2.572	2.273	2.303	2.284	2.375
EE glucosidase [h ⁻¹]	0.033	0.015	0.022	0.023	0.031	0.025
EE peptidase [h ⁻¹]	0.953	0.847	0.954	1.102	0.996	0.837
EE phosphatase [h ⁻¹]	0.577	0.613	0.580	0.575	0.630	0.621
TO glucosidase [mol l ⁻¹ h ⁻¹]	0.050	0.023	0.033	0.035	0.046	0.038
TO peptidase [mol l ⁻¹ h ⁻¹]	1.416	1.268	1.407	1.607	1.469	1.249
TO phosphatase [mol l ⁻¹ h ⁻¹]	0.858	0.919	0.866	0.858	0.946	0.934
Thy UT [nmol l ⁻¹ h ⁻¹]	nn	nn	nn	nn	nn	nn
Leu UT [nmol l ⁻¹ h ⁻¹]	nn	nn	nn	nn	nn	nn

Table 3: Solubility of MUF- and AMC- labelled substrate analogues

substrate analogue	solubility	Chrost et al. (1989)	Degrassi et al. (1999)	Chrost et al. (2006)	in this study	comments
MUF α -D-galactoside					H ₂ O (deionized)	ok
MUF α -D-glucoside	Methylcellosolve				Methylcellosolve	good solubility
MUF α -D-mannoside					Methylcellosolve	use of vortex shaker
MUF β -D-galactoside		H ₂ O			H ₂ O (deionized)	use of vortex shaker, flocculation (white)
MUF β -D-glucoside	Methylcellosolve	H ₂ O			H ₂ O (deionized)	use of vortex shaker (~35 min)
MUF β -D-lactoside					H ₂ O (deionized)	use of vortex shaker
MUF phosphate	Methylcellosolve	H ₂ O		H ₂ O	H ₂ O (deionized)	good solubility
MUF acetate			Acetone		Acetone	ok
MUF palmitate					Methylcellosolve	use of vortex shaker (~30 min)
L-Aspartic acid β -AMC					H ₂ O (deionized) & HCl	after dissolving too acidic; dilution with MOPS
L-Leucine AMC	Methylcellosolve	H ₂ O		Ethanol 99%	Ethanol 96%	use of vortex shaker (~5 min)

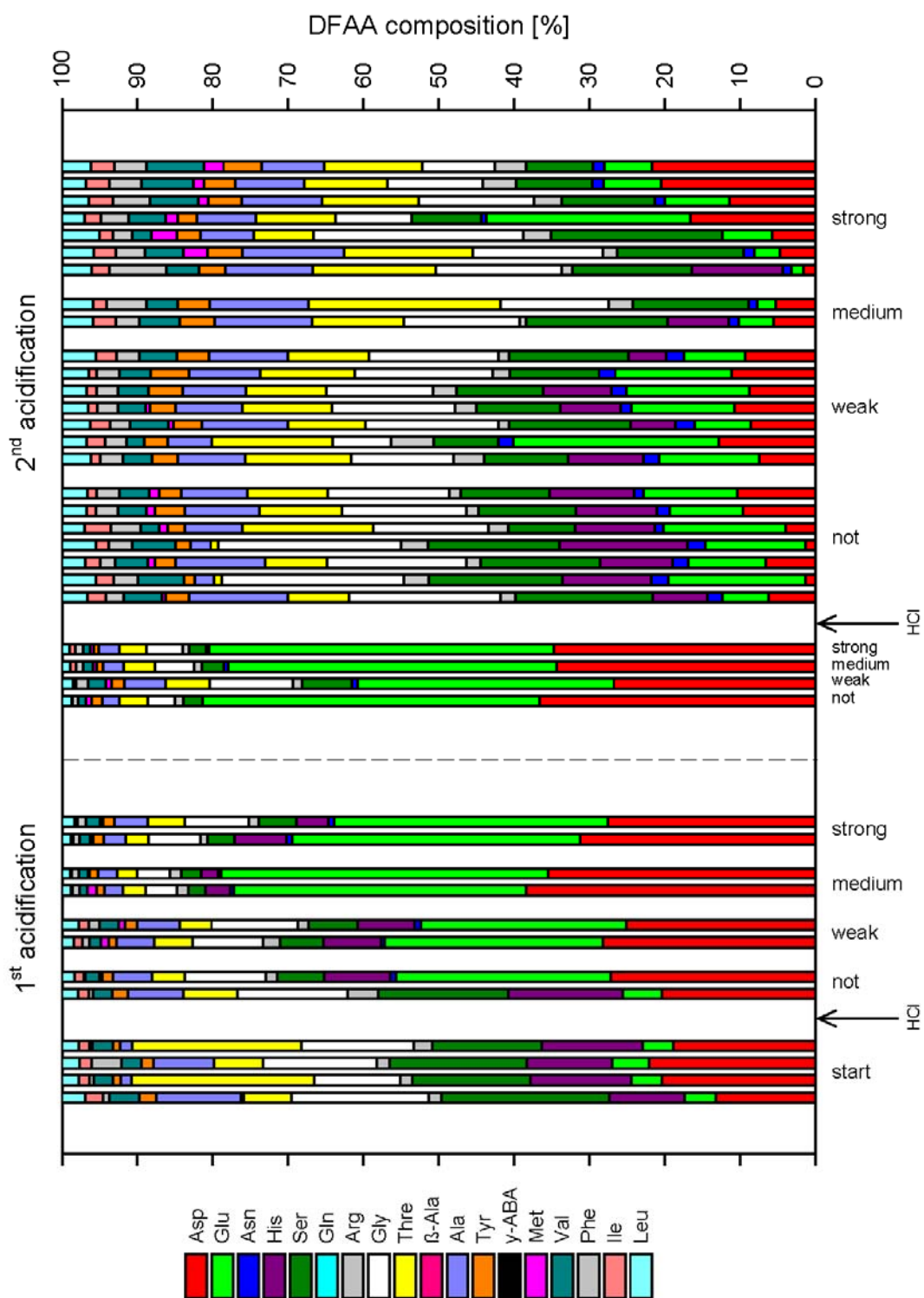


Figure 39: Dissolved free amino acid (DFAA) composition in the mesocosms (not, weakly and strongly acidified) of the 1st and 2nd acidification experiment. Temporal development within the treatments and acidification.

References

- AZAM, F. 1998. Microbial control of oceanic carbon flux: The plot thickens. *Science* **280**: 694-696.
- AZAM, F., T. FENCHEL, J. G. FIELD, J. S. GRAY, L. A. MEYERREIL, and F. THINGSTAD. 1983. The Ecological Role of Water-Column Microbes in the Sea. *Mar. Ecol.-Prog. Ser.* **10**: 257-263.
- AZAM, F., and F. MALFATTI. 2007. Microbial structuring of marine ecosystems. *Nat. Rev. Microbiol.* **5**: 782-791.
- BARCELOS E RAMOS, J., H. BISWAS, K. G. SCHULZ, J. LAROCHE, and U. RIEBESELL. 2007. Effect of rising atmospheric carbon dioxide on the marine nitrogen fixer *Trichodesmium*. *Glob. Biogeochem. Cycle* **21**.
- BURKHARDT, S., and U. RIEBESELL. 1997. CO₂ availability affects elemental composition (C:N:P) of the marine diatom *Skeletonema costatum*. *Mar. Ecol.-Prog. Ser.* **155**: 67-76.
- BURKHARDT, S., I. ZONDERVAN, and U. RIEBESELL. 1999. Effect of CO₂ concentration on C : N : P ratio in marine phytoplankton: A species comparison. *LIMNOL. OCEANOGR.* **44**: 683-690.
- CALDEIRA, K., and M. E. WICKETT. 2003. Anthropogenic carbon and ocean pH. *Nature* **425**: 365-365.
- CARACO, N. F., and R. MILLER. 1998. Effects of CO₂ on competition between a cyanobacterium and eukaryotic phytoplankton. *Can. J. Fish. Aquat. Sci.* **55**: 54-62.
- CHROST, R. J. 1991. Environmental Control of the Synthesis and Activity of Aquatic Microbial Ectoenzymes. *In* R. J. Chrost [ed.], *Microbial Enzymes in Aquatic Environments*. Brock/Springer Series in Contemporary Bioscience.
- CHROST, R. J., U. MUNSTER, H. RAI, D. ALBRECHT, P. K. WITZEL, and J. OVERBECK. 1989. Photosynthetic Production and Exoenzymatic Degradation of Organic-Matter in the Euphotic Zone of a Eutrophic Lake. *J. Plankton Res.* **11**: 223-242.

REFERENCES

- CHROST, R. J., and W. SIUDA. 2006. Microbial production, utilization, and enzymatic degradation of organic matter in the upper trophogenic layer in the pelagial zone of lakes along a eutrophication gradient. *LIMNOL. OCEANOGR.* **51**: 749-762.
- COFFIN, R. B., M. T. MONTGOMERY, T. J. BOYD, and S. M. MASUTANI. 2004. Influence of ocean CO₂ sequestration on bacterial production. *Energy* **29**: 1511-1520.
- COLE, J. J., S. FINDLAY, and M. L. PACE. 1988. Bacterial Production in Fresh and Saltwater Ecosystems - a Cross-System Overview. *Mar. Ecol.-Prog. Ser.* **43**: 1-10.
- COTNER, J. B., and B. A. BIDDANDA. 2002. Small players, large role: Microbial influence on biogeochemical processes in pelagic aquatic ecosystems. *Ecosystems* **5**: 105-121.
- DE NOBEL, W. T. 1997. Interaction of nitrogen fixation and phosphorus limitation in *Aphanizomenon flos-aquae* (Cyanophyceae). *J. Phycol.* **33**: 794-799.
- DEGRASSI, G., L. UOTILA, R. KLIMA, and V. VENTURI. 1999. Purification and properties of an esterase from the yeast *Saccharomyces cerevisiae* and identification of the encoding gene. *Appl. Environ. Microbiol.* **65**: 3470-3472.
- DELGIORGIO, P., D. F. BIRD, Y. T. PRAIRIE, and D. PLANAS. 1996. Flow cytometric determination of bacterial abundance in lake plankton with the green nucleic acid stain SYTO 13. *LIMNOL. OCEANOGR.* **41**: 783-789.
- ENGEL, A. 2004a. Polysaccharide aggregation as a potential sink of marine dissolved organic carbon. *Nature* **428**: 929-932.
- . 2004b. Transparent exopolymer particles and dissolved organic carbon production by *Emiliana huxleyi* exposed to different CO₂ concentrations: a mesocosm experiment. *Aquat. Microb. Ecol.* **34**: 93-104.
- ENGEL, A., and U. PASSOW. 2001. Carbon and nitrogen content of transparent exopolymer particles (TEP) in relation to their Alcian Blue adsorption. *Mar. Ecol.-Prog. Ser.* **219**: 1-10.

REFERENCES

- ENGEL, A. and others 2005. Testing the direct effect of CO₂ concentration on a bloom of the coccolithophorid *Emiliana huxleyi* in mesocosm experiments. *LIMNOL. OCEANOGR.* **50**: 493-507.
- FALKOWSKI, P. and others 2000. The global carbon cycle: A test of our knowledge of earth as a system. *Science* **290**: 291-296.
- FUHRMAN, J. A., and F. AZAM. 1982. Thymidine Incorporation as a Measure of Heterotrophic Bacterioplankton Production in Marine Surface Waters - Evaluation and Field Results. *Mar. Biol.* **66**: 109-120.
- GAO, K., Y. ARUGA, K. ASADA, and M. KIYOHARA. 1993. Influence of Enhanced Co₂ on Growth and Photosynthesis of the Red Algae *Gracilaria Sp* and *G-Chilensis*. *J. Appl. Phycol.* **5**: 563-571.
- GASOL, J. M., and P. A. DEL GIORGIO. 2000. Using flow cytometry for counting natural planktonic bacteria and understanding the structure of planktonic bacterial communities. *Sci. Mar.* **64**: 197-224.
- GERVAIS, F., and U. RIEBESELL. 2001. Effect of phosphorus limitation on elemental composition and stable carbon isotope fractionation in a marine diatom growing under different CO₂ concentrations. *LIMNOL. OCEANOGR.* **46**: 497-504.
- GIORDANO, M., J. BEARDALL, and J. A. RAVEN. 2005. CO₂ concentrating mechanisms in algae: Mechanisms, environmental modulation, and evolution. *Annual Review of Plant Biology* **56**: 99-131.
- GRANELI, E., K. WALLSTROM, U. LARSSON, W. GRANELI, and R. ELMGREN. 1990. Nutrient Limitation of Primary Production in the Baltic Sea Area. *Ambio* **19**: 142-151.
- GROSSART, H. P., M. ALLGAIER, U. PASSOW, and U. RIEBESELL. 2006. Testing the effect of CO₂ concentration on the dynamics of marine heterotrophic bacterioplankton. *LIMNOL. OCEANOGR.* **51**: 1-11.
- GRUBER, N., and J. N. GALLOWAY. 2008. An Earth-system perspective of the global nitrogen cycle. *Nature* **451**: 293-296.
- HEIN, M., and K. SAND-JENSEN. 1997. CO₂ increases oceanic primary production. *Nature* **388**: 526-527.

- HIETANEN, S., J. M. LEHTIMAKI, L. TUOMINEN, K. SIVONEN, and J. KUPARINEN. 2002. Nodularia spp. (Cyanobacteria) incorporate leucine but not thymidine: importance for bacterial-production measurements. *Aquat. Microb. Ecol.* **28**: 99-104.
- HOPPE, H. G. 1983. Significance of Exoenzymatic Activities in the Ecology of Brackish Water - Measurements by Means of Methylumbelliferyl-Substrates. *Mar. Ecol.-Prog. Ser.* **11**: 299-308.
- HOUGHTON, J. and others [eds.]. 2001. *Climate Change 2001: The Scientific Basis: Contribution of Working Group 1 to the Third Assessment Report of the Intergovernmental Panel on Climate Change*. Cambridge University Press.
- HUBER, A. L., and K. S. HAMEL. 1985. Phosphatase-Activities in Relation to Phosphorus-Nutrition in Nodularia-Spumigena (Cyanobacteriaceae) .2. Laboratory Studies. *Hydrobiologia* **123**: 81-88.
- IPCC. 2007. *Intergovernmental Panel on Climate Change (IPCC) 4th assessment report (AR4)*.
- JORGENSEN, N. O. G. 1987. Free Amino-Acids in Lakes - Concentrations and Assimilation Rates in Relation to Phytoplankton and Bacterial Production. *LIMNOL. OCEANOGR.* **32**: 97-111.
- KAMJUNKE, N., and S. JAEHNICHEN. 2000. Leucine incorporation by *Microcystis aeruginosa*. *LIMNOL. OCEANOGR.* **45**: 741-743.
- KAPLAN, A., and L. REINHOLD. 1999. CO₂ concentrating mechanisms in photosynthetic microorganisms. *Annual Review of Plant Physiology and Plant Molecular Biology* **50**: 539-+.
- KIRCHMAN, D., H. DUCKLOW, and R. MITCHELL. 1982. Estimates of bacterial growth from changes in uptake rates and biomass. *Appl. Environ. Microbiol.* **44**: 1296-1307.
- KIRCHMAN, D., E. K'NEES, and R. HODSON. 1985. Leucine incorporation and its potential as a measure of protein synthesis by bacteria in natural aquatic systems. *Appl. Environ. Microbiol.* **49**: 599-607.

REFERENCES

- KOCH, S. 2007. Growth and calcification of the coccolithophore *Emiliana huxleyi* under different CO₂ concentrations. Diploma-Thesis. Carl von Ossietzky Universität Oldenburg.
- KONONEN, K. 1996. Initiation of cyanobacterial blooms in a frontal region at the entrance to the Gulf of Finland, Baltic Sea. *LIMNOL. OCEANOGR.* **41**: 98-112.
- KORELEFF, F. 1983. Determination of total phosphor by alkaline persulphate oxidation, p. 136-139. *In* K. Grasshoff, M. Ehrhardt and K. Kremling [eds.], *Methods of seawater analysis*. Verlag Chemie, Weinheim.
- KÖRTZINGER, A. 2006. Der marine Kohlenstoffkreislauf - eine biogeochemische Betrachtung. *In* G. Hempel, I. Hempel and S. Schiel [eds.], *Faszination Meeresforschung*. Hauschild.
- LEE, S., and J. A. FUHRMAN. 1987. Relationships between Biovolume and Biomass of Naturally Derived Marine Bacterioplankton. *Appl. Environ. Microbiol.* **53**: 1298-1303.
- LEONARDOS, N., and R. J. GEIDER. 2005. Elevated atmospheric carbon dioxide increases organic carbon fixation by *Emiliana huxleyi* (Haptophyta), under nutrient-limited high-light conditions. *J. Phycol.* **41**: 1196-1203.
- LINDROTH, P., and K. MOPPER. 1979. High-Performance Liquid-Chromatographic Determination of Subpicomole Amounts of Amino-Acids by Precolumn Fluorescence Derivatization with Ortho-Phthaldialdehyde. *Analytical Chemistry* **51**: 1667-1674.
- LUNAU, M., M. WURST, J. PIONTEK, H. P. GROSSART, U. RIEBESELL, and A. ENGEL. 2008. Potential effects of ocean acidification on microbial organic matter degradation during an offshore mesocosm experiment. *Ocean Science Meeting*, March 2-7, 2008.
- MONTOYA, J. P., M. VOSS, P. KÄHLER, and D. G. CAPONE. 1996. A simple, high-precision, high-sensitivity tracer assay for N₂ fixation. *Appl. Environ. Microbiol.* **62**: 986-993.

REFERENCES

- MUENSTER, U. 1985. Investigations about structure, distribution and dynamics of different organic substrates in the DOM of Lake Pluzsee. *Archiv fuer Hydrobiologie, Supplement* **70**: 429-480.
- NIEMI, A. 1979. Blue-green algal blooms and N:P ratio in the Baltic Sea. *Acta Bot. Fenn.*, 110, 57-61, (1979).
- PASSOW, U. 2002. Transparent exopolymer particles (TEP) in aquatic environments. *Progress in Oceanography* **55**: 287-333.
- PASSOW, U., and A. L. ALLDREDGE. 1995. A dye-binding assay for the spectrophotometric measurement of transparent exopolymer particles (TEP). *LIMNOL. OCEANOGR.* **40**: 1326-1335.
- PETIT, J. R. and others 1999. Climate and atmospheric history of the past 420,000 years from the Vostok ice core, Antarctica. *Nature* **399**: 429-436.
- PIONTEK, J., N. HÄNDEL, and A. ENGEL. 2007a. Effects of rising temperature and pCO₂ on bacterial degradation processes in marine systems. European Geosciences Union, General Assembly 2007.
- PIONTEK, J., M. LUNAU, N. HÄNDEL, S. JANSEN, T. NEU, and A. ENGEL. 2007b. Effects of rising temperature and decreasing pH on degradation activity of marine bacterioplankton. 10th Symposium on Aquatic Microbial Ecology, September 2-7 2007.
- QIU, B. S., and K. S. GAO. 2002. Effects of CO₂ enrichment on the bloom-forming cyanobacterium *Microcystis aeruginosa* (Cyanophyceae): Physiological responses and relationships with the availability of dissolved inorganic carbon. *J. Phycol.* **38**: 721-729.
- RAVEN, J. 2005. Ocean acidification due to increasing atmospheric carbon dioxide. Royal Society.
- RAVEN, J. A. 2003. Inorganic carbon concentrating mechanisms in relation to the biology of algae. *Photosynthesis Research* **77**: 155-171.
- REDFIELD, A. C., B. M. KETCHUM, and F. A. RICHARDS. 1963. The influence of organism on the composition of seawater, p. 26-79. *In* M. N. Hill [ed.], *In The Sea*. Wiley Interscience: New York.

REFERENCES

- RIEBESELL, U. 2004. Effects of CO₂ Enrichment on Marine Phytoplankton. *J. Oceanogr.* **60**: 719-729.
- RIEBESELL, U. and others 2007. Enhanced biological carbon consumption in a high CO₂ ocean. *Nature* **450**: 545-550.
- RIEBESELL, U., D. A. WOLFGLADROW, and V. SMETACEK. 1993. Carbon-Dioxide Limitation of Marine-Phytoplankton Growth-Rates. *Nature* **361**: 249-251.
- RIEMANN, B., and F. AZAM. 1992. Measurements of bacterial protein synthesis in aquatic environments by means of leucine incorporation. *Marine Microbial Food Webs* **6**: 91-105.
- ROTHSCHILD, L. J. 1994. Elevated CO₂ - Impact on Diurnal Patterns of Photosynthesis in Natural Microbial Ecosystems, p. 285-289. *Life Sciences and Space Research Xxv. Advances in Space Research.* Pergamon Press Ltd.
- SABINE, C. L. and others 2004. The Oceanic Sink for Anthropogenic CO₂. *Science* **305**: 367-371.
- SCIANDRA, A. and others 2003. Response of coccolithophorid *Emiliana huxleyi* to elevated partial pressure of CO₂ under nitrogen limitation. *Mar. Ecol.-Prog. Ser.* **261**: 111-122.
- SIMON, M., and F. AZAM. 1989. Protein content and protein synthesis rates of planktonic marine bacteria. *Marine Ecology Progress Series* **51**: 201-213.
- STAL, L. J. and others 2003. BASIC: Baltic Sea cyanobacteria. An investigation of the structure and dynamics of water blooms of cyanobacteria in the Baltic Sea - responses to a changing environment. *Cont. Shelf Res.* **23**: 1695-1714.
- STERNER, R. W., and J. J. ELSER. 2002. *Ecological Stoichiometry: The Biology of Elements from Molecules to the Biosphere.* Princeton University Press.
- STODEREGGER, K., and G. J. HERNDL. 1998. Production and release of bacterial capsular material and its subsequent utilization by marine bacterioplankton. *LIMNOL. OCEANOGR.* **43**: 877-884.

REFERENCES

- TAMMINEN, T. 1995. Nitrate and Ammonium Depletion Rates and Preferences During a Baltic Spring Bloom. *Mar. Ecol.-Prog. Ser.* **120**: 123-133.
- TORTELL, P. D. 2000. Evolutionary and ecological perspectives on carbon acquisition in phytoplankton. *LIMNOL. OCEANOGR.* **45**: 744-750.
- VOSS, M., D. BOMBAR, N. LOICK, and J. W. DIPPNER. 2006. Riverine influence on nitrogen fixation in the upwelling region off Vietnam, South China Sea. *Geophys. Res. Lett.* **33**.
- YAMASHITA, E., F. FUJIWARA, X. LIU, and E. OHTAKI. 1993. Measurements of carbon dioxide in the Seto Inland Sea of Japan. *J. Oceanogr.* **49**: 559-569.
- ZEEBE, R. E., and D. WOLF-GLADROW. 2001. *CO₂ in seawater: Equilibrium, Kinetics, Isotopes.* Elsevier Oceanography Series.
- ZEHR, J. P. and others 2001. Unicellular cyanobacteria fix N₂ in the subtropical North Pacific Ocean. *Nature* **412**: 635-638.

EIDESSTATTLICHE ERKLÄRUNG

Hiermit versichere ich, dass ich diese Arbeit selbstständig verfasst und keine anderen als die angegebenen Hilfsmittel benutzt habe.

Oldenburg, 20. April 2008